AD-A017 460

ATMOSPHERIC EFFECTS ON 1.06 MICRON LASER-GUIDED
WEAPONS

Vance A. Hedin

Air Force Institute of Technology
Wright-Patterson Air Force Base, Ohio
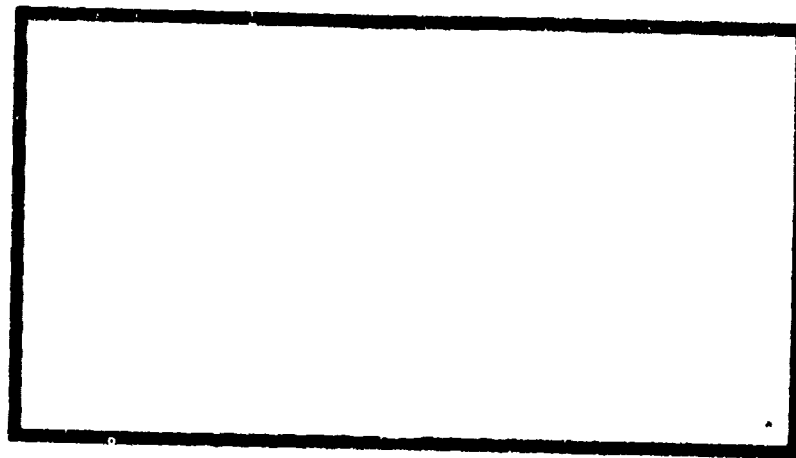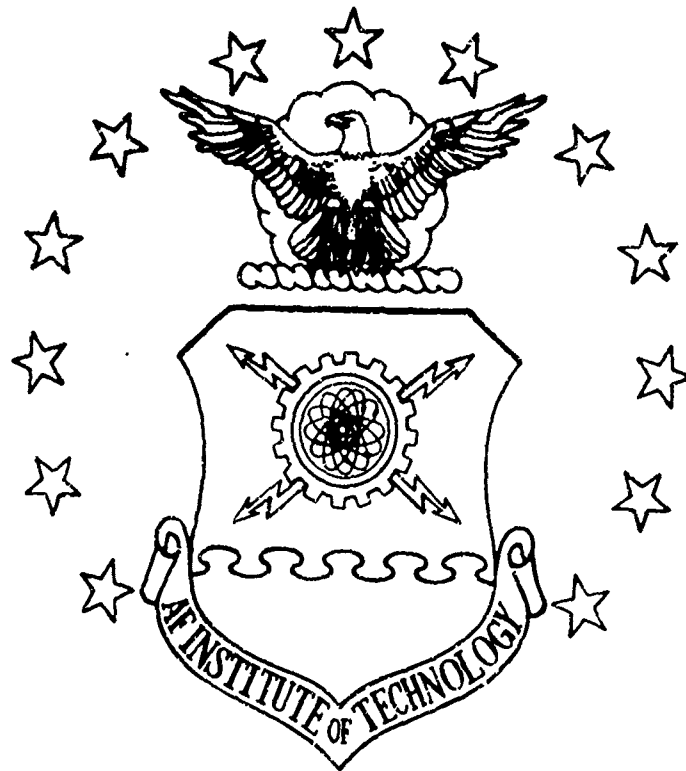
March 1975

329048
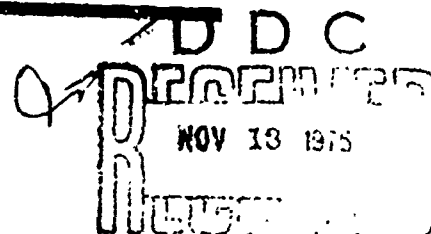
ADA017460

UNITED STATES AIR FORCE
AIR UNIVERSITY
AIR FORCE INSTITUTE OF TECHNOLOGY
Wright-Patterson Air Force Base, Ohio

DDC
RECEIVED
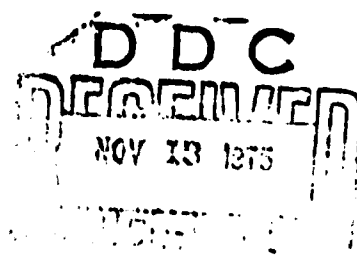NOV 18 1975

119

ATMOSPHERIC EFFECTS
ON
1.06 MICRON LASER-GUIDED WEAPONS

THESIS

GEO/PH/75-5   VANCE A. HEDIN
                            CAPTAIN   USAF

Approved for public release; distribution unlimited

REPORT DOCUMENTATION PAGE		READ INSTRUCTIONS BEFORE COMPLETING FORM
1. REPORT NUMBER GEO/PH/75-5	2. GOVT ACCESSION NO.	3. RECIPIENT'S CATALOG NUMBER
4. TITLE (and Subtitle) Atmospheric effects on 1.06 micron Laser-Guided Weapons		5. TYPE OF REPORT & PERIOD COVERED MS Thesis
		6. PERFORMING ORG. REPORT NUMBER
7. AUTHOR(s) Vance A. Hedin Captain USAF		8. CONTRACT OR GRANT NUMBER(s)
9. PERFORMING ORGANIZATION NAME AND ADDRESS Air Force Institute of Technology (AFIT/EN) Wright-Patterson AFB, Ohio 45433		10. PROGRAM ELEMENT, PROJECT, TASK AREA & WORK UNIT NUMBERS
11. CONTROLLING OFFICE NAME AND ADDRESS Operations Evaluation Group AF/SAV Assistant Chief of Staff, Studies and Analysis Hq USAF, Washington, D.C.		12. REPORT DATE March 1975
		13. NUMBER OF PAGES 119
14. MONITORING AGENCY NAME & ADDRESS(if different from Controlling Office)		15. SECURITY CLASS (of this report) Unclassified
		15a. DECLASSIFICATION DOWNGRADING SCHEDULE

16. DISTRIBUTION STATEMENT (of this Report)

Approved for public release; distribution unlimited

17. DISTRIBUTION STATEMENT (of the abstract entered in Block 20, if different from Report)

18. SUPPLEMENTARY NOTES

Approved for public release; IAW AFR 190-17

JERRY C. HIX, Captain, USAF
Director of Information

19. KEY WORDS (Continue on reverse side if necessary and identify by block number)

Laser-Guided System Lock-on Range
Aerosol Attenuation of 1.06 micron Laser Radiation
Rain Attenuation of 1.06 micron Laser Radiation
Atmospheric Transmittance of 1.06 micron Laser Radiation
Atmospheric Aerosol Models

Aerosol Mixing Layer
Atmospheric Propagation

20. ABSTRACT (Continue on reverse side if necessary and identify by block number)

With the advent of laser-guided weapons into the Air Force inventory, it has become an item of high interest to decision makers at many levels, from the aircrews who must deliver the weapons, to the high planning levels of the Air Staff, to better understand the significant limitations that weather places on these weapons. This thesis presents an easily useable model for predicting maximum lock-on ranges for 1.06 micron laser-guided weapons as a function of two significant weather factors: surface meteorological range

DD 1 JAN 73 1473   EDITION OF 1 NOV 65 IS OBSOLETE

Abstract (continued)

and rainfall rate. In addition, a number of sample caluclations based on the model are presented. The most important factor limiting transmittance and maximum lock-on range of a 1.06 micron system in a precipitation free environment is the aerosol content of the atmosphere. Aerosol effects depend on both the aerosol concentration and aerosol particle size distribution. Two aerosol altitude profiles are compared in this study: the Homogeneous Mixing Layer model as developed by Coolidge and an approximation of the model described by McClatchey. Incorporated in these models are several aerosol particle size distributions described by Dermendjian including combinations of maritime and continental distributions. Also included is the effect of rainfall on maximum lock-on range. It is found that computations of lock-on range using these two models give significantly different results in many cases. Recent information gives overwhelming evidence that the Homogeneous Mixing Layer model is the most representative atmospheric model, indicating it should be used for lock-on range calculations.

ATMOSPHERIC EFFECTS

ON

1.06 MICRON LASER-GUIDED WEAPONS

THESIS

Presented to the Faculty of the School of Engineering

of the Air Force Institute of Technology

Air University

in Partial Fulfillment of the

Requirements for the Degree of

Master of Science

by

Vance A. Hedin
Captain   USAF

Graduate Electro-optics

March 1975

Approved for public release; distribution unlimited

Preface

This thesis is a continua⁺ı n of ꞏ study requested by Operations
Evaluation Group, Assistant Ch ꞏ of Staff, Studies a.d Analysis, USAF.
Atmospheric conditions have a significant effect on the effectiveness
of laser-guided weapons. The most effective use of these weapons, then,
requires an understanding of the effects of weather and a knowledge of
when these weapons can or cannot be effectively used in specif ice tacti-
cal situations. This thesis describes a study of the maximum lock-on
range which can be expected for a 1.06 micron laser-guided weapon under
varying meteorological ranges and rainfall rates. Two atmospheric
models were used for this study and their results compared. The results
were much different in many cases and point out the fact that we must
know what the air is really like to accurately predict such things as
maximum lock-on range. It has become apparer⁺ to the author during this
study that the atmosphere is exceedingly complex and continuously vary-
ing and we are still a long way from accurately measuring al¹ variables
in the atmosphere and getting a real time picture of them. At the same
time I have received an appreciation of the fact that many judicious
assumptions and approximations can be made which will give fairly re-
liable and useful results, especially if one is looking for relative
results caused by changing various parameters.

I would like to express my sincere appreciation to those people
who have given so much assistance to me in the course of this study.
I would like to thank the library staff and computer terminal staff of
the Air Force Institute of Technology (AFIT) for their helpfulness. I

Contents

List of Figures

List of Tables

Abstract

With the advent of laser-guided weapons into the Air Force inventory, it has become an item of high interest to decision makers at many levels, from the aircrews who must deliver the weapons, to the high planning levels of the Air Staff, to better understand the significant limitations that weather places on these weapons. This thesis presents an easily useable model for predicting maximum lock-on ranges for 1.06 micron laser-guided weapons as a function of two significant weather factors: surface meteorological range and rainfall rate. In addition, a number of sample calculations based on the model are presented. The most important factor limiting transmittance and maximum lock-on range of a 1.06 micron system in a precipitation free environment is the aerosol content of the atmosphere. Aerosol effects depend on both the aerosol concentration and the aerosol particle size distribution. Two vertical aerosol profiles are compared in this study: the Homogeneous Mixing Layer model as developed by Coolidge and an approximation of the model described by McClatchey. Incorporated in these models are several aerosol particle size distributions described by Dermendjian including combinations of maritime and continental distributions. Also included is the effect of rainfall on maximum lock-on range. It is found that computations of lock-on range using these two models give significantly different results in many cases. Recent information gives overwhelming evidence that the Homogeneous Mixing Layer model is the most representative atmospheric model, indicating it should be used for lock-on range calculations.

ATMOSPHERIC EFFECTS

ON

1.06 MICRON LASER-GUIDED WEAPONS

I. Introduction

Background

In recent years many laser-guided weapons have been developed and included in the Air Force inventory. Experience with these weapons has shown that they can be highly effective and extremely accurate under the proper conditions. However, one major problem in the use of these weapons is the significant limitations imposed on them by the weather. Under certain weather conditions the maximum lock-on range of these weapons can be greatly reduced due to the attenuation of the laser beam by the atmosphere or lock-on can even be prevented, thus prohibiting the use of these weapons entirely. It is, therefore, an item of great interest at many levels of decision making, from the aircrew who must decide optimum delivery tactics for expected weather conditions to the highest level of planning at the Air Staff who must make force structure decisions, to know the limitions imposed by atmospheric conditions on these weapons.

It is extremely important to quantify the effects of weather on laser-guided weapons and many studies have been accomplished in an attempt to do this. However, these studies have been limited in their scope and applicability to varying weather conditions, and recent findings indicate that many of their results may also be unrealistic.

Problem

It is desirable to have some method of predicting maximum lock-on ranges of laser weapons based on observable atmospheric conditions. The general purpose of this report, therefore, is to investigate the atmospheric attenuation of 1.06 micron laser radiation under varying weather conditions and to compare the results of transmittance and lock-on range calculations using different mathematical models to describe the atmosphere. The specific problem is to devise a simple method or model for predicting maximum lock-on ranges of 1.06 micron laser-guided weapons for varying surface meteorological ranges and rain rates.

Scope

Laser radiation with a wavelength of 1.06 microns is affected in the atmosphere mainly by aerosol particle scattering and absorption and to a lesser extent by molecular scattering and absorption. This report will, therefore, investigate the attenuation effects of different aerosol particle size distributions, including the generally accepted continental, maritime, and haze L distrubutions proposed by Deirmendjian (Ref 8, 9, 10) and will include the effects of different mixtures of continental and maritime hazes. These distributions will be used in two vertical aerosol profiles given by McClatchey (Ref ?6) and Coolidge (Ref 7) respectively. Included in this report will be the effects of varying surface meteorological ranges and rain rates.

This report does not examine details of various laser hardware parameters. Instead, the parameters of an assumed typical laser weapon design are used in the determination of constant transmittance curves

and maximum lock-on ranges for different atmospheric conditions. The parameters of an actual system can be easily included to determine the maximum lock-on range for that particular system. A sensitivity study of the effects of varying these parameters is included.

Three atmospheric related factors will be ignored in this report. The first is beam spreading due to turbulence. Several references indicate that this factor will have negligible effects on maximum lock-on range (Ref 4, 25, 30). The second factor which is ignored is the change of the refractive index of air with a change in altitude. This becomes significant only for long slant paths when the angle between the laser receiver and the surface is less than 10 degrees (Ref 26:41). The effects of clouds and fog also will be ignored. They have such a large attenuation effect that if they occurred between the target and the weapon they would effectively prevent any laser weapon lock-on (Ref 7:129; 34).

Assumptions

When modeling something as complex as atmospheric effects, certain assumptions must be made. These include the following: The laser radiation is assumed to be monochromatic and affected only by absorption and single scattering from the aerosol particles when the atmosphere is precipitation free. The atmosphere is assumed to be uniform at all horizontal ranges of interest from the target. Also, the aerosol particle size distribution is assumed to remain constant for all altitudes. An additional assumption will be that the target intercepts the entire laser beam coming from the designator. Numerous other assumptions will be discussed in later sections.

Issues

It is very difficult to experimentally obtain an accurate and complete aerosol particle size distribution due to the inherent properties of the aerosol particles, and the present experimental equipment and methods used for particle collection. Also, the atmosphere is a highly complex mixture of molecules and aerosols with the aerosol content of the atmosphere being affected by many different aerosol sources and removal mechanisms (Ref 21). Additionally, the atmosphere is in a continuous state of flux. It is, therefore, not surprising that there have been several different models developed in attempting to describe the atmosphere. The investigator must determine how well the atmospheric model used represents the geographical area, season, time of day, past history, and aerosol sources of the air mass of interest.

If attenuation of the laser beam is to be related to variable weather conditions, the additional consideration of meteorological range determination is introduced. This is a measurement which depends, to a large degree, on the subjective judgement of the weather observer when done visually. In fact, a net error of as much as $\pm 35\%$ has been noted when measurements were taken in daylight by a prime duty observer. The error can be even higher for night observations and for those taken by a secondary duty observer. The net error is less when taken with instruments such as the forward scatter visibility meter, but it can still be as much as $\pm 23\%$ (Ref 29:34).

Rainfall is another consideration. The size of the raindrops as well as the rainfall rate has an effect on attenuation. Different formulas, many of them being empirically derived, have been developed to

describe the attenuation effects of rain. Consideration must be given as to which of these will be most representative of the rainfall of interest.

Standards

The method of investigating atmospheric attenuation in this study was computer analysis. Mathematical models were developed using the different vertical profiles, aerosol particle size distributions, meteorological ranges, and rainfall rates to determine constant transmittance curves and maximum lock-on ranges. Computer programs were then developed to use these mathematical models. Sample calculations were done for each model using an electronic calculator and compared with the computer solutions to verify their accuracy.

The ultimate method of determining the accuracy of the results of this study would be to simultaneously and accurately measure all variables of the mathematical models and see if the theoretical results agree. However, this is not completely possible at the present time. In the absence of this, the results of this study give a basis for predicting laser attenuation and maximum lock-on ranges of a specific weapon under varying weather conditions. Additionally, it gives a good method of showing the relative effects of different surface meteorological ranges, aerosol particle size distributions, and vertical attenuation profiles on transmittance and maximum lock-on ranges.

Overview

The factors affecting the attenuation of laser radiation in the atmosphere are discussed in Chapter II. The characteristics of aerosols as they relate to atmospheric attenuation are then discussed in

Chapter III. Also in this chapter is a description of the McClatchey and Homogeneous Mixing Layer (HML) atmospheric models which are used in this study. Chapter IV contains the mathematical development of the two models and the equations which are used for constant transmittance curves and lock-on range calculations. Chapter V contains the results of transmittance and lock-on range calculations and an analysis of these results. Appendices A through B show additional results of these calculations. Also included in Chapter V are two approximations which can be used for easy computations of surface lock-on ranges. Conclusions and recommendations are contained in Chapter VI. Appendix F gives a brief development of the basic lock-on range equation and lists the laser parameters which are included in this equation. Appendix G presents a brief guide to the use of the Homogeneous Mixing Layer model for making lock-on range calculations.

II. Atmospheric Attenuation of Laser Radiation

As laser radiation propagates through the atmosphere some photons are scattered out of the beam and other photons are absorbed. These scatterers and absorbers are the atmospheric gases, molecules, aerosols, and water droplets. Assuming that there is some constant, σ_t, by which these atmospheric absorbers and scatterers may be described for given atmospheric conditions, then the intensity of radiation at any point in space is given by the Beer-Lambert law of extinction which is

$$I = I_0 \exp(-\sigma_t x) \qquad (1)$$

where I is the intensity at any given point,

I_0 is the initial intensity,

σ_t is the total extinction coefficient,

and x is the distance traveled by the radiation.

The total extinction coefficient includes all attenuation coefficients. These seperate coefficients are in general additive. On a clear day for example

$$\sigma_t = \sigma_a + \sigma_m \qquad (2)$$

where σ_a is the aerosol attenuation coefficient,

and σ_m is the molecular attenuation coefficient.

These coefficients are in turn the sum of absorbing and scattering coefficients, for example

$$\sigma_a = \alpha_a + \beta_a \qquad (3)$$

where α_a is the aerosol scattering coefficient,

and β_a is the aerosol absorbing coefficient.

Transmittance

The Beer-Lambert law states that if the matter is in the same physical state, the extinction is dependent on the amount of matter through which the radiation travels. If the extinction coefficient varies along the path of the radiation, which is the case in the atmosphere, then the radiation transmittance, or the ratio of radiation intensity passed to the original intensity, I/I_0, can be described as

$$\tau = \exp[-\int_0^L \sigma_t(1)d1] \qquad (4)$$

where τ is the transmittance,

$\sigma_t(1)$ is the total atmospheric extinction coefficient per unit length,

d1 is the incremental path length,

and L is the total path length.

Lock-on Range

It has been generally assumed that Beer-Lambert's law based on single scattering theory is valid for an optical thickness of less than 0.03, and for values of optical thicknesses greater than unity, secondary and multiple scattering effects become important. (Optical thickness as used here is defined as the product of the extinction coefficient and path length). However, this is for propagation of diffuse radiation (Ref 35). For a narrow beam of collimated radiation (or laser beam propagation) it has been found that single scattering theory can account for observed attenuation for values of optical

8

thicknesses of up to 25 (Ref 36:724).

When one considers the laser lock-on problem, one is considering a two way path for the laser radiation; designator to target, and target to receiver. From designator to target the radiation is a collimated beam and Beer-Lambert's law will hold strictly for this. However, because of the nature of most military targets, they give diffuse reflection of the laser radiation. Therefore, Beer-Lambert's law will not hold strictly in this case for optical thicknesses greater than unity. However, because of the pulsed nature of the laser signal, it can be assumed that only photons reaching the receiver which have not scattered can be discriminated. Other photons will have experienced multiple scattering and will show up as noise. Therefore, single scattering theory should still hold.

The lock-on range equation can now be given as

$$R_r^2 \exp\left[\int_0^{R_r} \sigma_t(l)\,dl\right] = K \exp\left[-\int_0^{R_d} \sigma_t(l)\,dl\right] \tag{5}$$

where R_r is the range from receiver to target (lock-on range),

   R_d is the range from designator to target,

   K is a constant dependent on laser design parameters and target characteristics,

and σ_t is the atmospheric attenuation coefficient per unit length (Ref 14:13-14). A brief development of this equation including an explicit expression for K is given in Appendix F, page 102. This is a transcendental equation that is dependent on the specific atmospheric extinction coefficient and is easily solved with the aid of a computer.

Attenuation Mechanisms

The mechanisms of molecular scattering and absorption, aerosol scattering and absorption, and attenuation by precipitation for various laser wavelengths are described by the rigorous theory cf Mie and are extensively covered in current literature. Therefore, they will not be extensively discussed in this report. This section will describe briefly the attenuation effects of molecules, aerosols, humidity, and precipitation on 1.06 micron laser radiation.

Molecules. Molecular attenuation, which is highly dependent on specific wavelength, has little effect on 1.06 micron laser radiation in comparison to other mechanisms (Ref 7, 16, 26, 31, 37). The relative effect on attenuation that molecules do have is dependent on altitude. This relative importance can be seen by looking at attenuation values from Table I on the following page. Using clear air values for which the relative effect would be the greatest and Midlatitude Summer gives a molecular attenuation of less than one percent of the total at the surface. It then increases up to a maximum of 18% at 7 km altitude and decreases to 9% at 15 km.

Molecular attenuation can be ignored for many calculations. As an example, Fig. 1, page 12, shows a comparison of maximum lock-on range curves computed with and without molecular attenuation using McClatchey's aerosol model. At an altitude of 8 km there is less than 2% difference between the lock-on ranges. The difference is even less at lower altitudes and only slightly more at higher altitudes. It is concluded that molecular attenuation can safely be ignored for lock-on range and transmittance calculations, not only for the McClatchey model but for other models as well. It should be noted that if one were concerned with

Table I

Values of Attenuation Coefficient/km as a Function of Altitude for λ = 1.06 microns, McClatchey Model
k_m = molecular absorption, σ_m = molecular scattering, k_a = aerosol absorption, σ_a = aerosol scattering (Ref 26:21)

λ = 1.06 μm

Alt (km)	TROPICAL k_m (km⁻¹)	TROPICAL σ_m (km⁻¹)	MIDLATITUDE SUMMER k_m (km⁻¹)	MIDLATITUDE SUMMER σ_m (km⁻¹)	MIDLATITUDE WINTER k_m (km⁻¹)	MIDLATITUDE WINTER σ_m (km⁻¹)	SUBARCTIC SUMMER k_m (km⁻¹)	SUBARCTIC SUMMER σ_m (km⁻¹)	SUBARCTIC WINTER k_m (km⁻¹)	SUBARCTIC WINTER σ_m (km⁻¹)	AEROSOL CLEAN k_a (km⁻¹)	AEROSOL CLEAN σ_a (km⁻¹)	AEROSOL HAZY k_a (km⁻¹)	AEROSOL HAZY σ_a (km⁻¹)
0	<E-06	8.04E-04	<E-06	8.20E-04	<E-06	8.01E-04	<E-06	8.38E-04	<E-06	8.39E-04	1.98E-02	6.79E-02	9.63E-02	3.31E-01
0-1		7.81E-04		7.81E-04		7.43E-04		7.88E-04		8.77E-04	1.31E-02	4.50E-02	5.82E-02	2.00E-01
1-2		6.99E-04		7.06E-04		7.52E-04		7.21E-04		7.70E-04	5.71E-03	1.86E-02	2.13E-02	7.31E-02
2-3		6.33E-04		6.38E-04		6.70E-04		6.50E-04		6.82E-04	2.43E-03	8.36E-03	7.78E-03	2.67E-02
3-4		5.72E-04		5.77E-04		5.99E-04		5.84E-04		6.08E-04	1.15E-03	3.94E-03	2.06E-03	8.76E-03
4-5		5.18E-04		5.21E-04		5.37E-04		5.24E-04		5.40E-04	7.23E-04	2.49E-03	1.04E-03	3.56E-03
5-6		4.69E-04		4.59E-04		4.80E-04		4.71E-04		4.82E-04	7.23E-04	1.81E-03	5.2E-03	1.81E-03
6-7		4.22E-04		4.21E-04		4.27E-04		4.23E-04		4.29E-04	4.27E-04	1.47E-03	4.72E-04	1.47E-03
7-8		3.80E-04		3.78E-04		3.80E-04		3.78E-04		3.81E-04	4.18E-04	1.44E-03	4.19E-04	1.44E-03
8-9		3.41E-04		3.39E-04		3.36E-04		3.38E-04		3.34E-04	4.15E-04	1.43E-03	4.15E-04	1.43E-03
9-10		3.04E-04		3.02E-04		2.97E-04		3.01E-04		2.88E-04	4.01E-04	1.38E-03	4.01E-04	1.38E-03
10-11		2.72E-04		2.69E-04		2.50E-04		2.64E-04		2.46E-04	3.84E-04	1.32E-03	3.84E-04	1.32E-03
11-12		2.41E-04		2.39E-04		2.22E-04		2.26E-04		2.10E-04	3.81E-04	1.31E-03	3.81E-04	1.31E-03
12-13		2.13E-04		2.11E-04		1.90E-04		1.95E-04		1.80E-04	3.75E-04	1.29E-03	3.75E-04	1.29E-03
13-14		1.88E-04		1.93E-04		1.63E-04		1.67E-04		1.56E-04	3.56E-04	1.22E-03	3.56E-04	1.22E-03
14-15		1.66E-04		1.56E-04		1.40E-04		1.44E-04		1.31E-05	3.42E-04	1.18E-03	3.42E-04	1.18E-03
15-16		1.44E-04		1.33E-04		1.20E-04		1.23E-04		1.12E-04	3.23E-04	1.11E-03	3.23E-04	1.01E-03
16-17		1.24E-04		1.14E-04		1.06E-04		1.06E-04		9.63E-05	3.13E-04	1.08E-03	3.13E-04	1.08E-03
17-18		1.05E-04		9.72E-05		8.80E-05		9.14E-05		8.25E-05	3.06E-04	1.05E-03	3.06E-04	1.05E-03
18-19		8.63E-05		8.29E-05		7.53E-05		7.86E-05		7.06E-05	2.72E-04	8.51E-04	2.77E-04	9.51E-04
19-20		7.16E-05		7.01E-05		6.45E-05		6.75E-05		6.05E-05	2.18E-04	7.46E-04	2.18E-04	7.48E-04
20-21		5.96E-05		6.03E-05		5.51E-05		5.80E-05		5.17E-05	1.59E-04	5.45E-04	1.59E-04	9.65E-04
21-22		4.88E-05		5.14E-05		4.70E-05		4.99E-05		4.42E-05	1.17E-04	4.03E-04	1.13E-04	4.03E-04
22-23		4.18E-05		4.38E-05		4.01E-05		4.28E-05		3.78E-05	8.99E-05	3.06E-04	8.80E-04	3.0E-04
23-24		3.55E-05		3.74E-05		3.43E-05		3.68E-05		3.23E-05	8.03E-05	2.28E-04	6.93E-05	2.38E-04
24-25		3.02E-05		3.18E-05		2.93E-05		3.15E-05		2.76E-05	5.66E-05	1.84E-04	5.66E-05	1.94E-04
25-30		2.01E-05		2.15E-05		1.95E-05		2.13E-05		1.81E-05	2.85E-05	8.79E-05	2.85E-05	9.79E-05
30-35		8.20E-06		8.89E-06		8.79E-06		9.00E-06		8.14E-06	8.02E-06	8.02E-06	8.02E-06	2.76E-05
35-40		4.37E-06		4.71E-06		3.05E-06		4.73E-06		3.66E-06	2.76E-06	2.76E-06	2.76E-06	7.26E-06
40-45		2.15E-06		2.31E-06		1.83E-06		2.33E-06		1.88E-06	2.11E-06	7.26E-06	2.11E-06	1.91E-06
45-50		1.04E-06		1.19E-06		1.19E-06		1.21E-06		<E-06	1.91E-06	1.91E-06		<E-06
50-70		<E-06		<E-06		<E-06		<E-06			<E-06	<E-06	<E-06	
70-100														

Fig. 1 Aerosol + Molecular Attenuation vs Aerosol Attenuation for McClatchey Model. Curves are Maximum Lock-on Range for 1.06 microns with Designator and Receiver Collocated.

transmittances at constant altitudes greater than 4 km, molecular
attenuation should not be ignored; for example, at 7 km an 18% error
would be introduced.

Aerosols. In the absence of precipitation, aerosol attenuation
has the largest effect on laser propagation. This is caused by both
scattering and absorption. Aerosols are defined as dispersed solid or
liquid particles in a gaseous solution, in this case air. The aerosol
particles vary in size from a cluster of a few molecules to particles
of about 20 microns in radius. Particles larger than this remain air-
borne for only a short time and only occur close to their sources
(Ref 21:111). Aerosol attenuation coefficients depend considerably on
the dimensions, chemical composition, and aerosol particle concentra-
tion. These are subject to great variability in time and space. Thus,
a quantitative estimate of the attenuation due to aerosols requires
reliable data about all fundamental characteristics of atmospheric
aerosols (Ref 37:224). An excellent summary of aerosols, with refer-
ences, is given by Coolidge (Ref 7).

Clouds and Fog. The attenuation effects of clouds and fog on 1.06
micron laser radiation is very significant. For example a path length
of 0.1 km through a cloud with a Dermendjian CL particle size distri-
bution would reduce the laser radiation to about 18% of the original
(Ref 7:129). Clouds and fog of almost any thickness, therefore, will
prevent a laser lock-on to the target. In order to include the effects
of clouds on laser lock-on one should do a statistical study on the
probabilities of clouds or fog being present, that is, the probabili-
ties of a cloud-free-line-of-sight. A study of this has been done by
Lund (Ref 24).

Humidity. It has been suggested that humidity would have a large effect on the aerosol particle size distribution and thus the aerosol attenuation. However, Bullrich, et al, (Ref 5) found that the growth rate of all particle sizes was approximately the same up to a relative humidity of 95%. Zuev, et al, (Ref 38) and Andreyev, et al, (Ref 1) also found no definite relation between relative humidity and the aerosol attenuation coefficient for the infrared region of the spectrum. It can be concluded that up to 90-95% relative humidity, there is no humidity effects on aerosol attenuation of 1.06 micron laser radiation.

Rain. Attenuation due to rain (for drops of radii greater than one half of the wavelength) is es_ ntially independent of the specific wavelength in the visible to far infrared of the spectrum (Ref 15, 20, 32). This attenuation is due almost entirely to scattering. The theory for determining rain attenuation, like that for other mechanisms, is based on Mie theory. However, discrepancies exist between theory and experimental results. This is mainly because of difficulties involved in relating rain drop diameters and distribution of drop sizes to the rainfall rate. The techniques for measuring rainfall rate and the inconsistencies of the rate along the transmission path have also presented large problems to the experimentalist.

There have been several relationships developed, both experimentally and theoretically, to describe rain attenuation. Some of these are shown in Table II on the following page where the attenuation is related to rainfall rate.

Table III shows additional relationships for the rainfall coefficients and some interesting relationships for meteorological range if rainfall is the only limiting factor and a contrast of 0.055 is used.

14

Table II

Rainfall Attenuation Coefficients (Ref 32:801)

These relations are given for β, in km^{-1}, R in mm hr^{-1}

Author	Rainfall type	β - R
Atlas (1953)	Mean	$\beta_r = 0.31R^{0.67}$
Best (1950)	Mean	$\beta_r = 0.25R^{0.61}$
Chu and Hogg (1968)	Thunderstorm	$\beta_r = 0.18R^{0.67}$
Miller (1973)	Thunderstorm	$\beta_r = 0.12R^{0.78}$
Poliakova (1960)	Mean	$\beta_r = 0.21R^{0.74}$
Simms and Mueller (1972)	Thunderstorm	$\beta_r = 0.13R^{0.80}$
Wessels (1972)	Mean	$\beta_r = 0.25R^{0.79}$

Table III

Attenuation Coefficients(km^{-1}) and Meteorological Range(km) as a Function of Rainfall Rate(mm/hr) (Ref 2:488)

Author	Type	σ_r	MR
Atlas	Bergeron	$\sigma_r = 0.25R^{0.63}$	$MR = 11.6R^{-0.63}$
Blanchard	Warm Orographic	$\sigma_r = 1.20R^{0.33}$	$MR = 2.4R^{-0.33}$
Marshall and Palmer	Mean	$\sigma_r = 0.31R^{0.67}$	$MR = 9.3R^{-0.67}$

It is shown here that the type of rainfall also has some effect on the relationship of rainfall rate and attenuation or meteorological range.

The coefficient in each of these equations is a function of the nature of the drop size distribution, increasing roughly as the square root of the number concentration per unit volume and decreasing as the normalized spectrum broadens. The exponent is an insensitive function only of the variation of velocity with drop diameter (Ref 2:487).

The relationship of attenuation due to rainfall rate chosen for this study was that recently derived by Shipley at the University of Wisconsin, Madison, Wisconsin (Ref 32). It was developed using monostatic lidar as a means of determining rainfall attenuation.

Correlation of lidar-derived rainfall attenuation and gage measured rainfall gave

$$\sigma_r = 0.16R^{0.74} \text{ km}^{-1} \qquad (6)$$

This relationship was chosen at least partially arbitrarily but also because (1) of the method of measurement, (2) it compares well with the work of other authors, and (3) it was derived in a midlatitude location with both stratus and thunderstorm rainfall being used in its development.

Snow. Snow presents a difficult problem. The assumption which is made for solutions using Mie theory, that the particle is spherical, is not valid for snow, However, if it is assumed that snow particles will scatter the same as they would if they were melted drops as Gilbertson does (Ref 20:90), an approximation for the attenuation can be made. Using values from references 20 and 3 this relationship is

$$\sigma_s = 0.56R^{0.57} \text{ km}^{-1} \qquad (7)$$

This assumption could introduce serious error. More experimental data is necessary in order to verify the attenuation due to snow.

III. Aerosol Characteristics

Since atmospheric aerosols play such a dominant role in the attenuation of 1.06 micron laser radiation it is important to quantify their characteristics.

Meteorological Range

An important characteristic of aerosol particles is that they directly affect visibility or meteorological range in the form of haze. Therefore, their attenuation effects can be determined from observed meteorological range using a relationship first expressed by Koschmieder (Ref 22) and later expanded by Middleton (Ref 27). Koschmieder's law is expressed by

$$MR = \frac{3.912}{\sigma_a} \tag{8}$$

where MR is meteorological range (km) and σ_a is the aerosol attenuation coefficient (km^{-1}). Meteorological range in white light is defined as the maximum distance at which an observer can barely detect a large dark object against a white background. It is the distance at which the contrast of the object to the background is reduced to 0.02 of its original value at the eye of the observer.

The above relationship is assumed to be valid at the discrete wavelength of 0.55 microns which is the approximate center of eye sensitivity for ordinary color vision in daylight. To determine the attenuation of other wavelengths on the basis of meteorological range it is only necessary to find the proper ratio of attenuation at the desired wavelength to that of 0.55 microns. This can be accomplished

by using Mie scattering calculational models.

Aerosol Particle Size Distribution

A very important consideration in estimating haze attenuation for various wavelengths is the size distribution of the aerosol particles (Ref 8). Aerosol particles scatter photons most effectively if their radii are about equal to the wavelength of radiation (Ref 28). Using Mie theory, it is shown that the contribution to scattering of different particle sizes and concentrations depends very much on which wavelength is being used with particles less than 0.04 microns having little effect (Ref 23:105).

To illustrate the importance of the particle size distribution, Dermendjian (Ref 8) gives an example where the particles of 0.35 to 4.48 microns were 5% of the total concentration but because of their large geometric cross-section produced 80% of the scattering. It cannot be emphasized too strongly that if one is to calculate attenuation due to aerosols at a specific wavelength it is extremely important to know the particle size distribution.

Particle size distributions and densities are controlled by the particle production and removal mechanisms. Therefore, these properties depend on the geographic area and past history of the air mass being considered.

There have been several analytical functions proposed to describe aerosol distributions. Two of these which have been used extensively are the Dermendjian Continental Haze and the Dermendjian Maritime Haze distributions and variations of these original models. The names are descriptive of the sources of these aerosols. The continental haze is

of the form of a power law first described by Junge (Ref 21)

$$n(r) = Ar^{-\kappa} \tag{9}$$

The maritime haze is a modified gamma distribution described by Dermendjian (Ref 10) and is of the form

$$n(r) = ar^{\alpha}\exp(-br^{\gamma}) \qquad 0 \le r \le \infty \tag{10}$$

In these equations n(r) is the volume concentration at the radius r and A, κ, a, α, b, and γ are positive constants. These two distributions are shown graphically in Fig. 2.
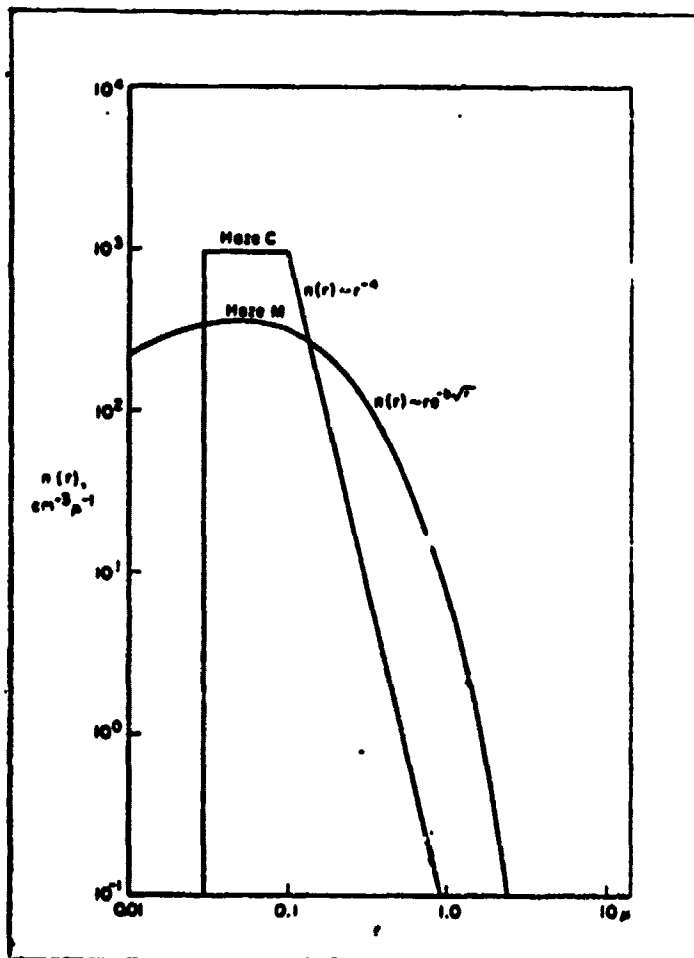
Fig. 2 Continental and Maritime Size Distribution Functions. (Ref 9:188)

The two general differences in the maritime and continental

hazes are as follows: (1) the number of particles in the maritime is

less than in the continental and (2) a greater portion of the maritime

particles are in the large particle range. An additional size distri-

bution model called the Haze L was also proposed by Dermendjian as a

replacement for the power law description of the continental type

aerosol. This is also a modified gamma distribution.

This report discusses the effect of these three distributions on

1.06 micron laser radiation attenuation. Even though these distribu-

tions are useful quantitatively, it is important to realize that these

are characteristic distributions and that in specific instances, con-

ditions may deviate considerably from the mean distribution.

Coolidge did an extensive study comparing aerosol attenuation

coefficients per particle per cm^3 per km path length for these and

other particle size distributions using Mie theory calculations (Ref 7).

Included in this study were the calculations of attenuation ratios of

1.0636 micron to 0.55 micron wavelengths. In doing this he used a

complex index of refraction of 1.53 - 0.031i for 0.55 microns and

1.51 - 0.046i for 1.0636 microns corresponding to average data re-

ported by Hanel and Fischer for Germany (Ref 7.66). The normalized

size distributions Coolidge used are shown in Table IV on the following

page. Partial results of this study are shown in Fig. 3, page 22.

These show that 100% maritime gives higher per particle attenuation,

with aerosol attenuations at 1.0636 microns approximately equal to

that of 0.55 microns. As the percentage of maritime is reduced and

continental increased, the attenuation at 1.0636 becomes less than that

at 0.55 microns, although the decrease is not significant until the

percentage maritime is less than 10%. This suggests that in coastal regions and ocean areas, 1.0636 micron attenuation may not be significantly less than that in the visible spectrum while in continental areas it may be significantly less.

Table IV

Aerosol Size Distributions
Radius, r, in microns (Ref 7:78)

Model	Distribution	
Deirmendjian Maritime	$5.333 \times 10^6 \times r \times e^{(-8.9443 \times \sqrt{r})}$	
Deirmendjian Continental $.02\mu \to 20\mu$	0 9.677419×10^4 $9.677419 \times r^{-4}$	$r < .02\mu$ $.02\mu \leq r \leq .1\mu$ $.1\mu < r \leq 20\mu$
Maritime + Continental	$5.333 \times 10^6 \times r \times e^{(-8.9443 \times \sqrt{r})}$ $5.333 \times 10^6 \times r \times e^{-(8.9443 \times \sqrt{r})} + 9.677419 \times 10^4$ $5.333 \times 10^6 \times r \times e^{-(8.9443 \times \sqrt{r})} + 9.677419 \times r^{-4}$	$r < .02\mu$ $.02\mu \leq r \leq .1\mu$ $.1\mu < r < 20\mu$
Deirmendjian Haze L	$4.9757 \times 10^8 \times r^{+2} \times e^{(-15.1186 \sqrt{r})}$	
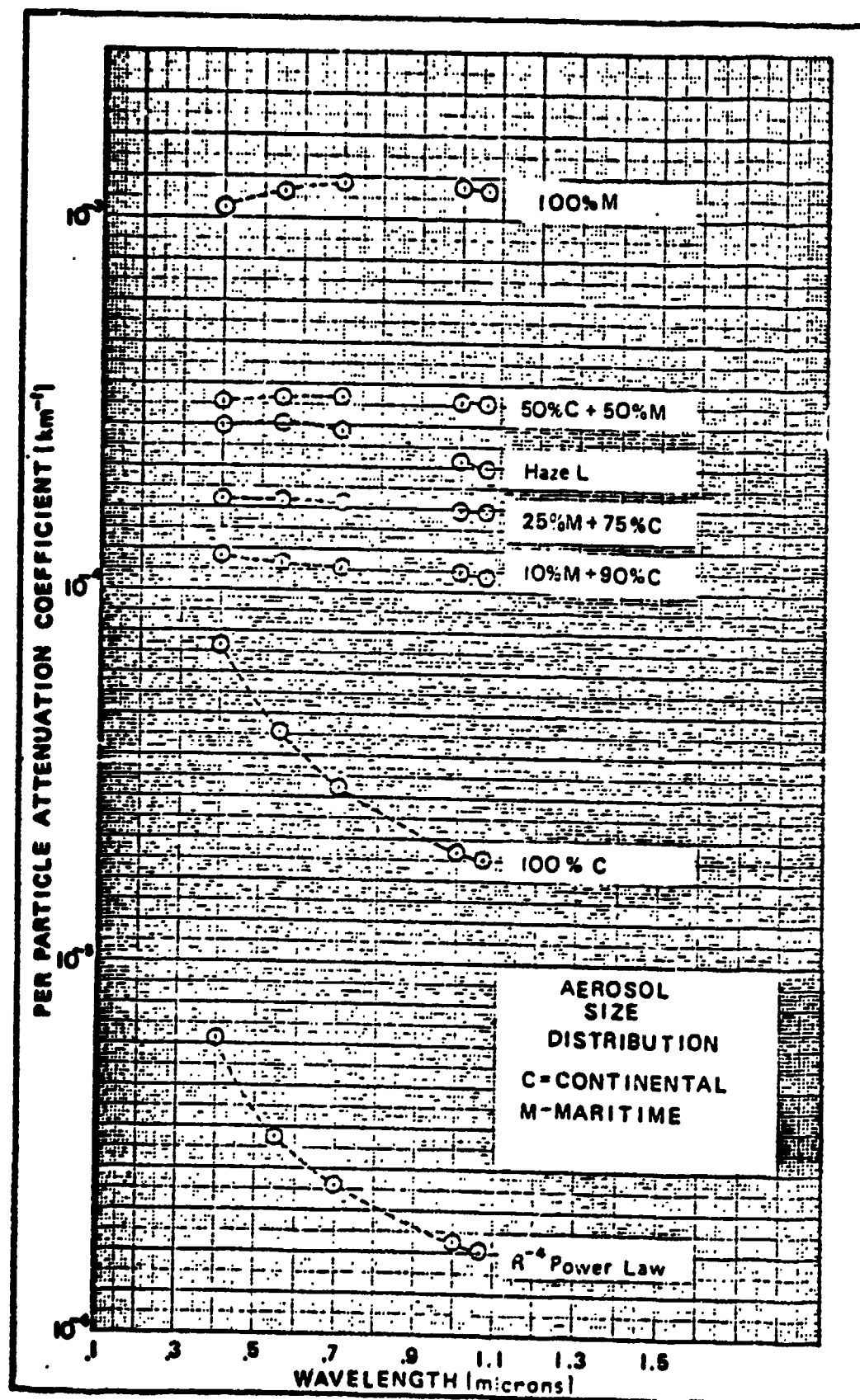
Fig. 3 Aerosol Attenuation Coefficient Curves for Different
Aerosol Size Distributions (Ref 7:80).

Table V shows the ratios of 1.0636 micron attenuation coefficients to that of 0.55 microns for several aerosol distributions calculated by Coolidge. It is these figures which were used in this study for making transmittance and lock-on range calculations for various aerosol particle size distributions.

Table V

Ratios of 1.0636 micron Attenuation Coefficients to 0.55 micron Attenuation Coefficients for Several Aerosol Distributions (Ref 7:58)

Aerosol Distribution	$\dfrac{\sigma_a(1.0636\mu)}{\sigma_a(0.55\mu)} = \alpha$
Haze L	.796
100% Continental ($.03\mu - 20\mu$)	.539
Maritime ($.003\mu - 20\mu$)	1.004
25% Maritime + 75% Continental	.932
50% Maritime + 50% Continental	.977

Vertical Attenuation Profiles

There are several models used to describe the change in aerosol attenuation with altitude. This thesis discusses two of these and compares the results of using them to compute slant ranges for constant

transmittance curves and for lock-on ranges. These two models are (1) that used by McClatchey (Ref 26) and (2) the Homogeneous Mixing Layer model as developed by Coolidge (Ref 7).

McClatchey Model. This model, which is based on work done earlier by Elterman (Ref 17, 18, 19), has been widely used for attenuation determinations. In this model McClatchey combines five model atmospheres for temperature, pressure, and absorbing gas concentrations with two aerosol models describing a "clear" and "hazy" atmosphere corresponding to meteorological ranges of approximately 23.5 and 5 km at ground level respectively. The aerosol size distribution is the same for both aerosol models at all altitudes and is similar to the Demendjian Continental Haze with a large particle cutoff of 10 microns.

The aerosol attenuation coefficients are computed at 1 km intervals up to 25 km and at 5 km intervals from there to 50 km altitude. Those up to 5 km, which comprise the mixing layer, follow one of two exponentially decreasing functions corresponding to the clear and hazy conditions mentioned above. Those above 5 km closely follow exponential functions which are not affected by surface conditions. Table I, page 11, shows these coefficients computed for a wavelength of 1.06 microns.

This model has several serious drawbacks: (1) in its present form surface meteorological range cannot be used as a continuous variable in determining attenuation coefficients, (2) it is based on only one particle size distribution, (3) the concept of an exponentially decreasing mixing layer of height 5 km does not seem to be borne out by recent measurements, and (4) the coefficients given are a discontinuous function which makes them difficult and time consuming to

24

use, even with a computer.

This report will, in a later section, propose an approximation which will, (1) describe the aerosol attenuation coefficient as a continuous function for ease in computations, (2) make it possible to use surface meteorological range as a continuous variable, and (3) make the model useable for various combinations of maritime and continental hazes.

Homogeneous Mixing Layer Model. This model consists of a homogeneous or slowly exponentially decreasing mixing layer of variable height, generally from 0.15 to 3 km, with a general mean of about 1.5 km, depending on surface meteorological conditions. Above the mixing layer or haze layer the aerosol attenuation coefficient shows either a sharp decrease or a more gradual transition through a 200 m layer to a clear air attenuation with a meteorological range of 40 km or better. The attenuation coefficient then shows a gradual exponential decrease which is frequently less than the density lapse rate of 7-8 km scale height. The scale height as used here is the height at which the attenuation coefficient has decreased by a factor of e^{-1}.

This model is based to a large extent on measurements taken by Duntley, et al, (Ref 11, 12, 13). The concept of a homogeneous mixing layer is also borne out by Zuev (Ref 38) and Tenneke (Ref 33) among others. The use of this model with different aerosol particle size distributions comprises the bulk of the study going into this report.

IV. Development of the Atmospheric Models

This chapter will describe the development of the mathematical formulas used in the McClatchey and Homogeneous Mixing Layer models. Two separate quantities were computed for each model. These were slant range calculations for constant transmittance curves and laser lock-on ranges for a given set of laser design parameters.

Transmittance (General)

Transmittance is described by Equation (4) which is repeated here

$$\tau = \exp\left[-\int_0^L \sigma_t(1)d1\right] \tag{4}$$

If one desired to find L for a given transmittance, the form of the equation could be changed to

$$\ln\frac{1}{\tau} = \int_0^L \sigma_t(1)d1 \tag{11}$$

The integration could then be performed and the equation solved for L. This will be done in following sections for specific conditions.

Lock-on Range (General)

The basic formula used for computing lock-on range is Equation (5) which is repeated here

$$R_r{}^2 \exp\left[\int_0^{R_r} \sigma_t(1)d1\right] = K\exp\left[-\int_0^{R_d} \sigma_t(1)d1\right] \tag{5}$$

There are two cases for which this equation will apply: (1) designator and receiver collocated and (2) designator and receiver separated.

For the first case, $R_r = R_d = R$. Transposing and taking the

26

square root of each side of Equation (5) then gives

$$R = \sqrt{K} \exp\left[-\int_0^R \sigma_t(1)d1\right] \qquad (12)$$

Taking the natural logarithm of both sides yields

$$\ln\frac{\sqrt{K}}{R} = \int_0^R \sigma_t(1)d1 \qquad (13)$$

The integral on the right side can be solved and the resulting transcendental equation can then be solved for R.

If the designator and receiver are separated, Equation (5) becomes

$$R_r^2 = K \exp\left[-\int_0^{R_r} \sigma_t(1)d1 -\int_0^{R_d} \sigma_t(1)d1\right] \qquad (14)$$

Taking the square root and the natural logarithm of both sides yields

$$2\ln\frac{\sqrt{K}}{R_r} = \int_0^{R_r} \sigma_t(1)d1 + \int_0^{R_d} \sigma_t(1)d1 \qquad (15)$$

Again, the integrations must be performed and the resulting transcendental equation solved for R_r. In this study these equations were solved with the aid of a computer by using the Newton-Raphson method.

Homogeneous Mixing Layer Model

In this model, for reasons explained earlier, molecular attenuation will be disregarded. Therefore, in the absence of precipitation the attenuation coefficient will be determined by the aerosol content of the air. Using Koschmieder's law and the ratio $\sigma_{a(1.0636)}/\sigma_{a(0.55)}$, or α, from Table V, page 23, for the particle size distribution of interest

$$\sigma_{a(1.0636)} = \alpha\sigma_{a(0.55)} \qquad (16)$$

or $\qquad \sigma_a(1.0636) = \alpha \dfrac{3.912}{MR}$ $\qquad\qquad$ (17)

This can also be described as

$$\sigma_a(1.0636) = \dfrac{\beta}{MR} \qquad\qquad (18)$$

where $\qquad\qquad\qquad\qquad \beta = \alpha(3.912)$ $\qquad\qquad$ (19)

Eq (18) is the attenuation coefficient in the mixing layer. For the exponentially decreasing coefficient above the mixing layer

$$\sigma_a(1.0636) = \dfrac{\beta}{MR_{hi}} \exp(-\dfrac{h}{H_p}) \qquad\qquad (20)$$

where σ_a is the attenuation coefficient (km^{-1}),

$\qquad MR_{hi}$ is the meteorological range above the mixing layer (km),

$\qquad$ h is the altitude (km),

and $\quad H_p$ is the scale height (km).

The attenuation coefficient for haze only for the HML model is now

$$\sigma_a(1.0636) = \begin{cases} \dfrac{\beta}{MR} & 0 \le h \le H \\[3mm] \dfrac{\beta}{MR_{hi}} \exp(-\dfrac{h}{H_p}) & h > H \end{cases} \qquad (21)$$

where H = mixing layer height. This value can now be substituted in Eqs (11), (13), (15). Fig. 4 on the following page shows the two regions of this model and transmittance paths in these regions.

R = slant range
L_1 = path in mixing layer
L_2 = path above mixing layer
h = altitude
H = mixing layer height
θ = elevation angle
z = variable for integration
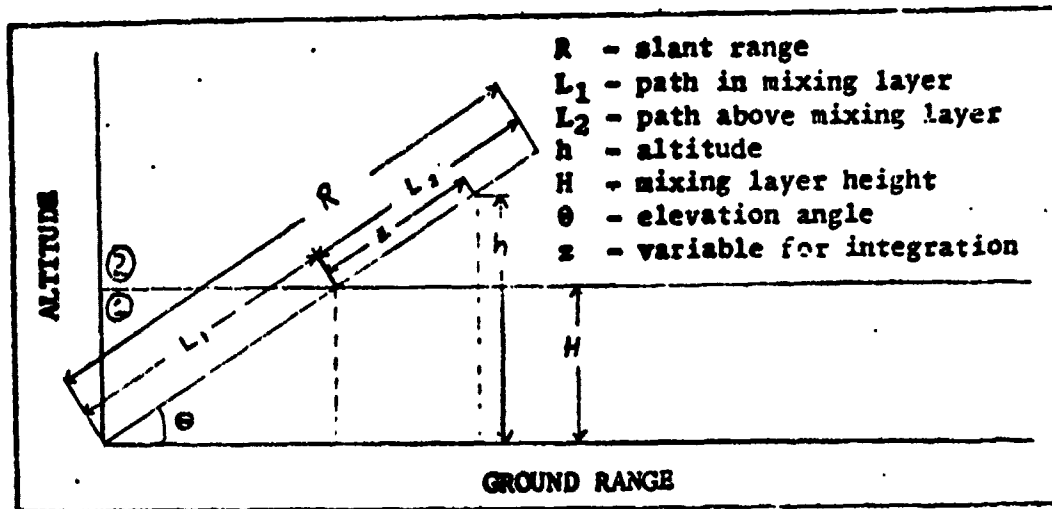
Fig. 4 Geometry of Slant Range Propagation

Constant Transmittance (Haze only). Using Eq (11) within the haze layer (region 1 of Fig. 4) yields

$$\ln \frac{1}{\tau} = \frac{\beta}{MR} L_1 \tag{22}$$

or

$$R = L_1 = \ln \frac{1}{\tau} \frac{MR}{\beta} \tag{23}$$

where R = the total slant range.

Above the mixing layer (region 2 of Fig. 4)

$$\tau = \exp - \left[\frac{\beta}{MR} L_1 + \int_{L_1}^{L_1 + L_2} \frac{\beta}{MR_{hi}} \exp(-\frac{h}{H_p}) \, dz \right] \tag{24}$$

L_1 is now a constant for any given elevation angle, θ, where

$$L_1 = \frac{H}{\sin \theta} \tag{25}$$

Also

$$h = z \sin \theta \tag{26}$$

Performing the integration and taking the natural logarithm of both sides yields

$$\ln \frac{1}{\tau} = \frac{\beta}{MR} L_1 + \frac{\beta}{MR_{hi}} \frac{H_p}{H} L_1 \exp\left(-\frac{H}{H_p}\right)\left[1 - \exp\left(-\frac{L_2 H}{H_p L_1}\right)\right] \quad (27)$$

Rearranging this formula gives

$$\exp\left(-\frac{H L_2}{H_p L_1}\right) = 1 - \frac{MR_{hi}H}{H_p} \exp\left(\frac{H}{H_p}\right)\left[\frac{\ln \frac{1}{\tau}}{\beta L_1} - \frac{1}{MR}\right] \quad (28)$$

Taking the natural log of both sides and multiplying by $H_p L_1 / H$ gives

$$L_2 = \frac{H_p}{H} L_1 \ln\left[1 - \left(\gamma - \frac{1}{MR}\right)\frac{MR_{hi}H}{H_p} \exp\left(\frac{H}{H_p}\right)\right]^{-1} \quad (29)$$

where
$$\gamma = \frac{\ln \frac{1}{\tau}}{\beta L_1} \quad (30)$$

Total slant range, R, now equals $L_1 + L_2$. Therefore,

$$R = L_1\left\{1 + \frac{H_p}{H} \ln\left[1 - \left(\gamma - \frac{1}{MR}\right)\frac{MR_{hi}H}{H_p} \exp\left(\frac{H}{H_p}\right)\right]^{-1}\right\} \quad (31)$$

Note that R approaches infinity when

$$\left(\gamma - \frac{1}{MR}\right)\frac{MR_{hi}}{H_p} H \exp\left(\frac{H}{H_p}\right) = 1 \quad (32)$$

or
$$\gamma_{max} = \frac{H_p}{MR_{hi}H} \exp\left(-\frac{H}{H_p}\right) + \frac{1}{MR} \quad (33)$$

For a given H_p and MR_{hi} this condition depends only on the mixing layer height and the surface meteorological range. This condition implies that for a given beam transmittance there is a minimum L_1 given by

$$L_{1min} = \frac{\ln \frac{1}{\tau}}{\beta Y_{max}} \tag{34}$$

and a maximum elevation angle given by

$$\Theta_{max} = \sin^{-1} \frac{H}{L_{1min}} \tag{35}$$

Two cases of slant range propagation exist. One case occurs when $H > L_{1min}$. Then Θ_{max} is 90 degrees and the constant τ curves are closed contours. For a given τ this would occur for low meteorological range conditions. The other case occurs when $H < L_{1min}$ and Θ_{max} is given by Eq (35). For a given transmittance this leads to an open constant curve which flares out and goes to infinity.

Constant Transmittance (Haze and Rain). The attenuation effects of raindrops and aerosols are additive; very little washout or changes of aerosol characteristics occur (Ref 7:133). Therefore,

$$\tau = \exp\left[-\left[\int_0^R (\sigma_a + \sigma_r)dl\right]\right] \tag{36}$$

where σ_a is attenuation due to aerosols,

and σ_r is attenuation due to rain.

In the haze layer, attenuation coefficients must be related to meteorological range for $\lambda = 0.55$ microns. One must ask how aerosols plus rain affect meteorological range observations. Using the criterion of 0.02 contrast as discussed earlier

$$\tau = 0.02 = \exp\left[-\int_0^{MR} (\sigma_a + \sigma_r) dl\right] \tag{37}$$

This leads to
$$\frac{\ln 50}{MR} = \sigma_a + \sigma_r \tag{38}$$

or
$$\sigma_a = \frac{3.912}{MR} - \sigma_r \tag{39}$$

This equation holds for $\lambda = 0.55$ microns. Putting this expression into Eq (16), page 27, and assuming that $\sigma_{a(1.0636)}$ is approximately equal to $\sigma_{a(1.06)}$, as is done throughout this report, yields the following expression for the total attenuation at $\lambda = 1.06$:

$$\sigma_t = \frac{\beta}{MR} + (1 - \alpha)\sigma_r \tag{40}$$

In the clear air above the mixing layer, visibility is limited by rain with haze having little or no effect on visibility. Also at altitude a meteorological range observation will not generally be made. Therefore, it is assumed that no correction need to be made to meteorological range for the effects of rain. Thus, Eq (20), page 28, holds above the mixing layer just as it did with no rain. To this, however, must be added σ_r. The total attenuation coefficient in the HML model then be

$$\sigma_t = \begin{cases} \dfrac{\beta}{MR} + (1 - \alpha)\sigma_r & 0 < h < H \\[3mm] \dfrac{\beta}{MR_{hi}} \exp(-\dfrac{h}{H_p}) + \sigma_r & h > H \end{cases} \tag{41}$$

Putting these values into the constant transmittance equation as before

will yield, for $h < H$

$$R = L_1 = \frac{\ln \frac{1}{\tau}}{\frac{\beta}{MR} + (1 - \alpha)\sigma_r} \qquad (42)$$

For $h > H$ the expression is

$$L_2 = \frac{H_p L_1}{H} \ln \left[\frac{A L_1}{L_1(B + A)\sigma_r L_2 - \ln \frac{1}{\tau}} \right] \qquad (43)$$

where

$$A = \frac{H_p}{MR_{hi}H} \exp(-\frac{H}{H_p}) \qquad (44)$$

and

$$B = \frac{\beta}{MR} + (1 - \alpha)\sigma_r \qquad (45)$$

This is a transcendental equation to be solved for L_2 where L_1 now equals $H/\sin\theta$. Then $R = L_1 + L_2$.

Note that L_2 cannot go to infinity as it did with haze only, as it occurs in the denominator of the logarithmic term as well as on the left hand side of the equation. So the constant transmittance curves will not flare out to infinity as they did with haze only. It may be noted here also that if one were concerned with snow attenuation, the snow attenuation coefficient could be substituted directly in the place of the rain coefficient.

Lock-on Range - Designator and Receiver Collocated (Haze only). For lock-on calculations where the designator and receiver are collocated, Eq (13), page 27 is used. In the haze layer this becomes

$$\boxed{\ln\frac{\sqrt{K}}{R} = \frac{\beta}{MR} R} \qquad (46)$$

Above the mixing layer, Eq (13) becomes

$$\ln\frac{\sqrt{K}}{R} = \int_0^{L_1} \frac{\beta}{MR}\,d1 + \int_0^{L_1+L_2} \frac{\beta}{MR_{hi}}\exp\left(-\frac{h}{H_p}\right)d1 \qquad (47)$$

or

$$\ln\frac{\sqrt{K}}{R} = \frac{\beta L_1}{MR} + \frac{\beta H_p L_1}{MR_{hi}H}\exp\left(-\frac{H}{H_p}\right)\left[1 - \exp\left(-\frac{HL_2}{H_pL_1}\right)\right] \qquad (48)$$

Then

$$\boxed{\ln\frac{\sqrt{K}}{L_1+L_2} = AL_1 + BL_1\exp(-CL_2)} \qquad (49)$$

where

$$B = \frac{\beta H_p}{MR_{hi}H}\exp\left(-\frac{H}{H_p}\right) \qquad (50)$$

$$A = \frac{\beta}{MR} + B \qquad (51)$$

and

$$C = \frac{H}{H_pL_1} \qquad (52)$$

This transcendental equation can now be solved for L_2 and added to L_1 where $L_1 = H/\sin\theta$.

Lock-on Range - Ground Based Designator (Haze only). The only situation studied in this report for designator and receiver being seperated was that of the ground based designator. The large number of possible situations with both designator and receiver airborne precluded a comprehensive look at them in the time allotted for this study.

Using Eqs (15) and (21), pages 27 and 28, the following equations were derived for the ground based designator: for $h < H$

$$\boxed{2\ln\frac{\sqrt{K}}{R_r} = \frac{\beta}{MR}(R_r + R_d)} \qquad (53)$$

34

For $h > H$

$$2 \ln \frac{\sqrt{K}}{L_1 + L_2} = A + B\left[1 - \exp(-CL_2)\right] \qquad (54)$$

where

$$A = \frac{\beta}{MR} (L_1 + R_d) \qquad (55)$$

$$B = \frac{\beta H_p L_1}{MR_{hi} H} \exp\left(-\frac{H}{H_p}\right) \qquad (56)$$

and

$$C = \frac{H}{H_p L_1} \qquad (57)$$

This equation can be solved for L_2 where, again, $L_1 = H/\sin\theta$. Then $R_r = L_1 + L_2$.

Lock-on Range - Designator and Receiver Collocated (Haze and Rain). With rain included with the haze, the attenuation coefficient used is that in Eq (41), page 32. For $h < H$

$$\ln\frac{\sqrt{K}}{R} = \left[\frac{\beta}{MR} + (1 - \alpha)\sigma_r\right]R \qquad (58)$$

For $h > H$

$$\ln\frac{\sqrt{K}}{R} = \int_0^{L_1}\left[\frac{\beta}{MR} - (1 - \alpha)\sigma_r\right]dl + \int_0^{L_1+L_2}\left[\frac{\beta}{MR_{hi}}\exp\left(-\frac{h}{H_p}\right) + \sigma_r\right]dl \qquad (59)$$

With simplification this yields

$$\ln\frac{\sqrt{K}}{L_1 + L_2} = L_1(B + A) + \sigma_r L_2 - AL_1\exp(-CL_2) \qquad (60)$$

where

$$A = \frac{\beta H_p}{MR_{hi} H} \exp\left(-\frac{H}{H_p}\right) \qquad (61)$$

$$B = \frac{\beta}{MR} + (1 - \omega)\sigma_r \tag{62}$$

and

$$C = \frac{H}{H_p L_1} \tag{63}$$

Again this is a transcendental equation which can be solved for L_2 with L_1 being a constant for any given elevation angle. Then $R = L_1 + L_2$.

McClatchey Model

The McClatchey model of the atmosphere, as described earlier, has been frequently used in attenuation calculations. As mentioned, some of its limitations include the following: (1) it is based on the continental haze particle size distribution only, (2) meteorological range is not a continuously variable parameter (values for meteorological ranges of 5 and 23.5 km are given), and (3) attenuation coefficients are given a. 1 km intervals instead of being a continuous function. This report attempts to alleviate these limitations by using several approximations.

Approximations. This model can be used to give approximate attenuation values for aerosol particle size distributions other than the continental haze with the use of the ratios $\sigma_{a(1.0636)}/\sigma_{a(0.55)}$ which were derived by Coolidge and shown in Table V, page 23. It is assumed here that $\sigma_{a(1.0636)}$ is not significantly different than $\sigma_{a(1.06)}$. With the use of the ratio for continental haze, $\sigma_{a(0.55)}$ can be determined for each 1 km interval from the values of $\sigma_{a(1.06)}$ of McClatchey shown in Table I, page 11, where $\sigma_{a(1.06)}$ is the sum of aerosol scattering and absorption. Thus

$$\sigma_{a(0.55)} = \frac{\sigma_{a(1.06)}}{0.539} \tag{64}$$

When $\sigma_{a(0.55)}$ is known, $\sigma_{a(1.06)}$ can be found for other distributions with the use of Eq (16), page 27, and Table V, page 23. These values can then be tabulated. If it is desired to include molecular attenuation, these values can be added to the aerosol attenuation coefficients. These values are tabulated for five different aerosol dis- in Tables VIII and IX in Appendix A, page 74, where Table VIII is for aerosol only and Table IX includes molecular attenuation from the mid-latitude summer profile.

If these values are to be used in this form for constant transmittance and lock-on range calculations they must be numerically integrated which requires a great deal of computer time. It can be seen from Fig. 5 on the following page that this model can be closely approximated with several exponential functions. In this study, two exponential functions were used for the regions 0-5 km and 5-18 km. This made it possible to reduce the computer cost of making calculations by a factor of approximately 20.

It is highly desirable to make this model useful with surface meteorological range as a continuously variable parameter. As stated earlier, this model was based largely on the work of Elterman. It was noted that if the values for surface attenuation coefficients derived with Elterman's method (Ref 19) for several meteorological ranges plotted on log-log paper they made a straight line and if the two surface attenuation coefficients of McClatchey for 5 and 23.5 km were plotted as a straight line it was parallel to the other. It was also noted that the slope of the line did not change for various particle size distributions. The relationship then derived was
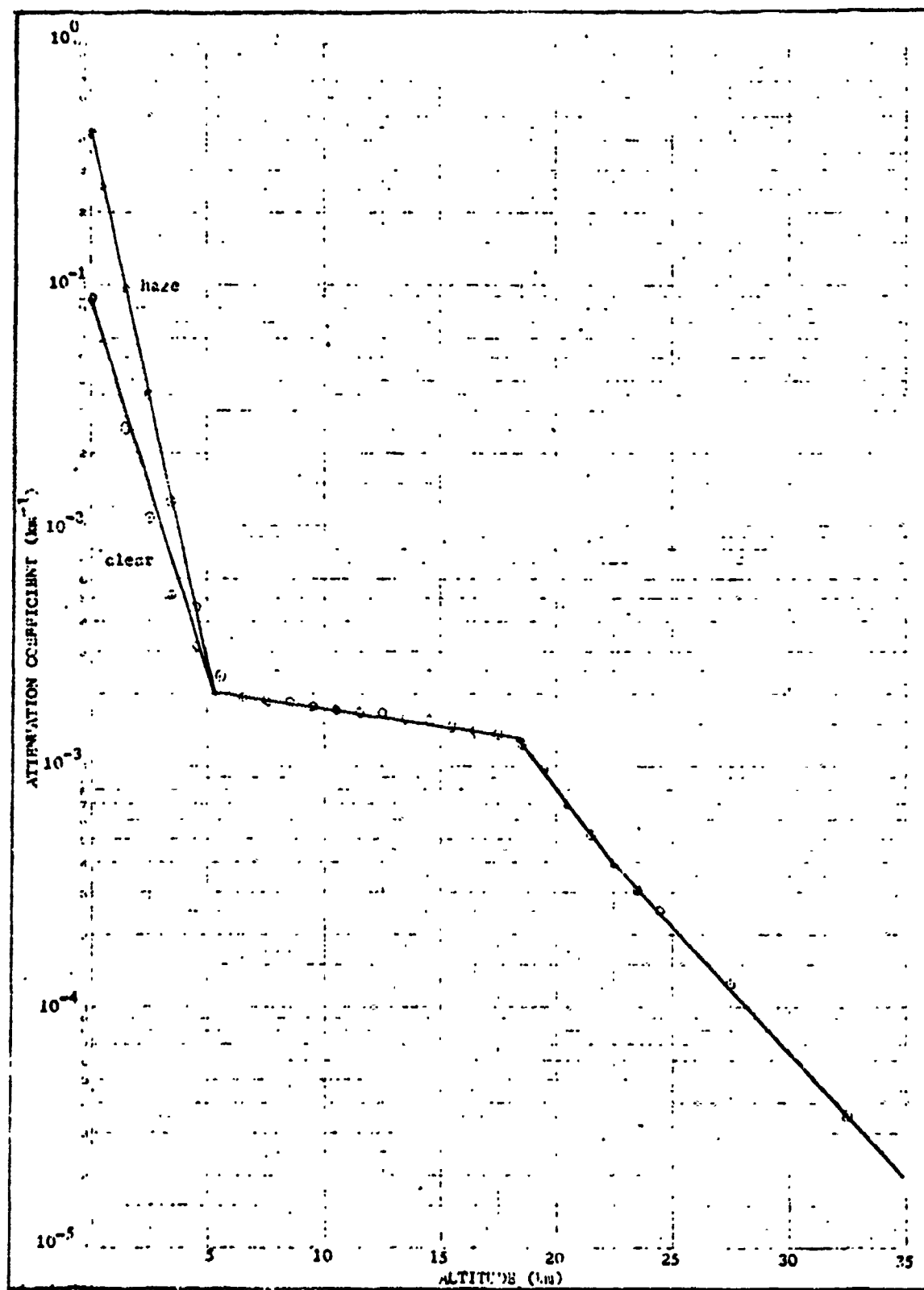
Fig. 5 Vertical Attenuation Profile for McClatchey Model

$$\beta_\rho = L(MR)^{-1.02} \tag{65}$$

where β_ρ is the surface attenuation coefficient,

L is a constant dependent on distribution used,

and MR is meteorological range.

This gives values very close to those of the Homogeneous Mixing Layer model at the surface.

It is also necessary to have the mixing layer scale heights as a function of meteorological range. To find this relationship, straight lines were drawn on semi-log paper from surface attenuation coefficients for several meteorological ranges to a common value at 5 km altitude. Scale heights were derived for each of these and they were in turn plotted on log-log paper. An approximate relationship was established of

$$H_{p1o} = N(MR)^\nu \tag{66}$$

where H_{p1o} is the scale height below 5 km, and N and ν are constants dependent on size distribution used.

In the region from 5-18 km, there is no effect from surface meteorological range. The attenuation depends solely on the aerosol distribution being used. The relationship here is

$$\sigma_a = \beta_e \exp\left(-\frac{h}{H_{phi}}\right) \tag{67}$$

where β_e and H_{phi} are constants dependent on the size distribution used with H_{phi} being the scale height above 5 km. The values for the constants in these relationships are listed in Table VI on the following page for four aerosol distributions. The results from the approximation

39

of the McClatchey model are now

$$\sigma_{a(1.06)} = \begin{cases} \beta_\rho \exp(-\dfrac{h}{H_{plo}}) & 0 < h < 5km \\[2em] \beta_e \exp(-\dfrac{h}{H_{phi}}) & 5 < h < 18km \end{cases} \tag{68}$$

It is these values which are used in constant transmittance and lock-on

range calculations.

Table VI

Constants in Approximation of McClatc! :. Aerosol Model
for Four Combinations of Maritime anu Continental Haze

Aerosol Mixture	$0 \leq h \leq 5$		$5 < h < 18$	
	β_ρ	H_{plo}	β_e	H_{phi}
Continental	$2.22(MR)^{-1.02}$	$0.675(MR)^{0.233}$	3.3×10^{-3}	21.0
25% Maritime	$3.79(MR)^{-1.02}$	$0.690(MR)^{0.22}$	4.9×10^{-3}	25.3
50% Maritime	$3.93(MR)^{-1.02}$	$0.680(MR)^{0.21}$	5.1×10^{-3}	25.4
100% Maritime	$4.10(MR)^{-1.02}$	$0.675(MR)^{0.22}$	5.2×10^{-3}	26.4

Transmittance. These calculations were made for haze only. No

rain was included but it could easily be done if desired as was shown

using the Homogeneous Mixing Layer model. Using the results of the

previous section in the same manner as was shown for the HML model,

the following results were obtained: for h < 5 km

$$R = \frac{H_{plo}}{\sin \theta} \ln\left[1 - \frac{\ln \frac{1}{T} \sin \theta}{\beta_\rho H_{plo}}\right]^{-1} \tag{69}$$

Note that R approaches infinity when the term shown in the logarithmic

argument approaches zero. This implies that

$$\theta_{max} = \sin^{-1}\frac{\beta_\rho H_{plo}}{\ln\frac{1}{\tau}} \tag{70}$$

For any given τ this depends on β_ρ and H_{plo} which are functions of meteorological range and particle size distribution. For $5 < h < 18$ km

$$L_2 = \frac{H_{phi}L_1}{5} \ln\left[1 - \frac{1}{B}\left(\frac{\ln\frac{1}{\tau}}{L_1} - A\right)\right]^{-1} \tag{71}$$

where

$$A = \frac{\beta_\rho H_{plo}}{5}\left[1 - \exp\left(-\frac{5}{H_{plo}}\right)\right] \tag{72}$$

and

$$B = \frac{H_{phi}}{5}\beta_e \exp\left(-\frac{5}{H_{phi}}\right) \tag{73}$$

Note that L_2 approaches infinity when

$$1 - \frac{1}{B}\left[\frac{\ln\frac{1}{\tau}}{L_1} - A\right] = 0 \tag{74}$$

or

$$L_{1min} = \frac{\ln\frac{1}{\tau}}{A + B} \tag{75}$$

Therefore,

$$\theta_{max} = \sin^{-1}\frac{5}{L_{1min}} \tag{76}$$

Finally $R = L_1 + L_2$ where L_1 is a constant for any given angle.

Lock-on Range. Proceeding in the same manner as before the following results were obtained for the lock-on range with receiver and

and designator collocated. For $h = 0$

$$\ln \frac{\sqrt{K}}{R} = \beta_\rho R \tag{77}$$

For $0 < h < 5$ km

$$\ln \frac{\sqrt{K}}{R} = B \left[1 - \exp(-AR) \right] \tag{78}$$

where

$$A = \frac{\sin \theta}{H_{plo}} \tag{79}$$

and

$$B = \frac{\beta_\rho H_{plo}}{\sin \theta} \tag{80}$$

For $5 < h < 18$ km

$$\ln \frac{\sqrt{K}}{L_1 + L_2} = CL_1 + DL_1 \left[1 - \exp\left(- \frac{5L_2}{H_{phi}L_1} \right) \right] \tag{81}$$

where

$$C = \frac{\beta_\rho H_{plo}}{5} \left[1 - \exp\left(- \frac{5}{H_{plo}} \right) \right] \tag{82}$$

and

$$D = \frac{\beta_e H_{phi}}{5} \exp\left(- \frac{5}{H_{phi}} \right) \tag{83}$$

Again this equation is to be solved for L_2 where L_1 is a constant for a given elevation angle. Finally $R = L_1 + L_2$.

V. Results and Analysis

This chapter contains the results of using the models developed in the preceding chapter and an analysis of these results. The atmospheric scale height used for the clear air in the HML model was 7.99 km. This is the value suggested by Coolidge and has been given as the scale height for the atmospheric mean density profile. This is different than the scale height as determined by Duntley et al. in experimental measurements of the volume extinction coefficient (Ref 11, 12, 13). The scale height found there was in the neighborhood of 20 km in several of the experiments. The scale height used for the approximation of the McClatchey model above 5 km was also in the neighborhood of 20 km, so these higher values have merit. However, in the absence of further experimental measurements and for the purposes of calculations, the scale height for the density profile was used.

The scale height is a sensitive parameter as can be seen in Fig. 6 on the following page. Here the two scale heights of 20 km and 7.99 km were used for comparison. At an elevation angle of 54 degrees, and with a meteorological range of 3.0 km, the scale height of 20 km gave a 13% shorter lock-on range than did 7.99 km.

A meteorological range of 40 km was used for clear air above the mixing layer in the HML model as it seems to be a worst case condition (Ref 7:112). A typical value for K of $6.7 \times 10^3 \text{km}^2$ was used (Ref 14:13-14).

Aerosol Mixtures

An attempt was made to see if a generalization could be found where the percentage of maritime haze mixed with continental haze
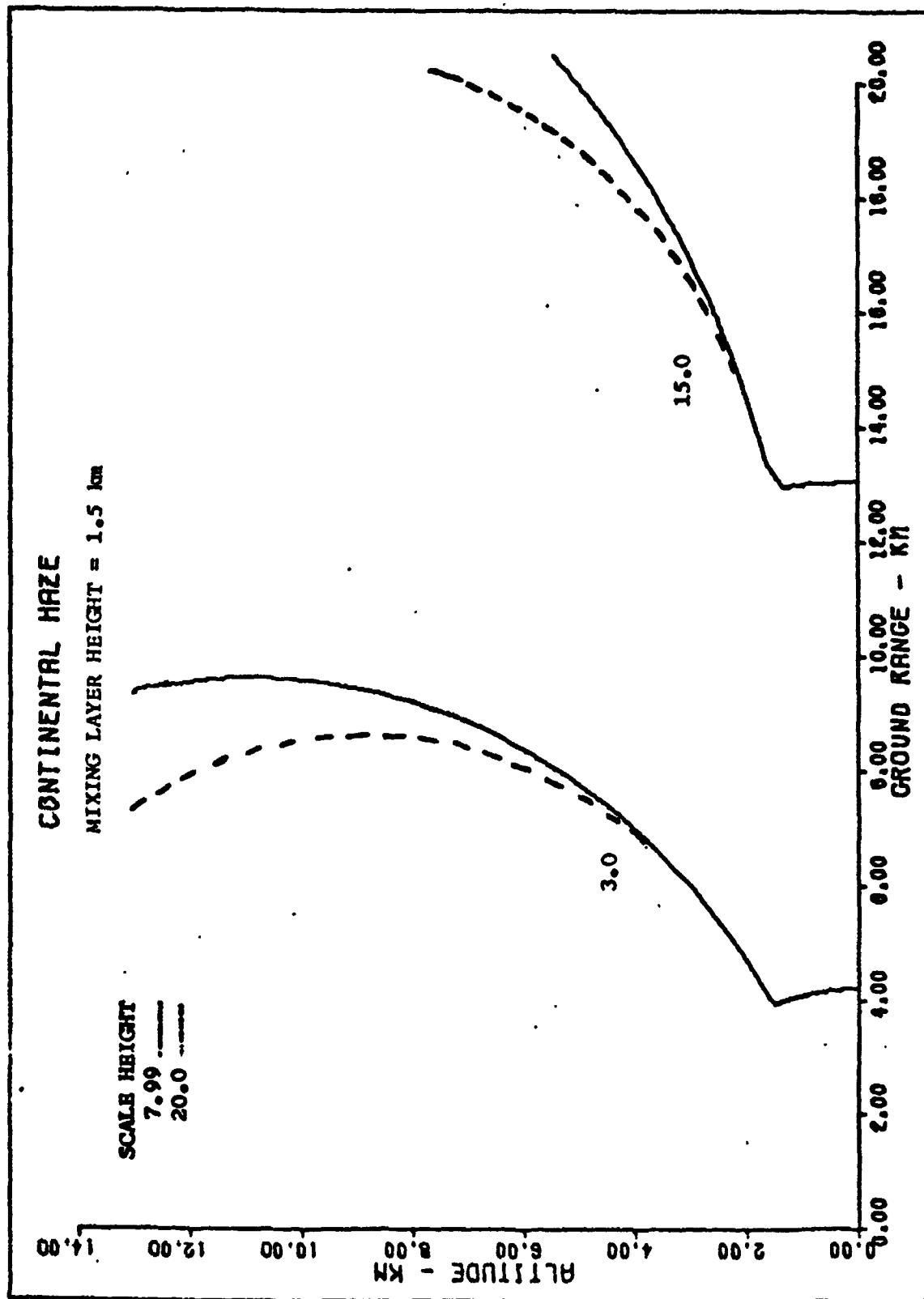
Fig. 6 Effects of Clear Air Scale Height in Homogeneous Mixing Layer Model on Maximum Lock-on Range at Two Meteorological Ranges – Designator and Receiver Collocated.

could be used as a continuous variable. It was found that the rela-
tionship for the ratio, α, of

$$\alpha = 0.78(\% \text{ maritime})^{0.057} \tag{84}$$

is a good approximation (within 1% of the values in Table V, page 23)
down to about 10% maritime (Ref 7:79). Below this the effects of add-
ing maritime to continental are changing too quickly for this relation
to be valid.

Constant Transmittance Slant Range

This section will describe the results of computing constant
transmittance curves for both the HML model and the McClatchey model.
These results are then compared.

Homogeneous Mixing Layer Model (Haze only). The calculations for
this model give the characteristically shaped curves shown in Fig. 7 on
the following page. Note that in the mixing layer the curve is cir-
cular. At low transmittances and high meteorological ranges, the curve
above the mixing layer flares out to infinity. At high transmittances
and low meteorological ranges the curves have a "keyhole" shape.

Figure 7 was computed for 100% continental haze. The results of
changing the haze composition slightly to 25% maritime distribution and
75% continental distribution gives a significant difference as shown in
Fig 8, page 47. As can be seen, the slant range for different haze dis-
tributions changes considerably for the same meteorological range condi-
tions. For example, at a meteorological range of 5 km and transmittance
of 0.1, the surface slant range is decreased from 5.43 km in 100% conti-
nental haze to 3.11 km in the 25% maritime mixture, a 42% reduction in
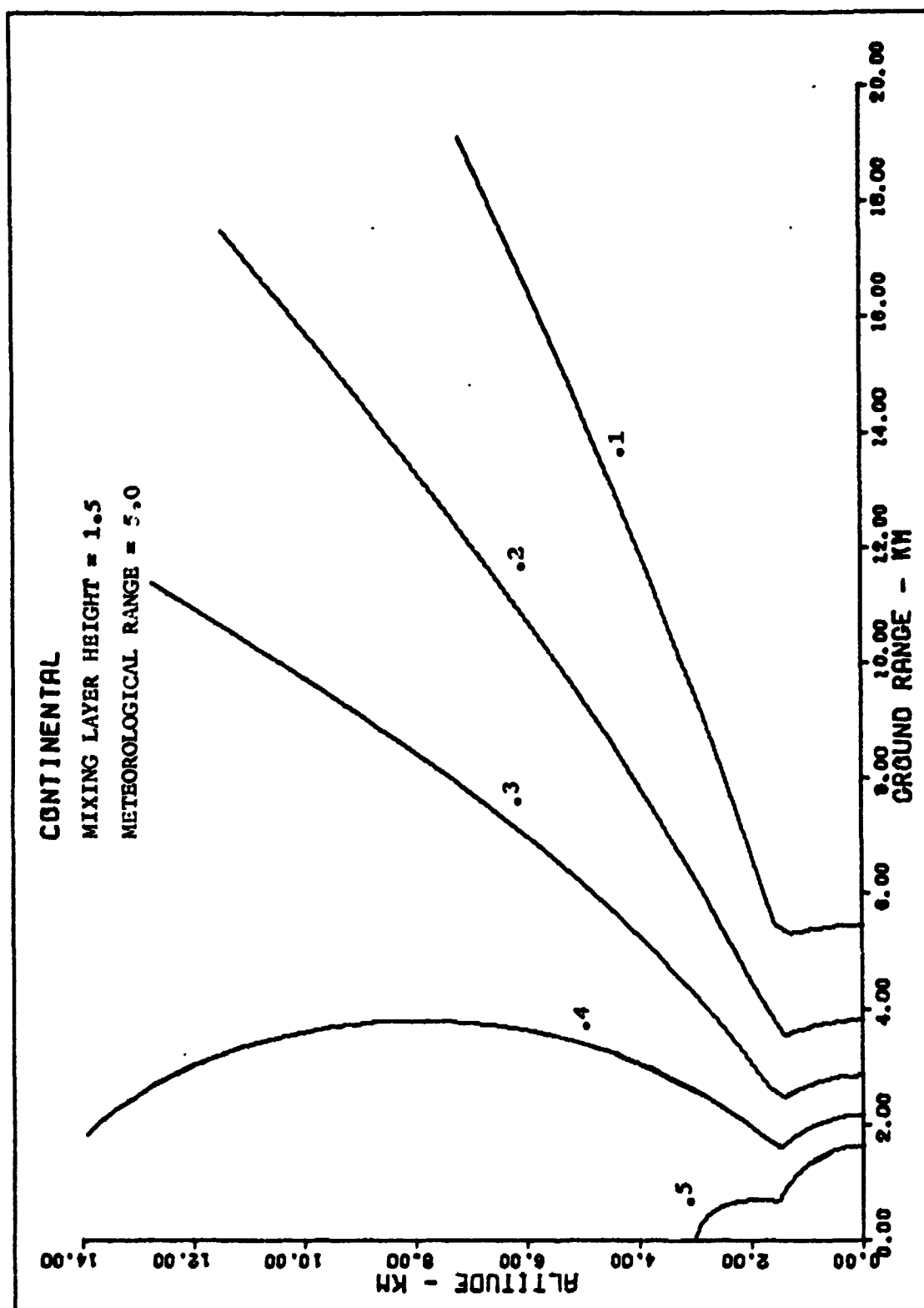
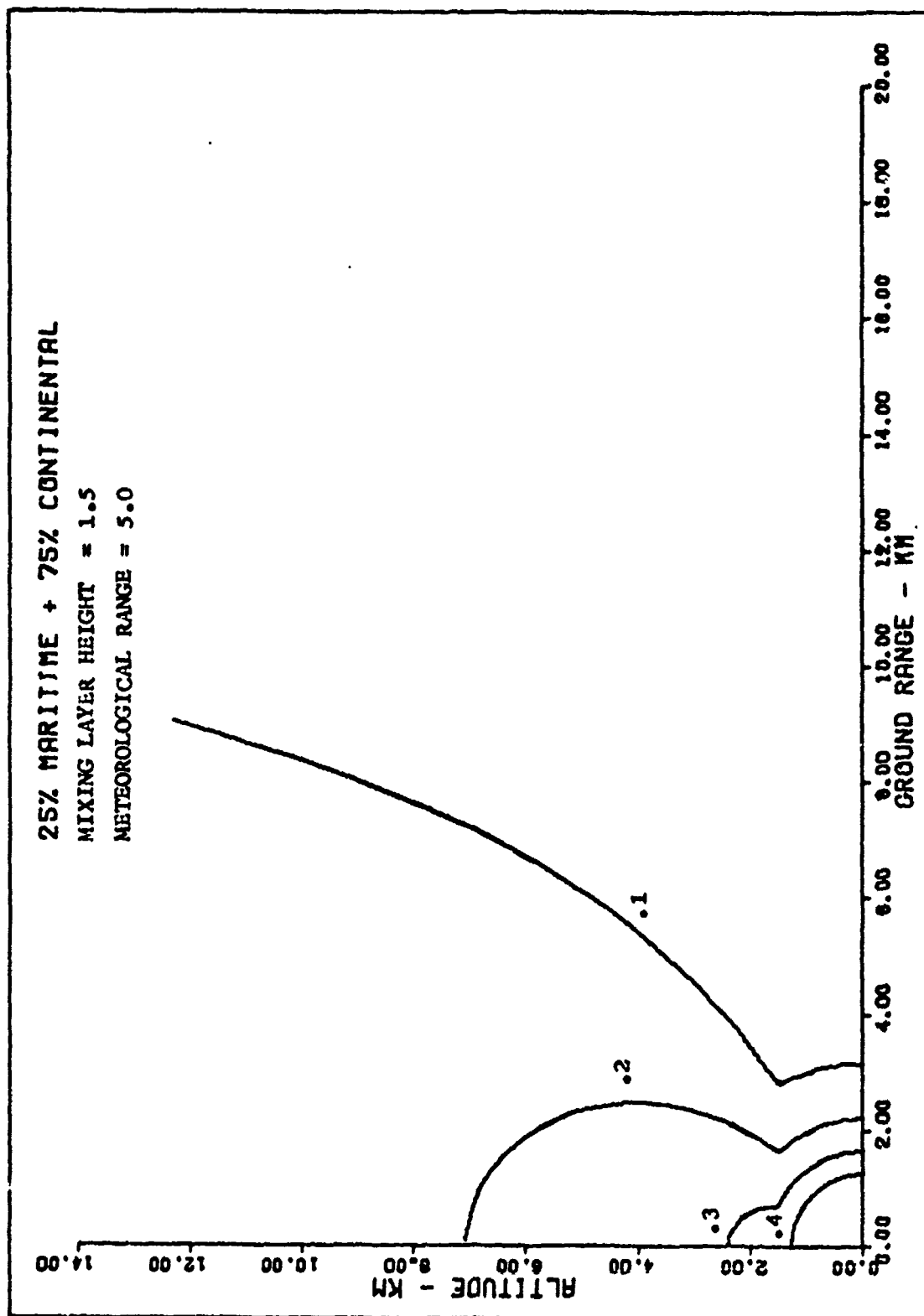Fig. 7 Transmittance of 1.06 microns – Homogeneous Mixing Layer Model

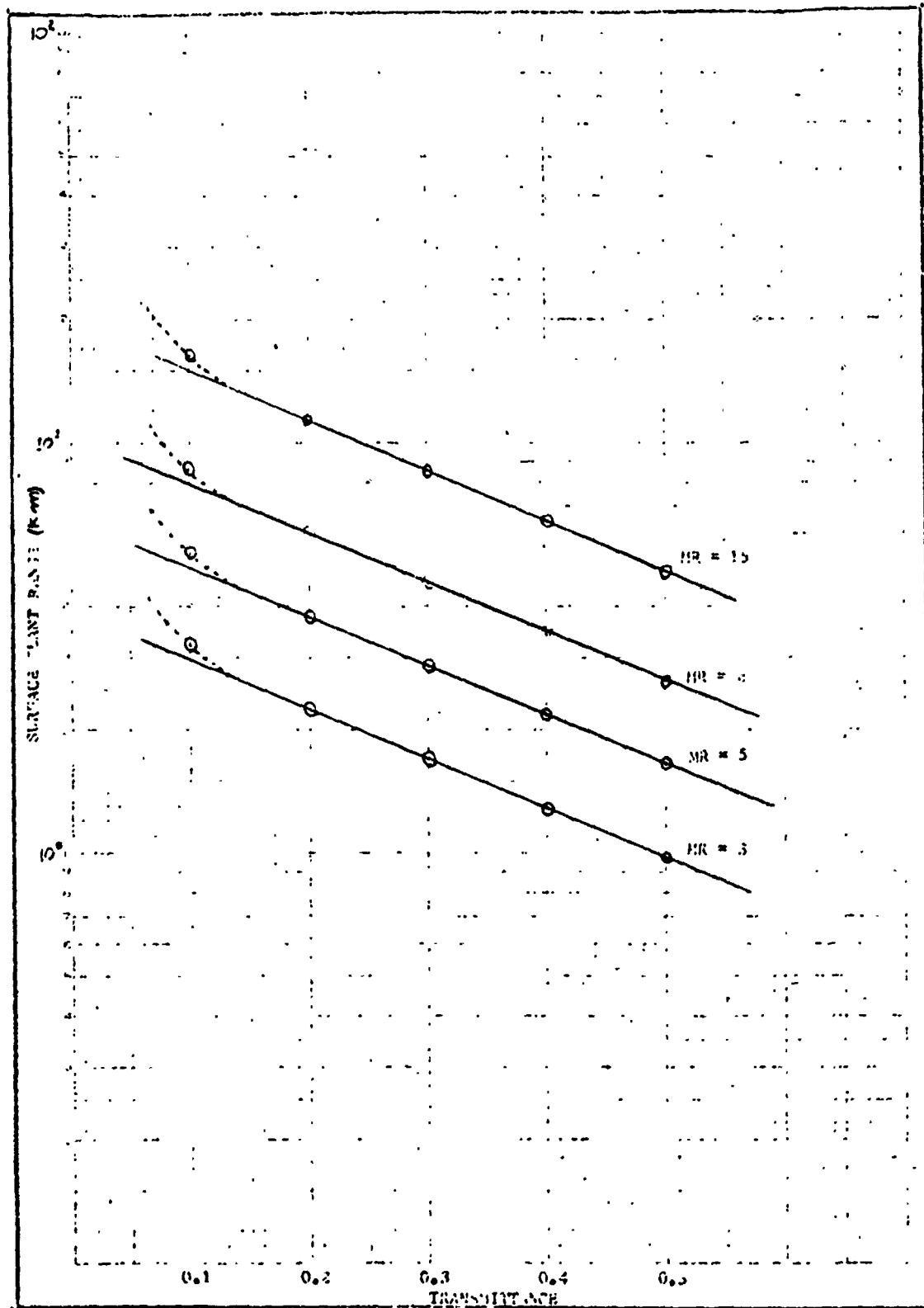Fig. 8 Transmittance of 1.06 microns — Homogeneous Mixing Layer Model.

Fig. 9 Surface Slant Range as a Function of Transmittance for Several Meteorological Ranges.

range. Significant effects on range can be realized with as little as 10% maritime (Ref 7). Results of additional constant transmittance calculations are shown in Figures 23A through 23E in Appendix B, page 77.

Fig. 9, page 48, shows surface slant range vs transmittance for several values of meteorological range. It is interesting to note that all points lie on an exponential curve for transmittances of 0.2 or greater. Below that value the points are starting to move to infinity for zero transmittance.

Homogeneous Mixing Layer Model (Haze with Rain). When Fig. 10 on the following page is compared to Fig. 7, page 46, it can be seen that rain can have a significant effect on transmittance. With an observed meteorological range of 5 km, and rain classified as light (2.5 mm/hr), the surface slant range for 0.1 transmittance can be decreased by 25%.

McClatchey Model. This model was used for transmittance calculations for various aerosol mixtures of continental and maritime hazes. An example of using this model is shown in Fig. 11, page 51. The shape of these curves is dramatically different from those of the HML model. The curves begin at the same point at the surface for a given transmittance, but at low transmittances and high meteorological ranges they flare out immediately from the surface. Also, at the higher transmittances the curves do not have the characteristic "keyhole" shape of the Homogeneous Mixing Layer model.

The differences in the slant ranges between the two models are significant. Slant ranges for the McClatchey model are usually greater, often much greater, than those of the Homogeneous Mixing Layer model.
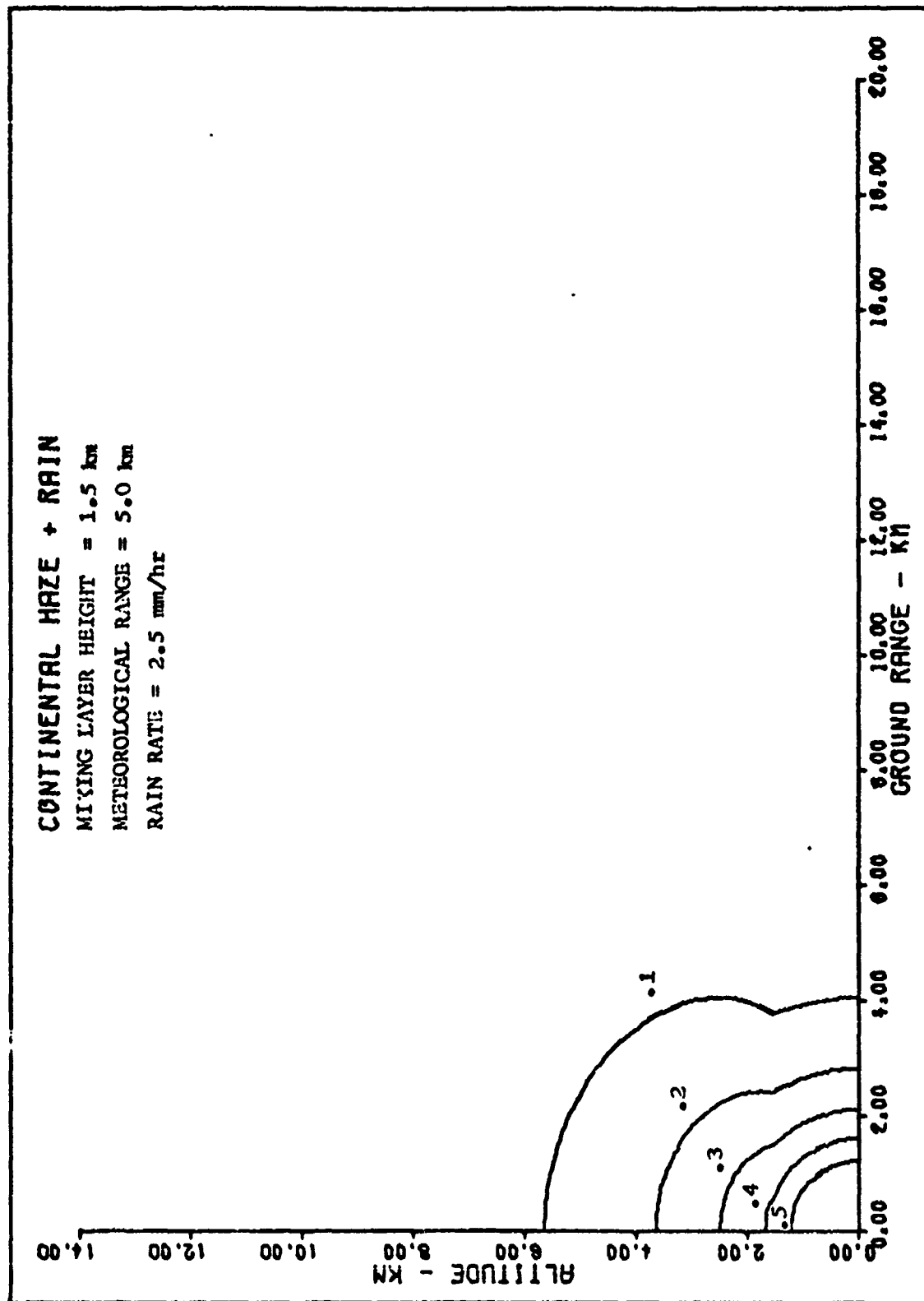
49

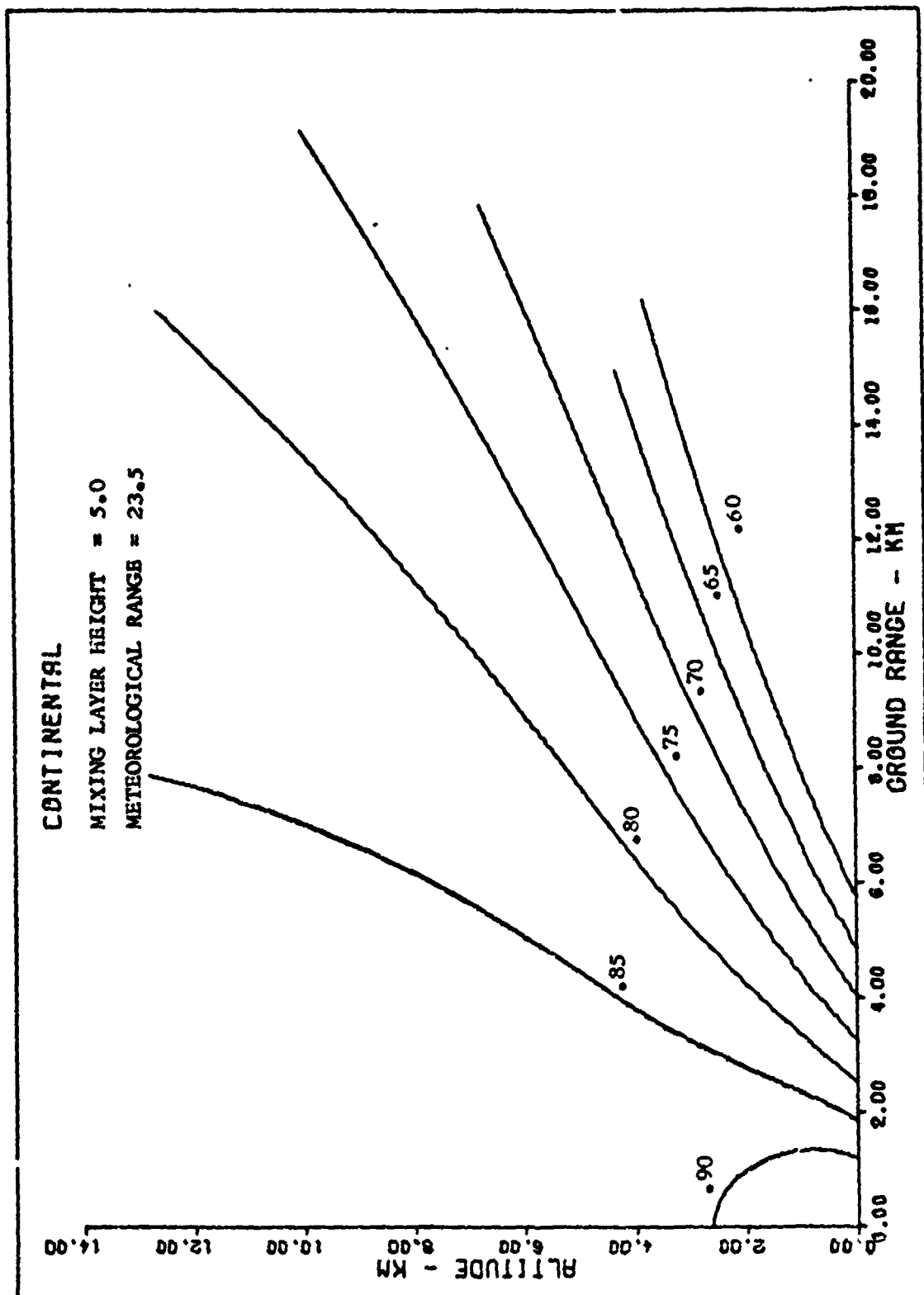Fig. 10 Transmittance of 1.06 microns – Homogeneous Mixing Layer

Fig. 11 Transmittance of 1.06 microns - McClatchey Model

Lock-on Range

Lock-on ranges were computed for both models. With the McClatchey model, different haze effects with designator and receiver collocated were studied. For the Homogeneous Mixing Layer model, the effects of various haze distributions on lock-on range were studied with the designator and receiver collocated and with a ground based designator. Also studied with this model were the effects of haze plus rain with the designator and receiver collocated.

McClatchey Model. A comparison between the two models is shown in Fig 12 on the following page. As can be seen the two models vary significantly. The McClatchey lock-on range curve flares out immediately from the surface and at the higher meteorological ranges they appear to be going to infinity.

A comparison was done with different mixtures of maritime and continental aerosols, shown in Figs. 13 and 14, pages 54 and 55. Here, as in the constant transmittance curves, the aerosol mixture has a significant effect. A mixture of 25% maritime and 75% continental will decrease a surface lock-on range, with a meteorological range of 5 km, from 6.1 to 4.1 km, a 33% decrease from that for 100% continental. It is interesting to note that if the amount of maritime is increased to 100% the lock-on range is reduced only an additional 4%. Fig. 15, page 56 shows the effect of aerosol mixture on surface lock-on range, with the values between 0 and 10% maritime being interpolated.

Fig. 16, page 57 shows lock-on ranges vs meteorological range for various altitudes. It is interesting to note that these can be closely approximated by a power law for any given altitude. However, no simple algebraic relationship was found which held for all altitudes.

52
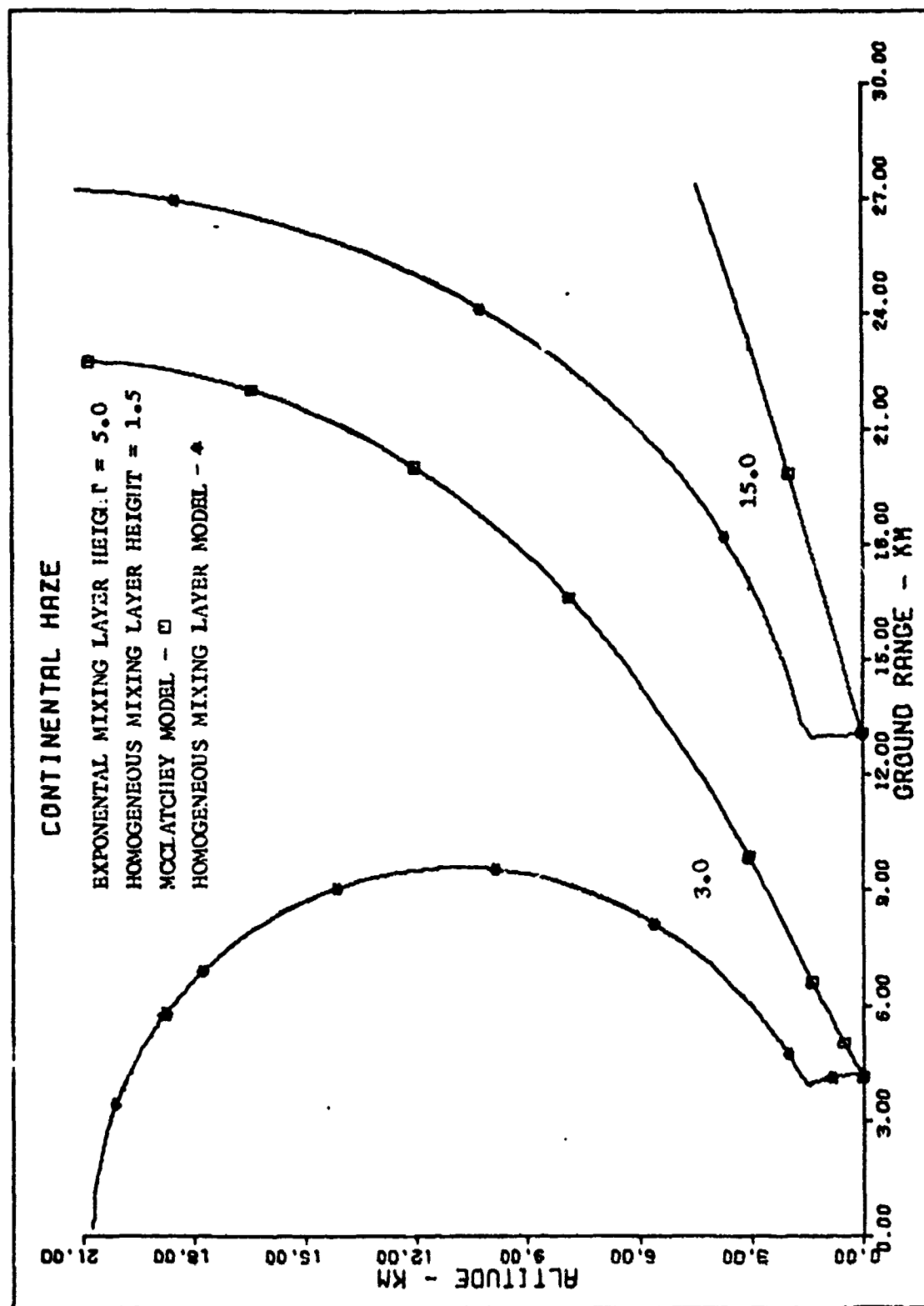
Fig. 12 Maximum Lock-on Range - 1.06 microns - Designator and Receiver Collocated.
McClatchey Model vs Homogeneous Mixing Layer Model at Two Meteorological Ranges.
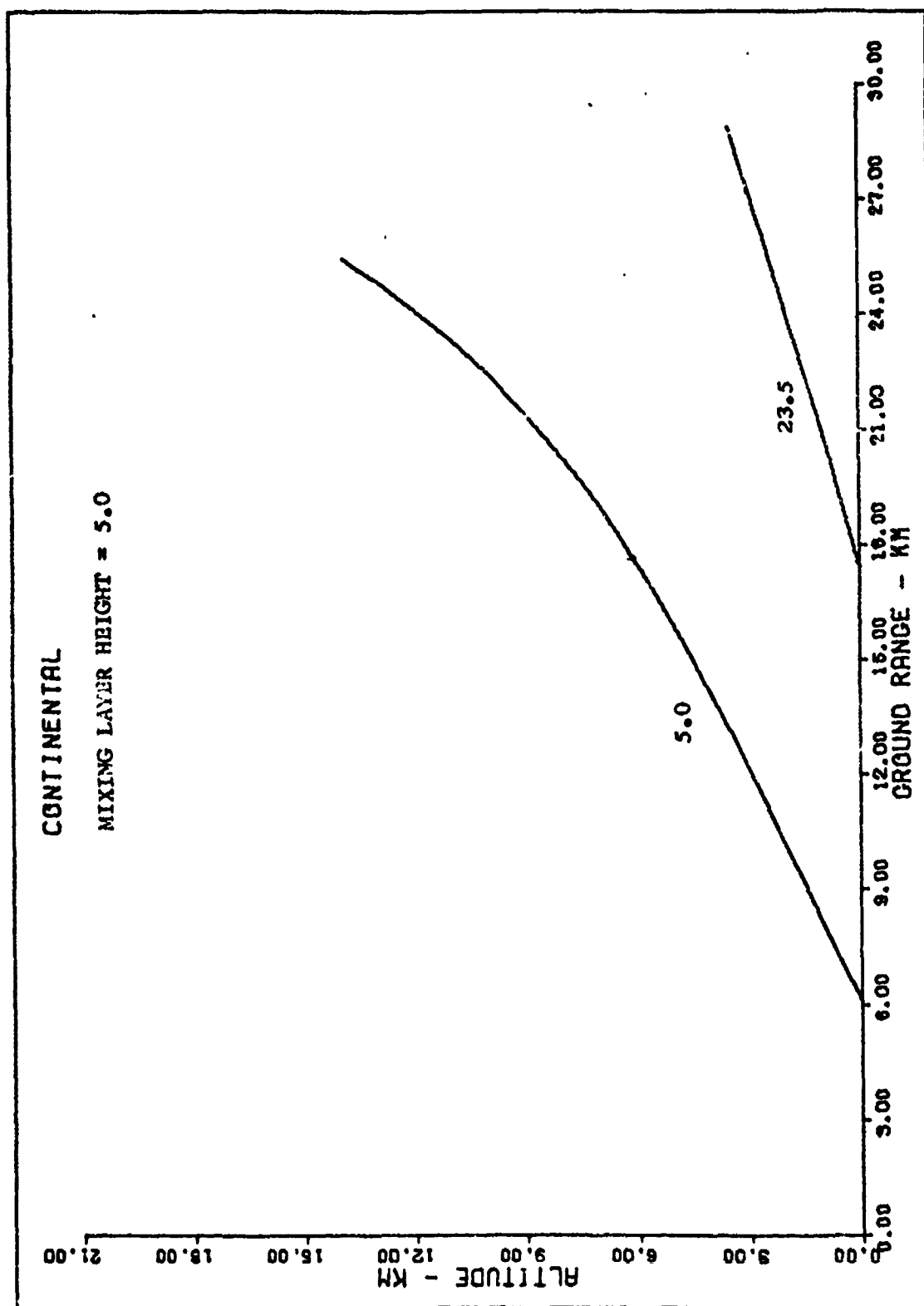
Fig. 13 Maximum Lock-on Range with Designator and Receiver Collocated at Two Meteorological Range Conditions, McClatchey Model.

Fig. 14 Maximum Lock-on Range with Designator and Receiver Collocated at Two Meteorological Range Conditions, McClatchey Model.

Fig. 15   Surface Lock-on Range as a Function of Aerosol Mixture for
Two Meteorological Ranges

Fig. 16 Lock-on Range as a Function of Meteorological Range for
Several Altitudes - McClatchey Model.

Homogeneous Mixing Layer Model (Haze only). The analysis described
for the McClatchey model with different aerosol mixtures also holds for
the HML model. In addition, it should be noted that the haze L distri-
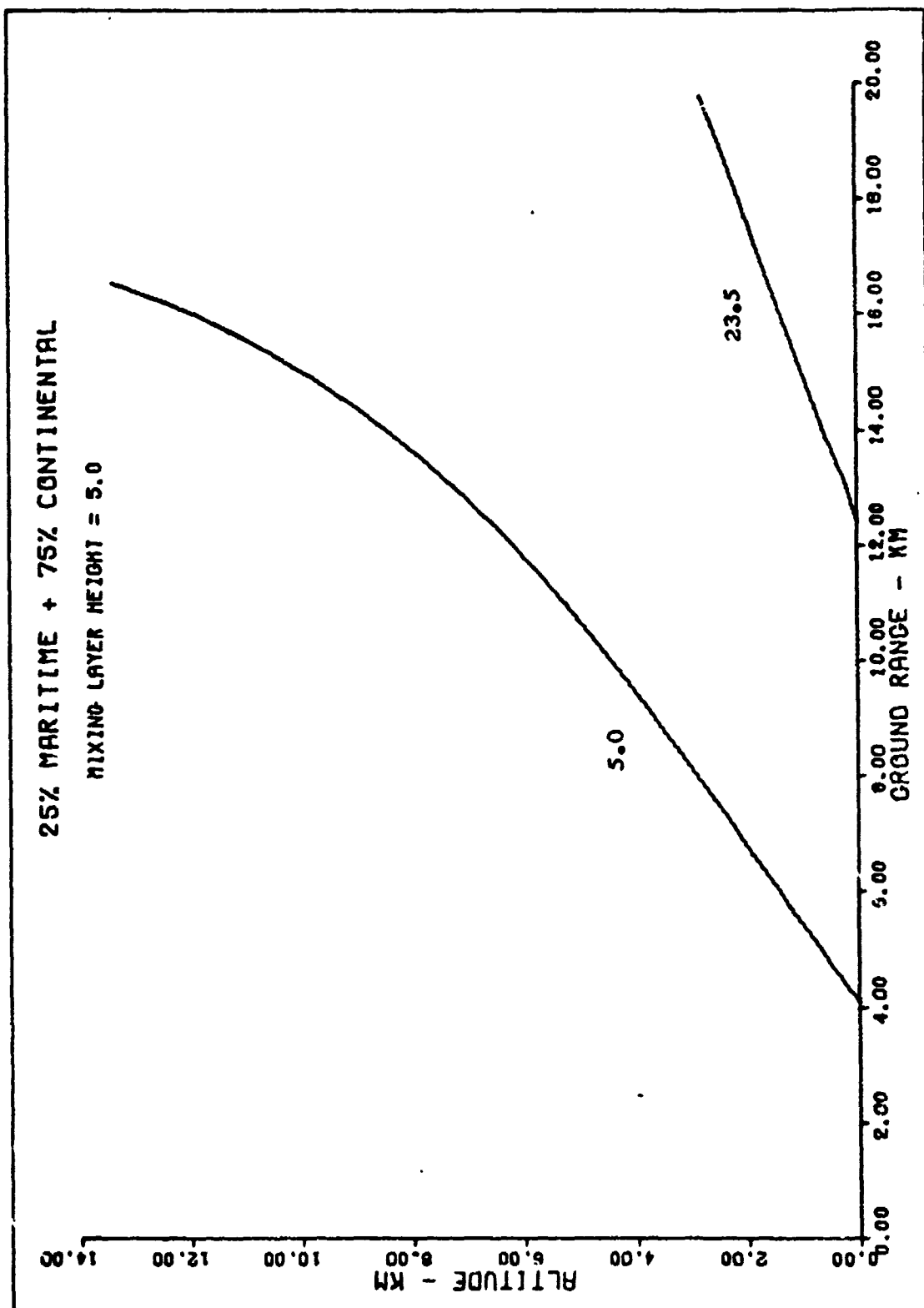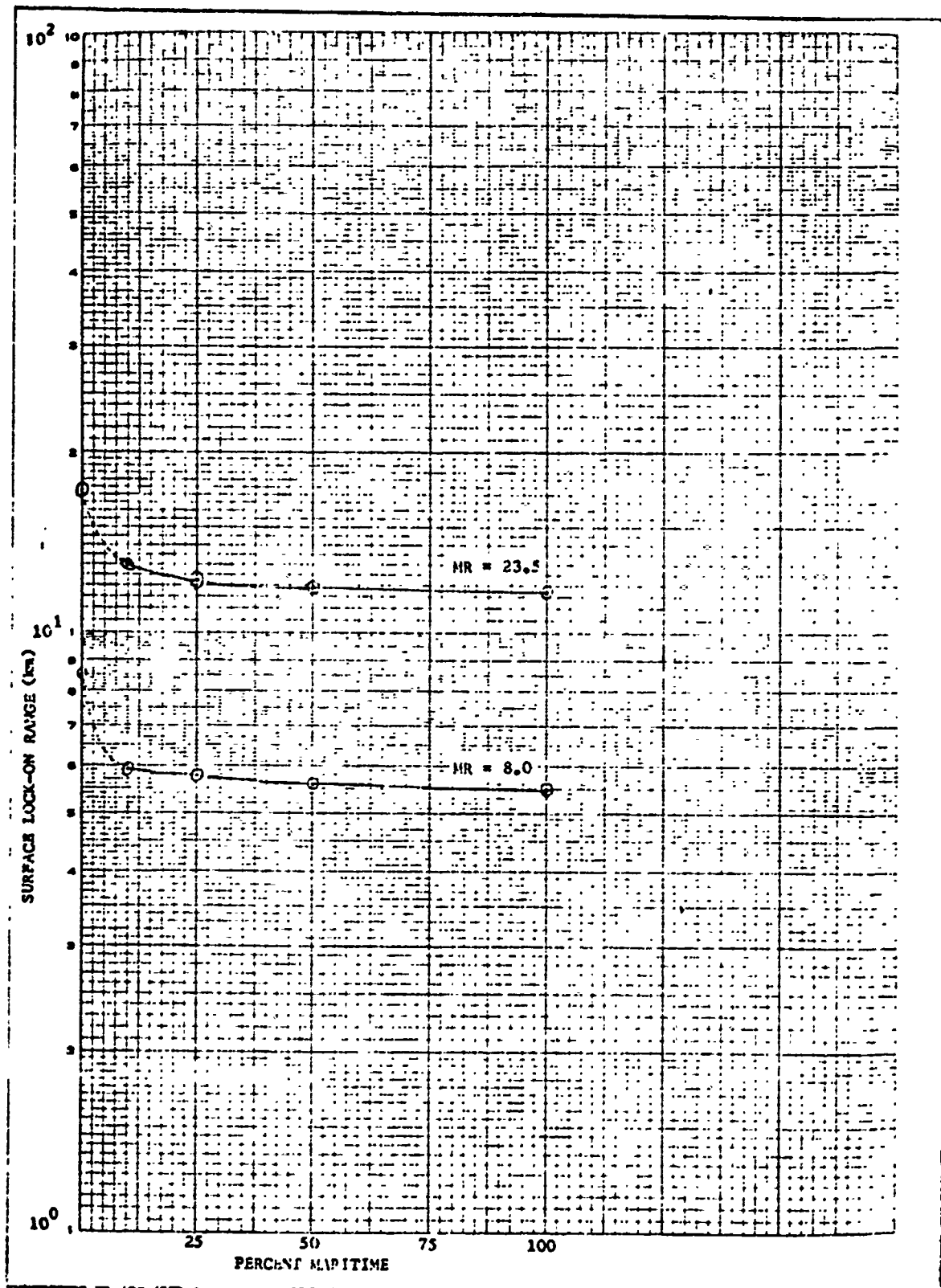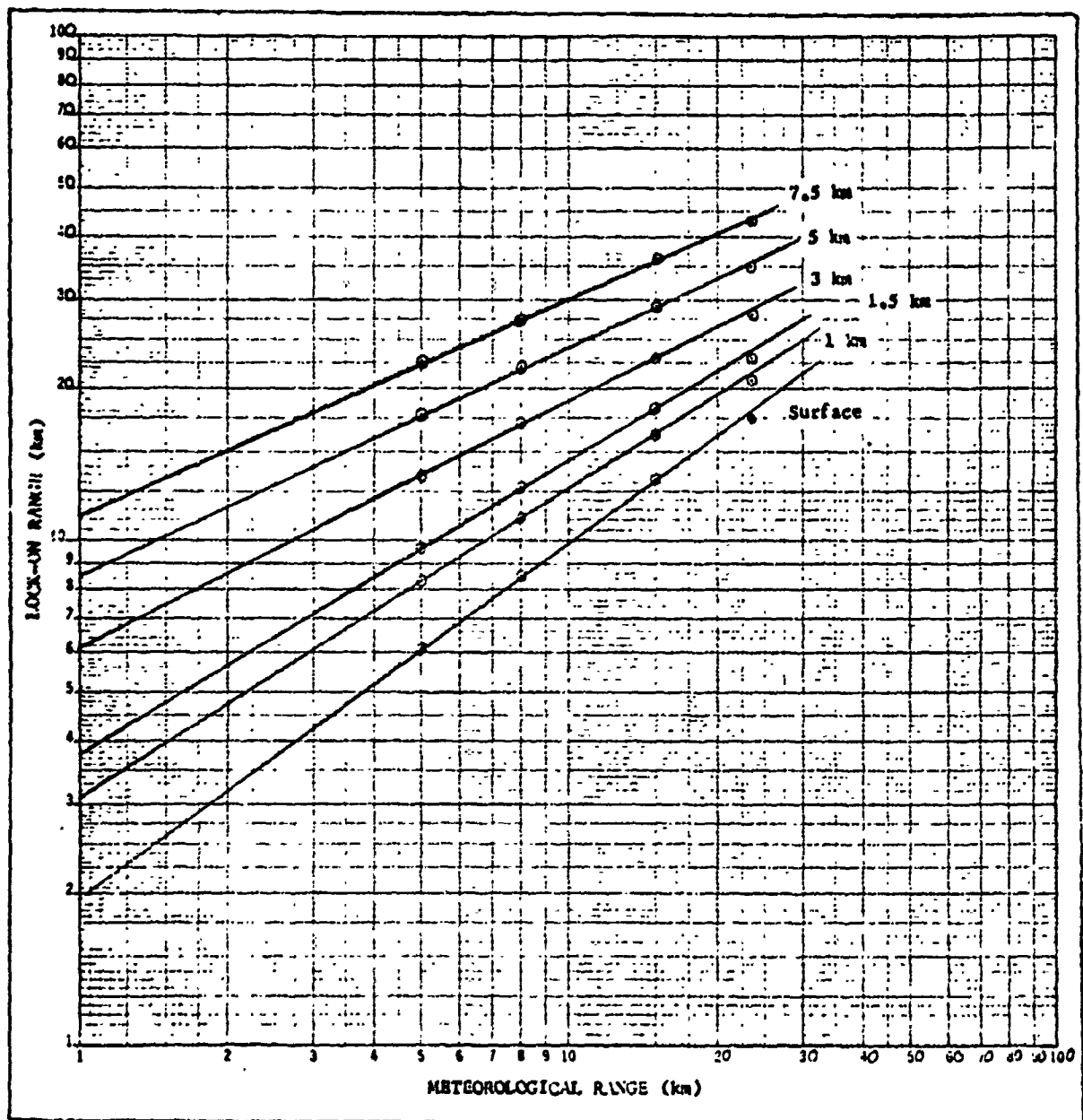bution, which was proposed as a replacement for the continental, gives
a significant decrease in lock-on range from that of the continental,
though the decrease is less than that given by a mixture of 25% maritime
and 75% continental. This can be seen by comparing Figs. 24A and 24B in
Appendix C, page 83. It should also be noted that the curves for the
HML model have different characteristics from those of the McClatchey
model; they have the "keyhole" shape of the constant transmittance
curves. This is true for all meteorological range conditions studied.

There may be large differences in the lock-on ranges between this
model and the McClatchey model (the differences at specific altitudes
are strongly dependent on the height of the uniform mixing layer, a
property which will be discussed later). For example, it can be seen
from Fig. 12, page 53, that at an altitude of 6 km with a meteorologi-
cal range of 3 km there is a 34% difference in lock-on range between the
two models. At higher altitudes the difference is even greater.

An additional difference in the results of using the two models can
be seen by comparing Figs. 16 and 17, pages 57 and 59. At the surface,
the relationship of lock-on range to meteorological range can be approx-
imated with a power law. At higher altitudes, however, this is not true
as it is with the McClatchey model. It can also be seen from Fig. 17
that the change in lock-on range is less with a change in altitude at
higher meteorological ranges than with lower. Figs. 24A through 24E
in Appendix C, page 83 show additional examples of lock-on range curves
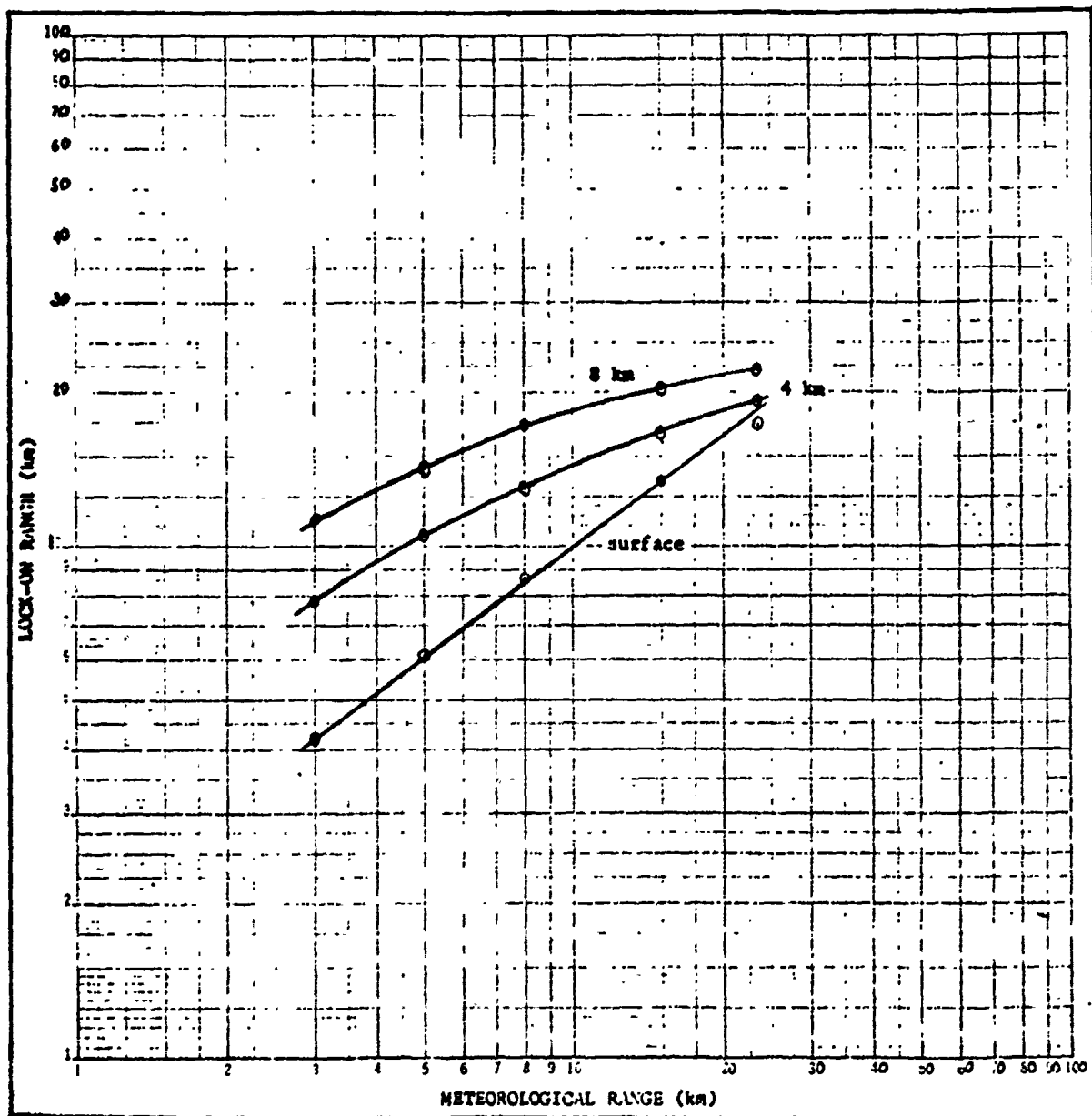with designator and receiver collocated.

58

Fig. 17   Lock-on Range as a Function of Meteorological Range for
Several Altitudes - Homogeneous Mixing Layer Model.

Homogeneous Mixing Layer Model (Haze with Rain). Rain can have a significant effect on laser lock-on ranges. For example, a "moderate" rainfall of 8.0 mm/hr in a meteorological range of 3 km and a continental haze reduces the lock-on range by 26%. Compare Fig 18, page 61, with Fig 6, page 44. It should be noted here that it was difficult to correlate realistic values of meteorological range to rainfall rates when both haze and rain contribute to lowered visibility. Using the values for meteorological range in Table III, page 15, it can be seen that 3 km is an unrealistic value for the higher rainfall rates in Fig. 18. Thus, the lock-on ranges for the higher rainfall rates are probably inaccurate.

Mixing Layer Height. The height of the mixing layer in the HML model has a significant effect on the lock-on ranges as can be seen from Figs. 25A through 25E in Appendix D, page 89. Fig. 19, page 62, shows lock-on ranges at 6 km altitude vs mixing layer height for several surface meteorological ranges. The data were taken from the continental haze model. It can be seen that as the mixing layer height decreases, a change in meteorological range has less effect on the lock-on range. This is because the laser beam is propagating through a higher percentage of clear air. An extreme example of this is shown in Fig. 20, page 63, where the mixing layer height is only 0.1 km. The curves corresponding to the different meteorological ranges are very close.

Ground Designator (Haze only). Lock-on ranges for an airborne receiver can be increased considerably with a ground designator, especially in low surface meteorological range conditions. For example, with the receiver at 6 km altitude, a surface meteorological range of
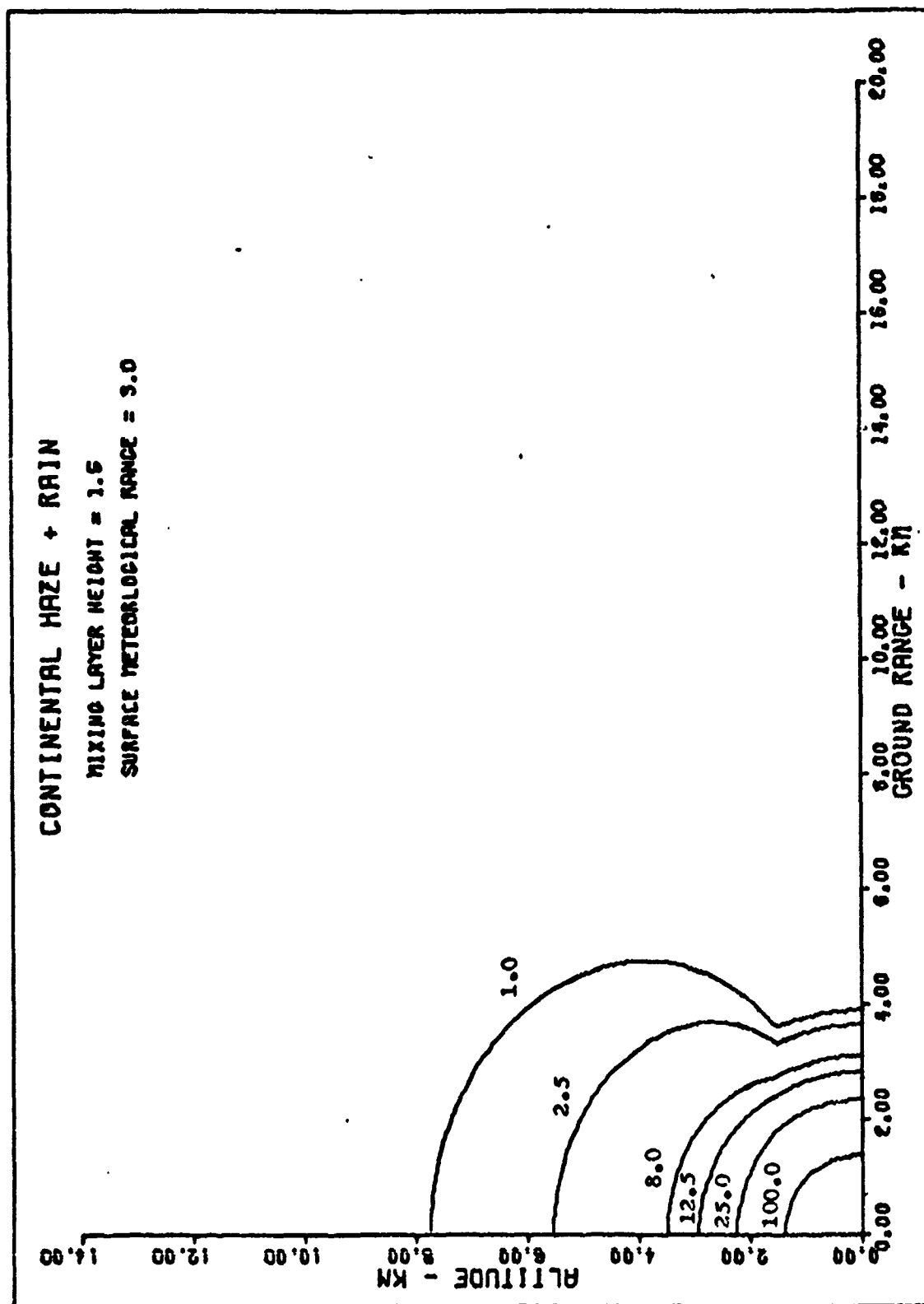
Fig. 18 Maximum Lock-on Range with Designator and Receiver Collocated for Various Rainfall Rates (mm/hr), Homogeneous Mixing Layer Model.
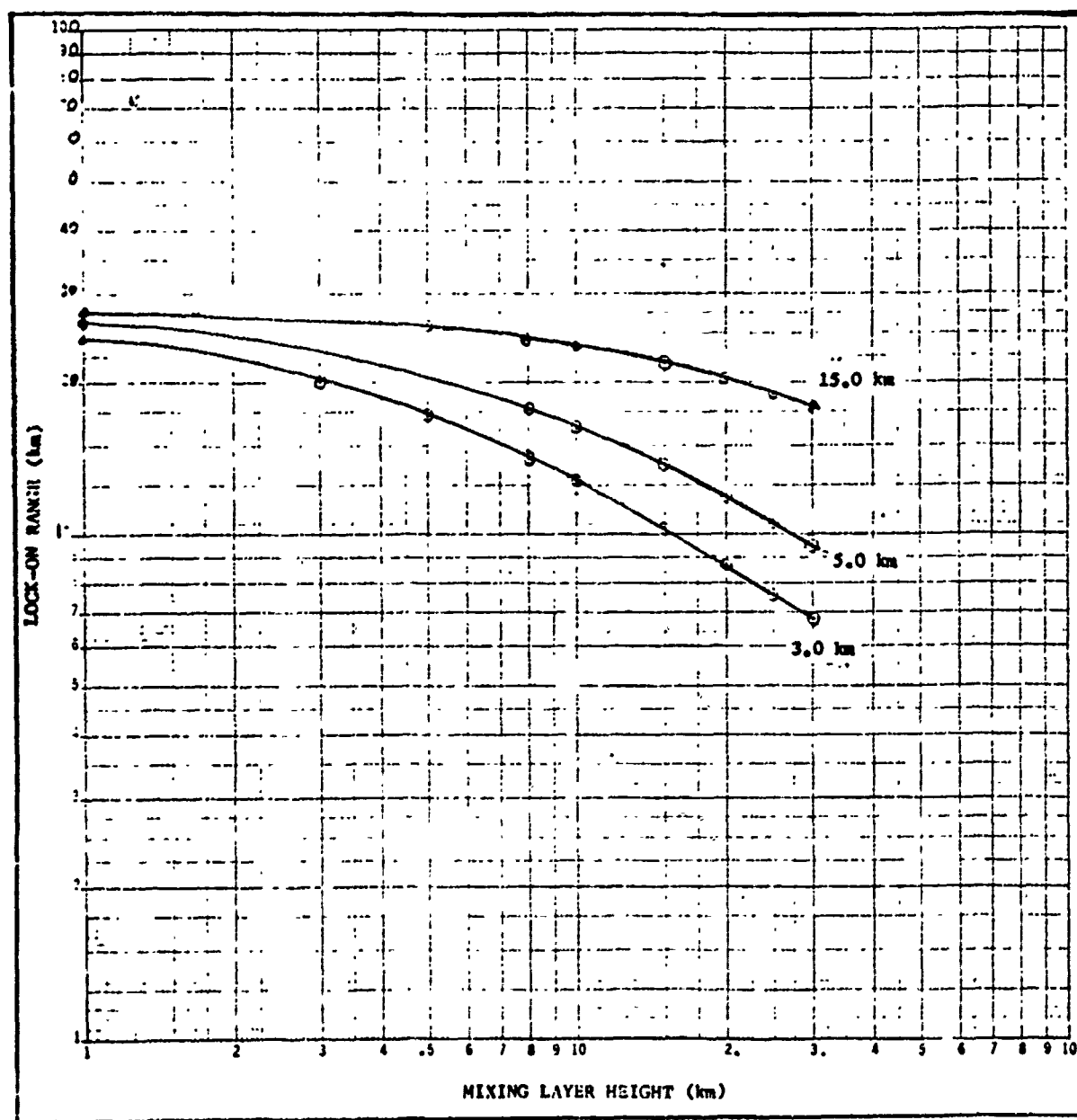
Fig. 19 Lock-on Range at 6 km Altitude vs Mixing Layer Height
for Several Meteorological Ranges – Homogeneous Mixing
Layer Model.

Fig. 20 Maximum Lock-on Range with Designator and Receiver Collocated at Several Meteorological Ranges, Homogeneous Mixing Layer Model.

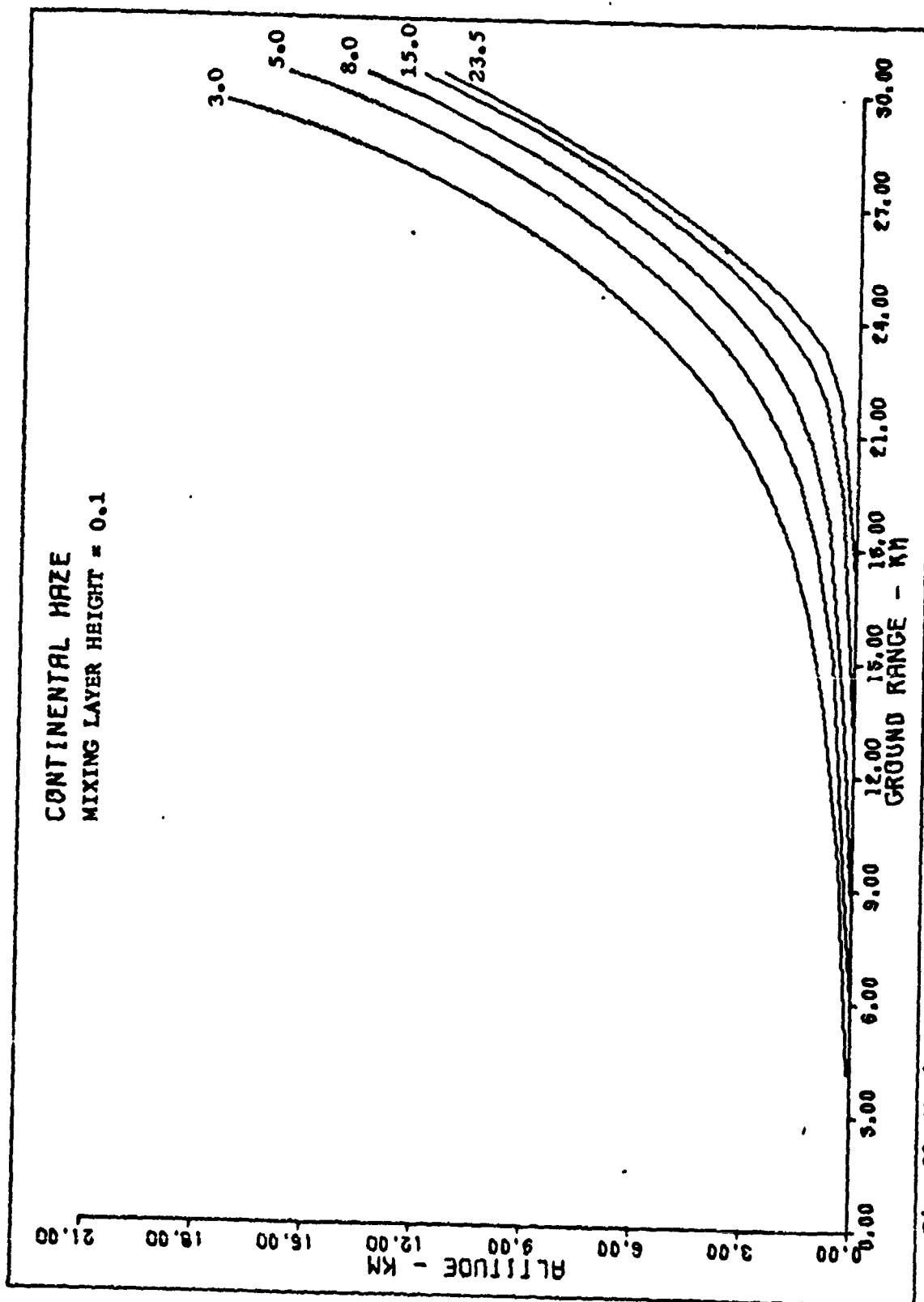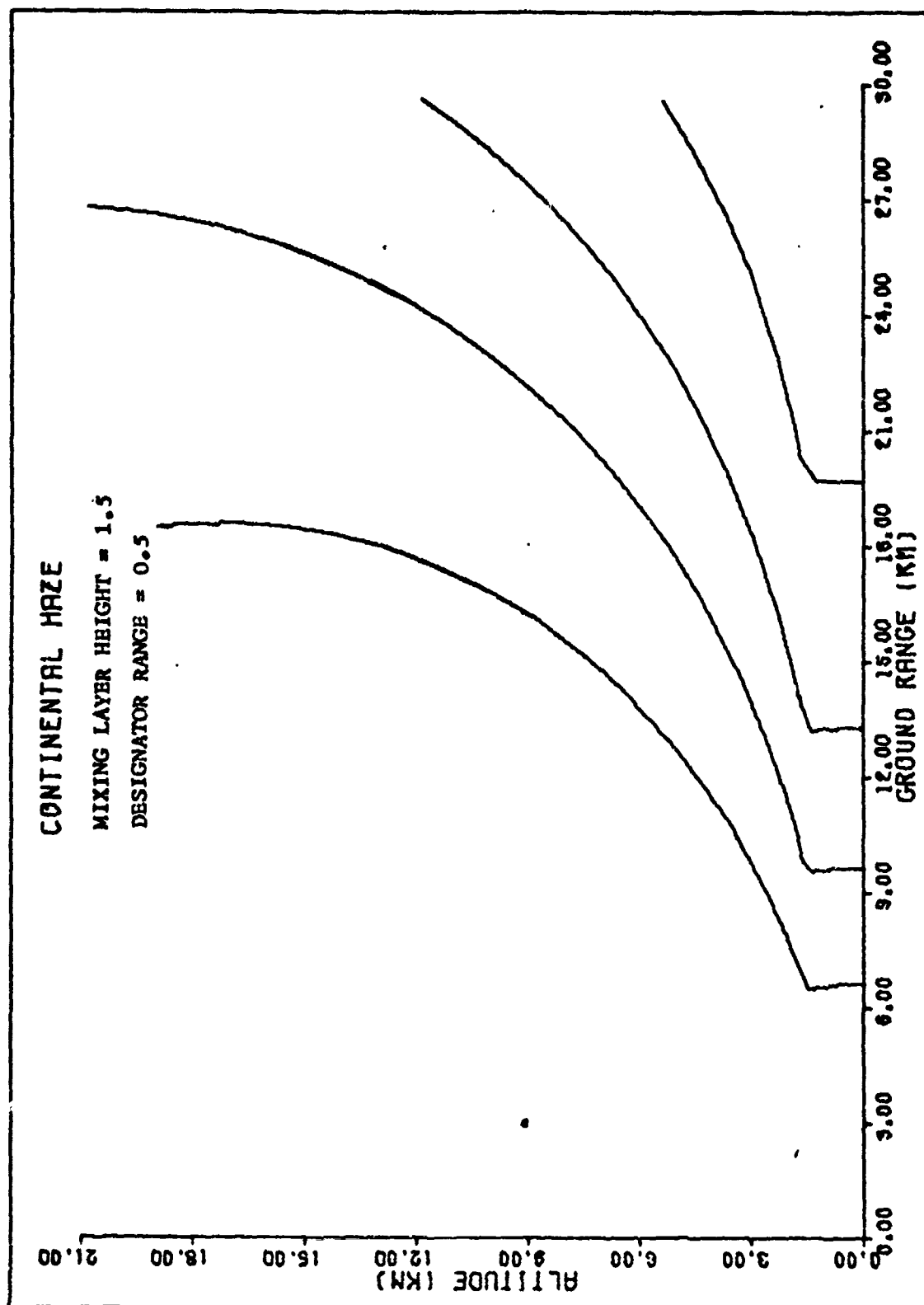Fig. 21 Maximum Lock-on Range with Ground Designator at Several Meteorological Ranges, Homogeneous Mixing Layer Model.
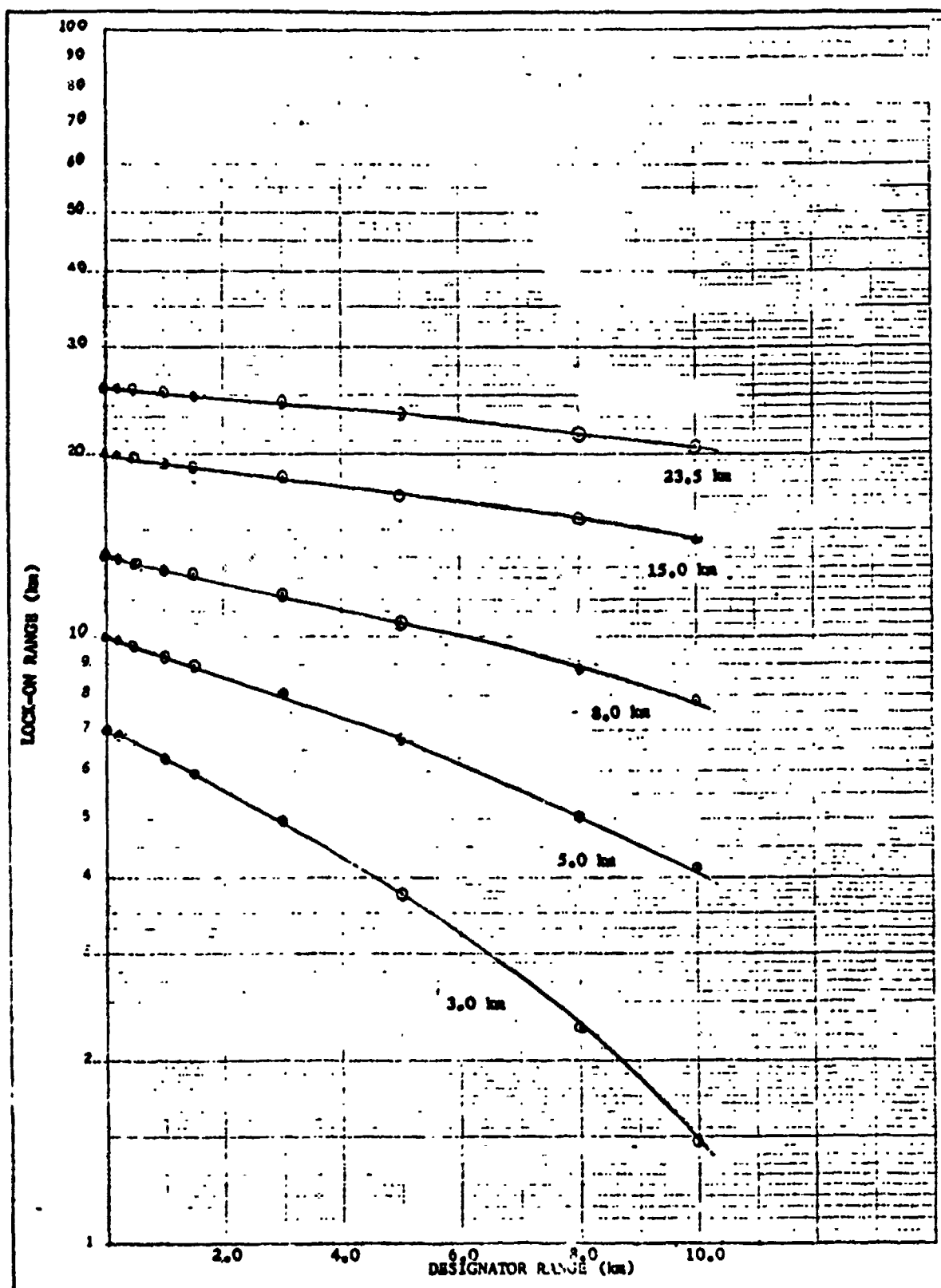
Fig. 22 Mixing Layer Lock-on Range vs Ground Designator Range
for Several Meteorological Ranges.

3 km, and the designator at 0.5 km from the target, the maximum lock-on range increases from 10.25 km with designator and receiver collocated to 15.1 km, an increase of 47%. Compare Fig. 21, page 64, to Fig. 6, page 44. Fig. 22 on the preceding page shows lock-on range in the mixing layer vs ground designator range for various meteorological range conditions. As the visibility increases, the position of the ground designator has less effect on the maximum lock-on range. Figs. 26A through 26E in Appendix B, page 95, show several examples of how position of the designator affects lock-on range.

Laser Design Parameters

A sensitivity study was accomplished to determine the effects on maximum lock-on ranges of changing various laser design parameters. This would change the value of $\sqrt{K}$ in Eq 5, page 9. The results are shown in Table VII. For example, if peak designator output power or target reflectance is doubled, $\sqrt{K}$ goes from 81.8 km to 116.6 km. The surface lock-on range is increased by 14% for a meteorological range of 23.5 km or 10% for 5 km meteorological range.

Table VII

Surface Lock-on Ranges for 100% Continental Air Mass
for Various Values of $\sqrt{K}$ and Meteorological Range

$\sqrt{K}$ (km)	Surface Meteorological Range (km)				
	3.0	5.0	8.0	15.0	23.5
116.6	4.60	6.75	9.50	14.71	19.77
81.8	4.22	6.13	8.53	13.03	17.29
69.3	4.04	5.86	8.13	12.29	16.19
58.2	3.86	5.56	7.68	11.52	15.08
26.1	3.05	4.28	5.74	8.22	10.33

Surface Lock-on Range Approximations

By using several approximations the surface lock-on range, with receiver and designator collocated, can be calculated fairly accurately by using a simple algebraic expression, with K, MR, and % maritime as variables. Thus it becomes an easy matter to determine the relative effects of changing these variables with a small electronic calculator or slide rule without solving the transcendental equations described earlier.

The first of these expressions, for 100% continental haze, is

$$R = \rho \ln \frac{K}{A} \qquad (85)$$

where

$$A = 0.74(MR)^{0.604} \qquad (86)$$

and

$$\rho = 0.40(MR)^{0.872} \qquad (87)$$

This relationship is good to within about 3% of computer values for values of $\sqrt{K}$ between 25 and 200 and within 6% for $\sqrt{K}$ of 400.

For mixtures of maritime and continental air masses, with % maritime greater than 10%, the relationship is

$$R = 0.455(\sqrt{K})^{0.257}(MR)^{0.73}(\% \text{ maritime})^{-0.037} \qquad (88)$$

This will give values within 3% of Eq (5), page 8, for values of $\sqrt{K}$ above 45 while as $\sqrt{K}$ decreases to 25 the error goes to 10%.

An attempt was made to find a simple algebraic relation for lock-on range at any given altitude as a function of meteorological range or surface lock-on range but no such relationship was found. Hence it is still necessary to use the transcendental equations for these solutions.

VI. Conclusions and Recommendations

This report has addressed the problem of quantifying the effects of weather on 1.06 micron laser-guided weapons. It has presented an easily useable model for computing maximum lock-on ranges at altitudes in and above the mixing layer for these weapons as a function of (1) surface meteorological range and (2) rainfall rates. Additionally, a simple expression was given for computing surface or mixing layer lock-on ranges.

The lock-on range is strongly affected by the aerosol concentration and particle size distribution. The concentration can be estimated rather quickly and easily through meteorological range observations. The particle size distribution is much more difficult and .ime consuming to measure, and several models have been proposed to describe the distribution.

Two aerosol altitude profiles were studied. The first was the Homogeneous Mixing Layer model as developed by Coolidge. The second was an approximation of the model described by McClatchey. Incorporated in each of these models were three different aerosol particle size distributions proposed by Dermendjian. These were (1) Haze L, (2) Continental, and (3) Maritime. Additionally, various mixtures of continental and maritime were used. Also included were various rainfall rates. The results of computations using these two models were analyzed and compared.

Conclusions

It is concluded that the effect of weather on the 1.06 micron laser-guided weapon can be quantified for a large range of weather conditions, provided that the aerosol characteristics of the atmosphere can be accurately modeled. It is further concluded that in the absence of more accurate information, useful relative information can be obtained by using models that are now available.

Based on recent conclusive evidence as referenced in this study, it is concluded that the most representative aerosol profile of the atmosphere is the Homogeneous Mixing Layer model. The most significant factors in this model as they relate to laser lock-on range are (1) surface meteorological range, (2) the aerosol particle size distribution, and (3) the height of the mixing layer. The scale height of the attenuation coefficient above the mixing layer has less significant effects.

Recommendations

In the past, lock-on range calculations have been done using the McClatchey atmospheric model. However it has been shown in this report that large differences occur in the results of using the McClatchey model and the Homogeneous Mixing Layer model. Because recent evidence is overwhelmingly in favor of the Homogeneous Mixing Layer model in the lower atmosphere, it is recommended that, until more precise information on the atmosphere becomes available, future studies and calculations be done using the Homogeneous Mixing Layer model.

Because of the significant limitations that atmospheric aerosols can impose on 1.06 micron laser guided-weapons and the need to quantify these limitations, the following recommendations are also made:

(1) better methods be developed to accurately and quickly (preferably in real time) determine experimentally the aerosol concentration and particle size distribution, (2) methods be developed for more accurately and quickly determining the vertical aerosol attenuation profile, including the height of the mixing layer, and (3) a method be developed for measuring directly the attenuation of 1.06 micron laser radiation. This last recommendation would lessen the need for accurately knowing the particle size distribution. Additionally, work needs to be done to better quantify rainfall effects as well as effects of other forms of precipitation on laser propagation.

There are methods which show promise in some of these areas. For example, reference 31 gives a summary of some methods used to determine mixing layer height and suggests a new method based only on surface measurements. This merits more study. Reference 6 describes a method for using lidar in mixing layer measurements. Reference 34 describes several instruments which can be used to measure weather variables.

Bibliography

1. Andreyev, S. D. et al. "Certain Characteristics of Spectral Transmission of Atmospheric Hazes in the Visible and Infrared." Izv., Atmospheric and Oceanic Physics, Vol 8, No. 12:1261-1267 (1972).

2. Atlas, R. "Optical Extinction by Rainfall." Journal of Meteorology, 10:486-488 (December 1953).

3. Atlas, D. and E. Kessler, III. "A Model Atmosphere for Widespread Precipitation." Aeronatical Engineering Review, 16:69-77 (February 1957).

4. Buck, A. I. "Effects of the Atmosphere on Laser Beam Propagation." Applied Optics, 6:703-706 (April 1967).

5. Bullrich, K. et al. "New Aspects of Scattering and Absorbing Properties of Atmospheric Aerosol Particles." Journal of Colloid and Interface Science, 39:546-550 (June 1972).

6. Collis, R. T. H. "Lidar." Applied Optics, 9:1782-1788 (August 1970).

7. Coolidge, C. H. Jr. Atmospheric Transmission of 1.06 Micron Laser Radiation: Application to Stand-off Missile Performance. Masters Thesis. Wright-Patterson AFB, Ohio: Air Force Institute of Technology, March 1974.

8. Deirmendjian, D. "The Role of Water Particles in the Atmospheric Transmission of Infra-red Radiation." Quarterly Journal of the Royal Meteorological Society, 85:404-411 (October 1959).

9. ------. "Scattering and Polarization Properties of Water Clouds and Hazes in the Visible and Infrared." Applied Optics, Vol. 3, No. 2: 187-196 (February 1964).

10. ------. Electromagnetic Scattering on Spherical Polydispersions. RAND Corporation Report Number R-456-PR. New York: American Elsevier Publishing Company, Inc., April 1969.

11. Duntley, S. Q. et al. Airborne Measurements of Optical Atmospheric Properties in Southern Germany. AFCRL-72-0255 and SIO Ref. 72-64. San Diego, California: University of California, San Diego Scripps Institution of Oceanography, Visibility Laboratory, July 1972. AD747490

12. ------. Airborne and Ground-based Measurements of Optical Atmospheric Properties in Central New Mexico. AFCRL-72-0413 and SIO Ref. 72-71. San Diego, California: University of California, San Diego Scripps Institution of Oceanography, Visibility Laboratory, September 1972.

13. ------. Airborne Measurements of Optical Atmospheric Properties, Summary and Review. AFCRL-72-0593 and SIO Ref. 72-82. San Diego, California: University of California, San Diego Scripps Institution of Oceanography, Visibility Laboratory, November 1972. AD754898

14. Electro-Optics Handbook, Burlington, Massachusetts: RCA Defense Electronics Products, May 1968.

15. Electro-Optics Handbook, Lancaster, Pennsylvania: RCA Electronic Components, 1974.

16. Elterman L. and R. B. Toolin. "Atmospheric Optics." Chapter 7 in Handbook of Geophysic and Space Environments, L. G. Hanscom Field, Bedford, Massachusetts: Air Force Cambridge Research Laboratory, 1964.

17. Elterman, L. Atmospheric Attenuation Model, 1964, in the Ultraviolet, Visible, and Infrared Regions for Altitudes to 50 km. AFCRL-64-740 and Environmental Research Papers No. 46. L. G. Hanscom Field, Bedford, Massachusetts: Air Force Cambridge Research Laboratories, September 1964. AD607859

18. ------. UV, Visible, and IR Attenuation for Altitudes to 50 km, 1968. AFCRL-68-0153 and Environmental Research Papers, No. 285. L. G. Hanscom Field, Bedford, Massachusetts: Air Force Cambridge Research Laboratories, April 1968. AD671938

19. ------. Vertical-Attenuation Model with Eight Surface Meteorological Ranges 2 to 13 Kilometers. AFCRL-70-0200 and Environmental Research Papers, No. 318. L. G. Hanscom Field, Bedford, Massachusetts: Air Force Cambridge Research Laboratories, March 1970.

20. Gilbertson, D. K. Study of Tactical Army Aircraft Landing Systems (TAALS). Technical Report ECOM-03367-4, Interim Report 1 July 1963 to 30 June 1964, Report No. 4. Burlington, Massachusetts: Radio Corporation of America, Defense Electronics Products, Aerospace Systems Division, January 1966. AD477727

21. Junge, C. E. Air Chemistry and Radioactivity. New York: Academic Press, 1963.

22. Koshmieder, H. "Theorie der horisontalen Sichtweite." Beitr. Physfrein Atm. 12:33-53 and 171-181, 1924.

23. Landsberg, H. E. and O. V. Miegham (Editors). Advances in Geophysics, Vol. 10, New York: Academic Press, 1964.

24. Lund, I. A. Haze-Free and Cloud-Free Lines-of-Sight Through the Atmosphere. AFCRL-72-0540, and Environmental Research Papers, No. 413. L. G. Hanscom Field, Bedford, Massachusetts: Air Force Cambridge Research Laboratories, 13 September 1972. AD751264

25. Mardis, J. V. Lock-on Ranges of Laser-Guided Systems. Masters Thesis. Wright-Patterson AFB, Ohio: Air Force Institute of Technology, June 1972.

26. McClatchey, R. A. et al. Optical Properties of the Atmosphere, (Third Edition). AFCRL-72-0497 and Environmental Research Papers, No. 411. L. G. Hanscom Field, Bedford, Massachusetts: Air Force Cambridge Research Laboratories, 24 August 1972.

27. Middleton, W. E. K. Vision Through the Atmosphere. Toronto: University of Toronto Press, 1952.

28. Moller, F. "Optics of the Lower Atmosphere." Applied Optics, Vol. 3, No. 2:157-165 (February 1964).

29. Muench, H. S. et al. Development and Calibration of the Forward Scatter Visibility Meter. AFCRL-TR-74-0145. Instrumentation Papers, No. 217. L. G. Hanscom Field, Bedford, Massachusetts: Air Force Cambridge Research Laboratories, 18 March 1974.

30. Muneck, R. J. "Turbulent Backscatter of Light." Journal of the Optical Society of America. 55:393 (July 1965).

31. Nozaki, K. Y. Mixing Depth Model Using Hourly Surface Observations. Part 1, Report 7053. Washington: USAF Environmental Technical Applications Center, November 1973.

32. Shipley, S. T. et al. "Measurement of Rainfall Rates by Lidar." Journal of Applied Meteorology, 13:800-807 (October 1974).

33. Tennekes, H. "The Atmospheric Boundary Layer." Physics Today, Vol. 27, No. 1:52-63 (January 1974).

34. Try, P. D. "Atmospheric Measurements for Close Air Support Evaluation." Paper presented at 34th Symposium, Military Operations Research Society, US Army Transportation Center, Fort Eustis, Virginia, 3-5 December 1974.

35. Van de Hulst, H. C. Light Scattering by Small Particles. New York: John Wiley and Sons, Inc., 1957.

36. Zuev, V. E. et al. Reports of the USSR Academy of Science, Physics of the Atmosphere and the Ocean Series. Vol 3, No. 7. 1967.

37. Zuev, V. E. Propagation of Visible and Infrared Waves in the Atmosphere. Moscow: Soviet Radio, 1970. AD753974

38. Zuev, V. E. et al. "Recent Results from Studies of Atmospheric Aerosols." Izv., Atmospheric and Oceanic Physics, Vol. 9, No. 4:371-385 (1973).

Appendix A

Aerosol Attenuation Values for McClatchey Model

Table VIII

Aerosol Attenuation Coefficients
for Several Particle Size Distributions - McClatchey Model

	CONTINENTAL		MARITIME		25%M-75%C		50%M-50%C		HAZE L	
ALT	CLEAR	HAZE	CLEAR	HAZE	CLEAR	HAZE	CLEAR	HAZE	CLEAR	HAZE
0	8.77E-02	4.27E-01	1.63E-01	7.95E-01	1.52E-01	7.38E-01	1.59E-01	7.73E-01	1.29E-01	6.30E-01
1	5.81E-02	2.55E-01	1.08E-01	4.80E-01	1.00E-01	4.46E-01	1.05E-01	4.67E-01	8.57E-02	3.81E-01
2	2.53E-02	9.44E-02	4.71E-02	1.76E-01	4.37E-02	1.63E-01	4.58E-02	1.71E-01	3.73E-02	1.39E-01
3	1.08E-02	3.45E-02	2.01E-02	6.42E-02	1.87E-02	5.96E-02	1.96E-02	6.25E-02	1.59E-02	5.09E-02
4	5.09E-03	1.29E-02	9.47E-03	2.35E-02	8.79E-03	2.18E-02	9.22E-03	2.28E-02	7.51E-03	1.86E-02
5	3.21E-03	4.60E-03	5.97E-03	8.56E-03	5.55E-03	7.95E-03	5.81E-03	8.33E-03	4.74E-03	6.79E-03
6	2.34E-03	2.34E-03	4.36E-03	4.36E-03	4.04E-03	4.04E-03	4.24E-03	4.24E-03	3.45E-03	3.45E-03
7	1.90E-03	1.90E-03	3.54E-03	3.54E-03	3.28E-03	3.28E-03	3.44E-03	3.44E-03	2.80E-03	2.80E-03
8	1.86E-03	1.85E-03	3.45E-03	3.46E-03	3.21E-03	3.21E-03	3.37E-03	3.37E-03	2.74E-03	2.74E-03
9	1.46E-03	1.85E-03	3.44E-03	3.44E-03	3.20E-03	3.20E-03	3.35E-03	3.35E-03	2.73E-03	2.73E-03
10	1.74E-03	1.73E-03	3.31E-03	3.31E-03	3.06E-03	3.03E-03	3.22E-03	3.22E-03	2.63E-03	2.63E-03
11	1.70E-03	1.70E-03	3.16E-03	3.16E-03	2.94E-03	2.94E-03	3.08E-03	3.08E-03	2.51E-03	2.51E-03
12	1.69E-03	1.69E-03	3.15E-03	3.15E-03	2.92E-03	2.92E-03	3.06E-03	3.16E-03	2.49E-03	2.49E-03
13	1.67E-03	1.67E-03	3.11E-03	3.11E-03	2.89E-03	2.39E-03	3.02E-03	3.02E-03	2.46E-03	2.46E-03
14	1.55E-03	1.55E-03	2.94E-03	2.94E-03	2.73E-03	2.73E-03	2.86E-03	2.86E-03	2.33E-03	2.33E-03
15	1.52E-03	1.52E-03	2.83E-03	2.83E-03	2.63E-03	2.63E-03	2.75E-03	2.75E-03	2.24E-03	2.24E-03
16	1.43E-03	1.43E-03	2.66E-03	2.66E-03	2.47E-03	2.47E-03	2.59E-03	2.59E-03	2.11E-03	2.11E-03
17	1.39E-03	1.34E-03	2.59E-03	2.59E-03	2.40E-03	2.40E-03	2.52E-03	2.52E-03	2.05E-03	2.05E-03
18	1.35E-03	1.33E-03	2.53E-03	2.53E-03	2.35E-03	2.35E-03	2.46E-03	2.46E-03	2.01E-03	2.01E-03
19	1.23E-03	1.23E-03	2.29E-03	2.29E-03	2.13E-03	2.13E-03	2.23E-03	2.23E-03	1.32E-03	1.32E-03
20	9.66E-04	9.60E-04	1.80E-03	1.80E-03	1.67E-03	1.67E-03	1.75E-03	1.75E-03	1.43E-03	1.43E-03
21	7.04E-04	7.04E-04	1.31E-03	1.31E-03	1.22E-03	1.22E-03	1.28E-03	1.28E-03	1.04E-03	1.04E-03
22	5.26E-04	5.2?E-04	9.68E-04	9.68E-04	8.93E-04	8.93E-04	9.42E-04	9.42E-04	7.67E-04	7.67E-04
23	3.95E-04	3.95E-04	7.35E-04	7.35E-04	6.82E-04	6.82E-04	7.15E-04	7.15E-04	5.83E-04	5.83E-04
24	3.07E-04	3.07E-04	5.71E-04	5.71E-04	5.30E-04	5.30E-04	5.50E-04	5.50E-04	4.53E-04	4.53E-04
25	2.51E-04	2.51E-04	4.67E-04	4.67E-04	4.34E-04	4.34E-04	4.55E-04	4.55E-04	3.7?E-04	3.7?E-04
30	1.26E-04	1.23E-04	2.35E-04	2.35E-04	2.18E-04	2.18E-04	2.28E-04	2.28E-04	1.85E-04	1.86E-04
35	3.56E-05	3.56E-05	6.63E-05	6.63E-05	6.15E-05	6.15E-05	6.42E-05	6.42E-05	5.22E-05	5.25E-05
40	9.37E-06	9.37E-06	1.74E-05	1.74E-05	1.62E-05	1.62E-05	1.70E-05	1.71E-05	1.33E-05	1.34E-05
45	1.91E-06	1.91E-06	3.56E-06	3.56E-05	3.30E-06	3.30E-06	3.46E-06	3.46E-06	2.92E-06	2.92E-06

Table IX

Aerosol + Molecular (Midlatitude Summer) Attenuation Coefficients for Several Particle Size Distributions – McClatchey Model

ALT	CONTINENTAL		MARITIME		25%H-75%C		50%H-50%C		HAZE L	
	CLEAR	HAZE	CLEAR	HAZE	CLEAR	HAZE	CLEAR	HAZE	CLEAR	HAZE
0	6.85E-02	4.28E-01	1.64E-01	7.96E-01	1.52E-01	7.39E-01	1.63E-01	7.74E-01	1.30E-01	6.31E-01
1	5.89E-02	2.59E-01	1.09E-01	4.81E-01	1.01E-01	4.47E-01	1.06E-01	4.66E-01	8.65E-02	3.82E-01
2	2.60E-02	9.51E-02	4.78E-02	1.76E-01	4.44E-02	1.64E-01	4.65E-02	1.72E-01	3.80E-02	1.40E-01
3	1.19E-02	3.51E-02	2.07E-02	6.49E-02	1.93E-02	6.02E-02	2.02E-02	6.31E-02	1.66E-02	5.16E-02
4	5.67E-03	1.32E-02	1.01E-02	2.40E-02	9.37E-03	2.23E-02	9.80E-03	2.34E-02	8.09E-03	1.92E-02
5	3.73E-03	5.12E-03	6.50E-03	9.08E-03	6.07E-03	8.47E-03	6.34E-03	8.85E-03	5.26E-03	7.31E-03
6	2.81E-03	2.81E-03	4.82E-03	4.82E-03	4.51E-03	4.51E-03	4.71E-03	4.71E-03	3.92E-03	3.92E-03
7	2.32E-03	2.32E-03	3.96E-03	3.96E-03	3.70E-03	3.70E-03	3.86E-03	3.86E-03	3.22E-03	3.22E-03
9	2.24E-03	2.24E-03	3.84E-03	3.84E-03	3.59E-03	3.53E-03	3.75E-03	3.75E-03	3.12E-03	3.12E-03
9	2.17E-03	2.17E-03	3.78E-03	3.78E-03	3.53E-03	3.53E-03	3.69E-03	3.69E-03	3.07E-03	3.07E-03
10	2.04E-03	2.04E-03	3.62E-03	3.62E-03	3.36E-03	3.34E-03	3.53E-03	3.53E-03	2.93E-03	2.93E-03
11	1.97E-03	1.97E-03	3.43E-03	3.43E-03	3.21E-03	3.21E-03	3.35E-03	3.36E-03	2.79E-03	2.79E-03
12	1.93E-03	1.93E-03	3.38E-03	3.38E-03	3.16E-03	3.16E-03	3.30E-03	3.30E-03	2.73E-03	2.73E-03
13	1.85E-03	1.84E-03	3.32E-03	3.32E-03	3.10E-03	3.10E-03	3.24E-03	3.24E-03	2.69E-03	2.68E-03
14	1.76E-03	1.76E-03	3.12E-03	3.12E-03	2.91E-03	2.91E-03	3.04E-03	3.04E-03	2.51E-03	2.51E-03
15	1.61E-03	1.61E-03	2.90E-03	2.90E-03	2.78E-03	2.78E-03	2.91E-03	2.91E-03	2.43E-03	2.43E-03
15	1.56E-03	1.56E-03	2.79E-03	2.79E-03	2.60E-03	2.60E-03	2.72E-03	2.72E-03	2.24E-03	2.24E-03
17	1.50E-03	1.50E-03	2.70E-03	2.70E-03	2.52E-03	2.52E-03	2.63E-03	2.63E-03	2.17E-03	2.17E-03
18	1.46E-03	1.46E-03	2.63E-03	2.63E-03	2.45E-03	2.45E-03	2.50E-03	2.50E-03	2.12E-03	2.11E-03
19	1.31E-03	1.31E-03	2.37E-03	2.37E-03	2.21E-03	2.21E-03	2.31E-03	2.31E-03	1.90E-03	1.90E-03
20	1.04E-03	1.04E-03	1.87E-03	1.87E-03	1.74E-03	1.74E-03	1.82E-03	1.82E-03	1.50E-03	1.50E-03
21	7.74E-04	7.64E-04	1.37E-03	1.37E-03	1.28E-03	1.23E-03	1.34E-03	1.34E-03	1.10E-03	1.10E-03
22	5.71E-04	5.71E-04	1.02E-03	1.02E-03	9.50E-04	9.50E-04	9.93E-04	9.93E-04	8.13E-04	8.13E-04
23	4.39E-04	4.39E-04	7.79E-04	7.79E-04	7.26E-04	7.26E-04	7.59E-04	7.59E-04	6.27E-04	6.27E-04
24	3.44E-04	3.44E-04	6.09E-04	6.09E-04	5.68E-04	5.68E-04	5.93E-04	5.93E-04	4.90E-04	4.90E-04
25	2.63E-04	2.83E-04	4.99E-04	4.99E-04	4.66E-04	4.66E-04	4.87E-04	4.87E-04	4.02E-04	4.02E-04
30	1.48E-04	1.48E-04	2.56E-04	2.56E-04	2.39E-04	2.39E-04	2.50E-04	2.50E-04	2.07E-04	2.07E-04
35	4.55E-05	4.59E-05	7.62E-05	7.62E-05	7.14E-05	7.14E-05	7.44E-05	7.44E-05	6.24E-05	6.24E-05
40	1.41E-05	1.41E-05	2.22E-05	2.22E-05	2.09E-05	2.09E-05	2.17E-05	2.17E-05	1.85E-05	1.85E-05
45	4.22E-06	4.22E-06	5.87E-06	5.87E-06	5.61E-06	5.61E-06	5.77E-06	5.77E-06	5.13E-06	5.13E-06

Appendix B

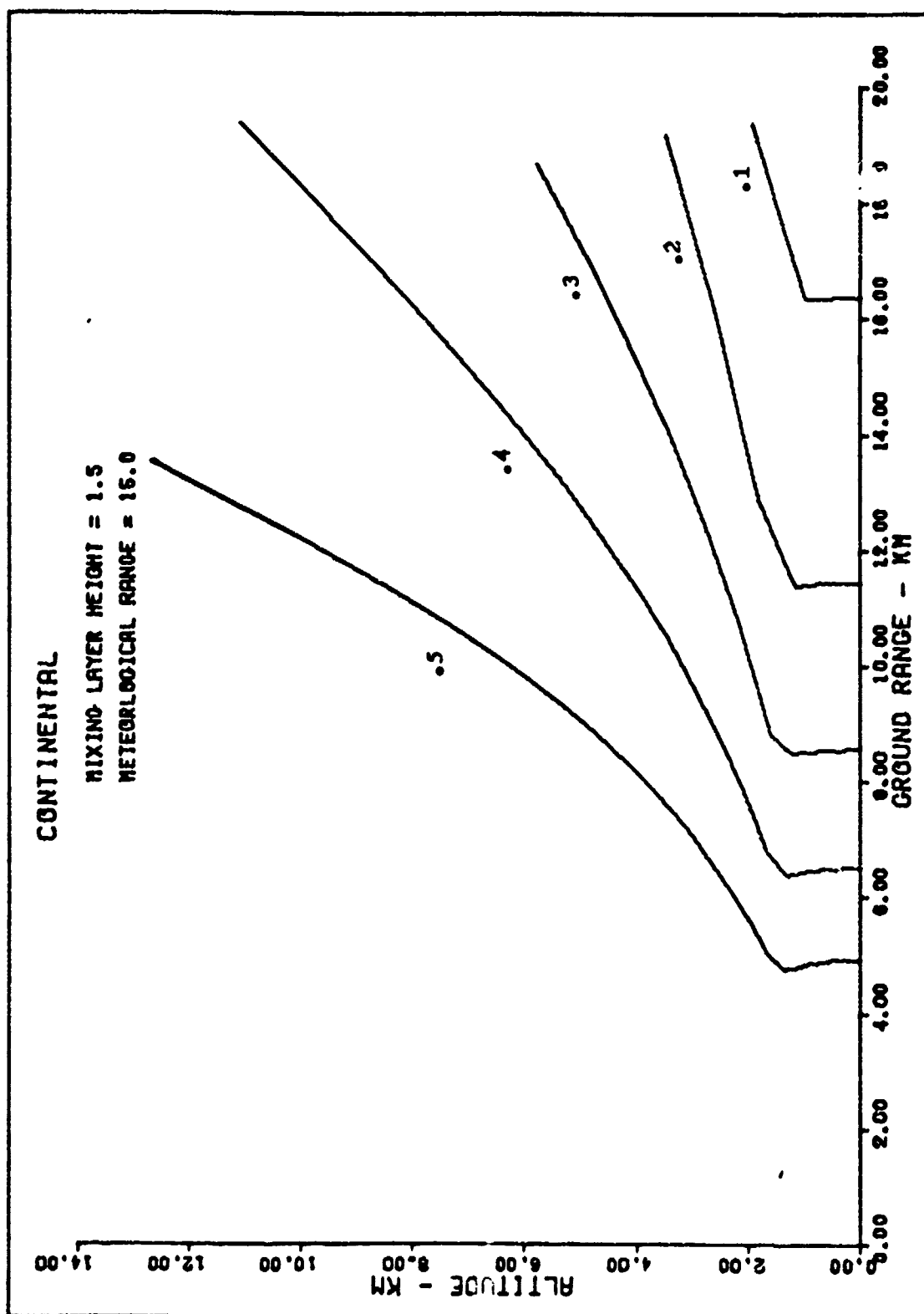Constant Transmittance Curves

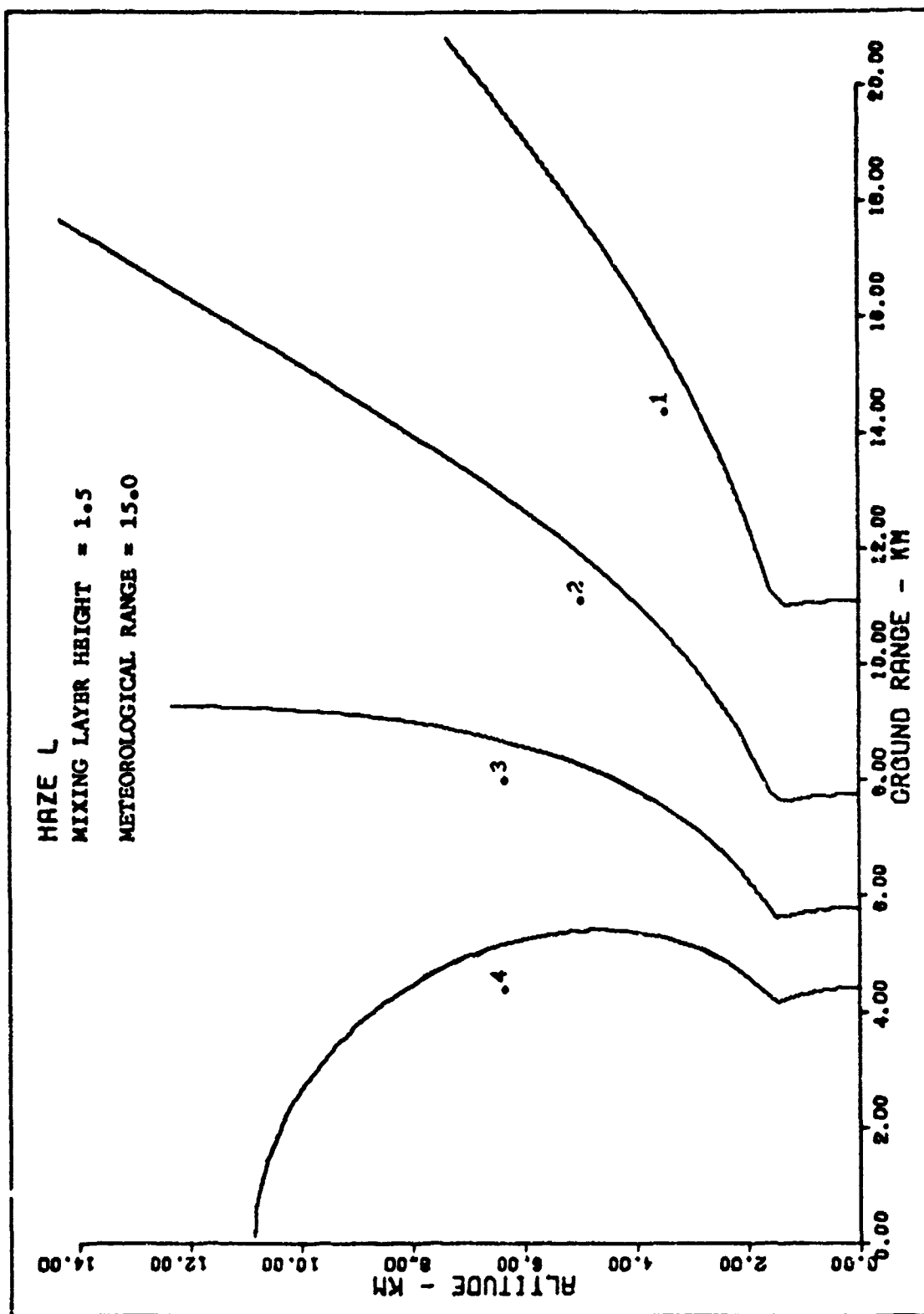Fig. 23 A Transmittance of 1.06 microns — Homogeneous Mixing Layer.

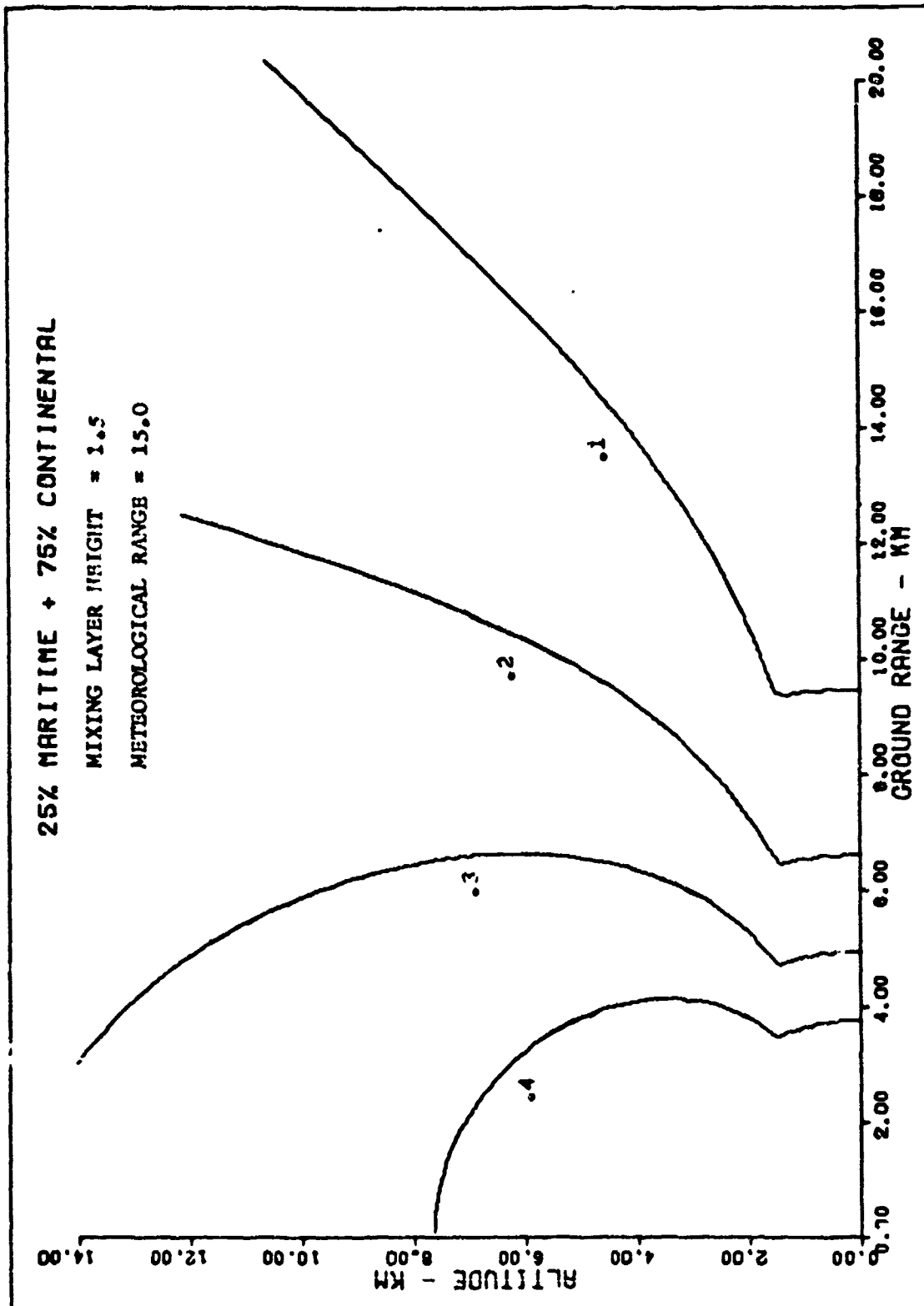Fig. 23 B Transmittance of 1.06 microns - Homogeneous Mixing Layer.

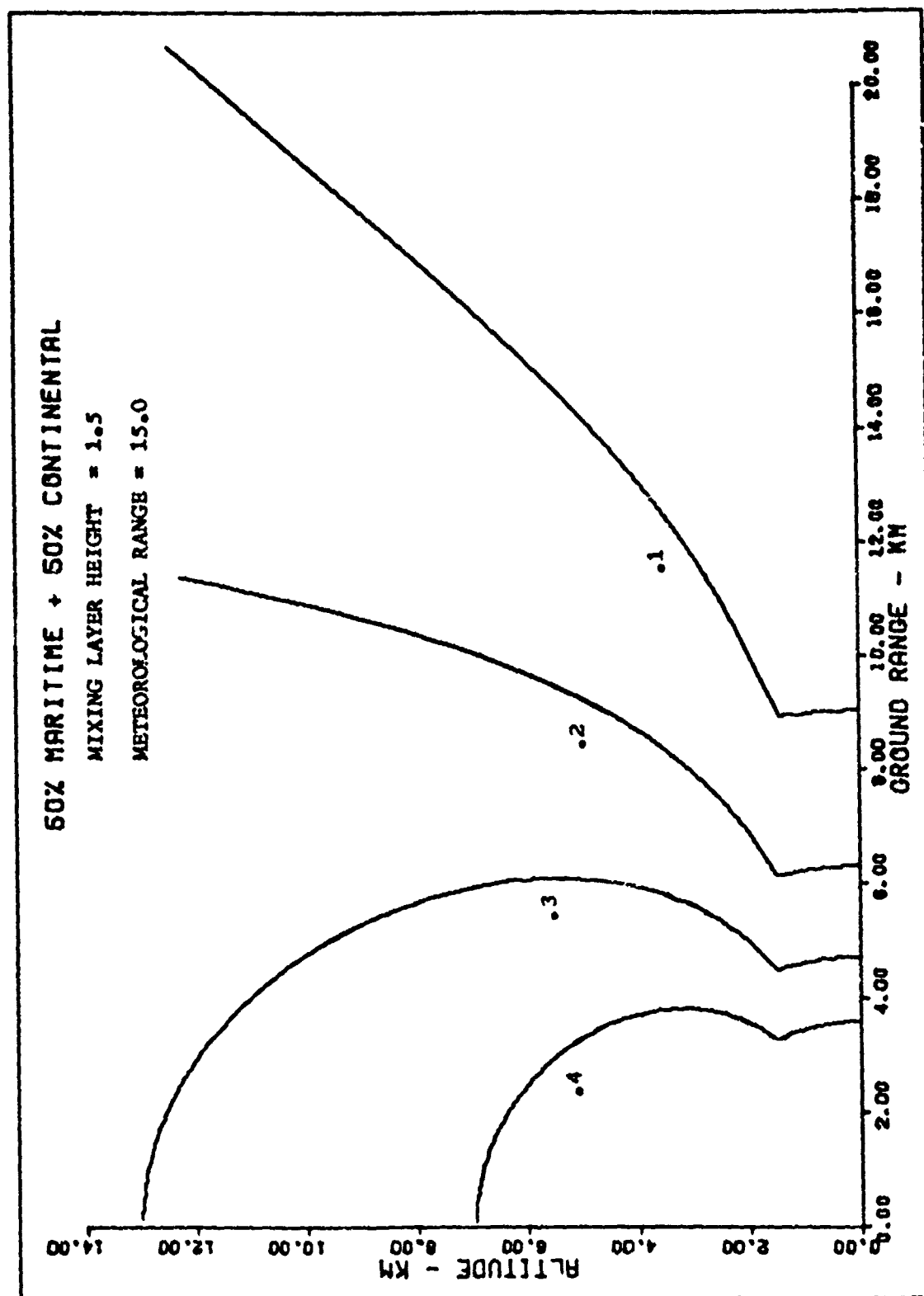Fig. 23 C Transmittance of 1.06 microns - Homogeneous Mixing Layer.

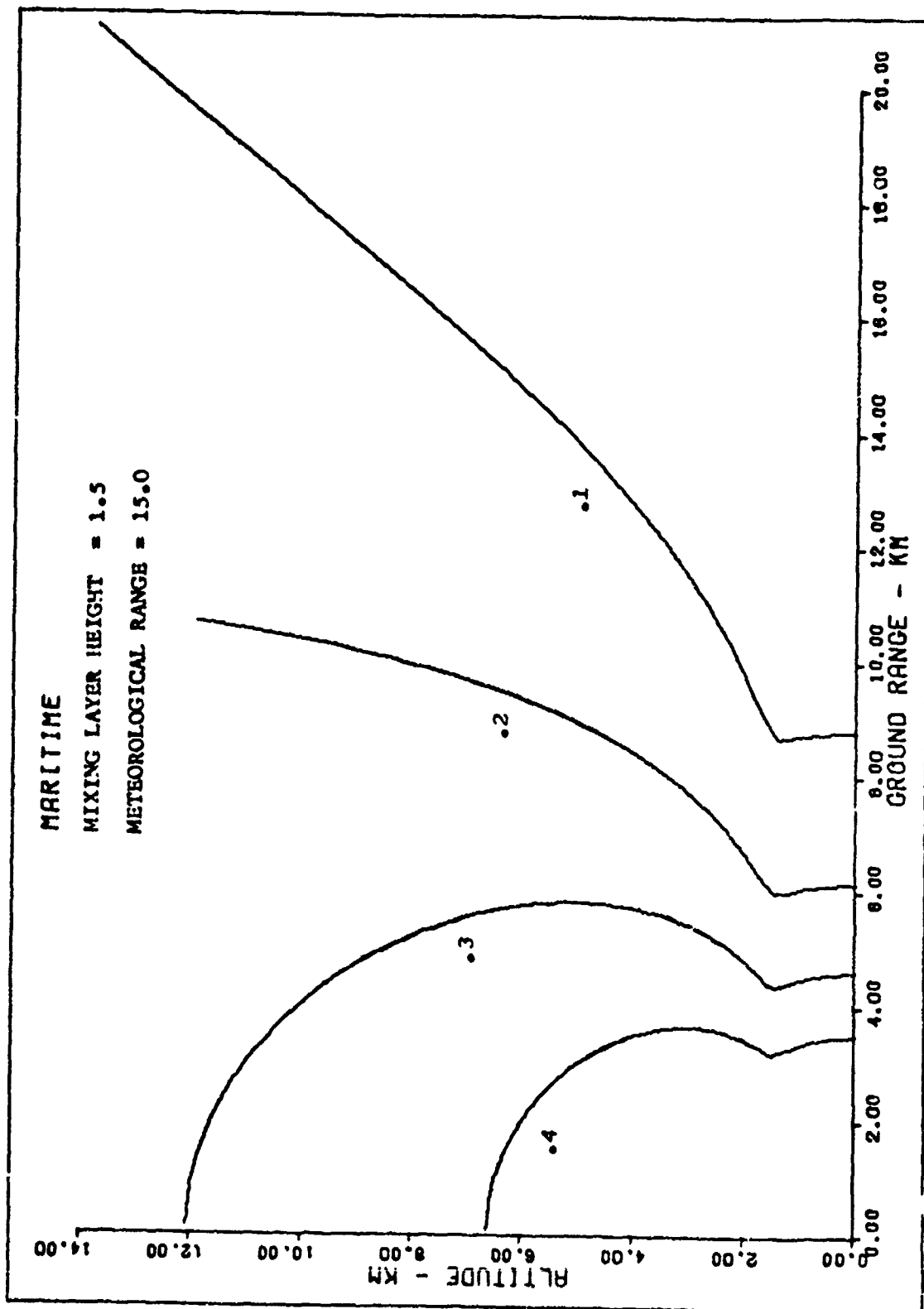Fig. 23 D Transmittance of 1.06 microns – Homogeneous Mixing Layer.

50% MARITIME + 50% CONTINENTAL

MIXING LAYER HEIGHT = 1.5

METEOROLOGICAL RANGE = 15.0

Fig. 23 E   Transmittance of 1.06 microns – Homogeneous Mixing Layer.

Appendix C

Maximum Lock-on Range Curves - Designator and Receiver Collocated
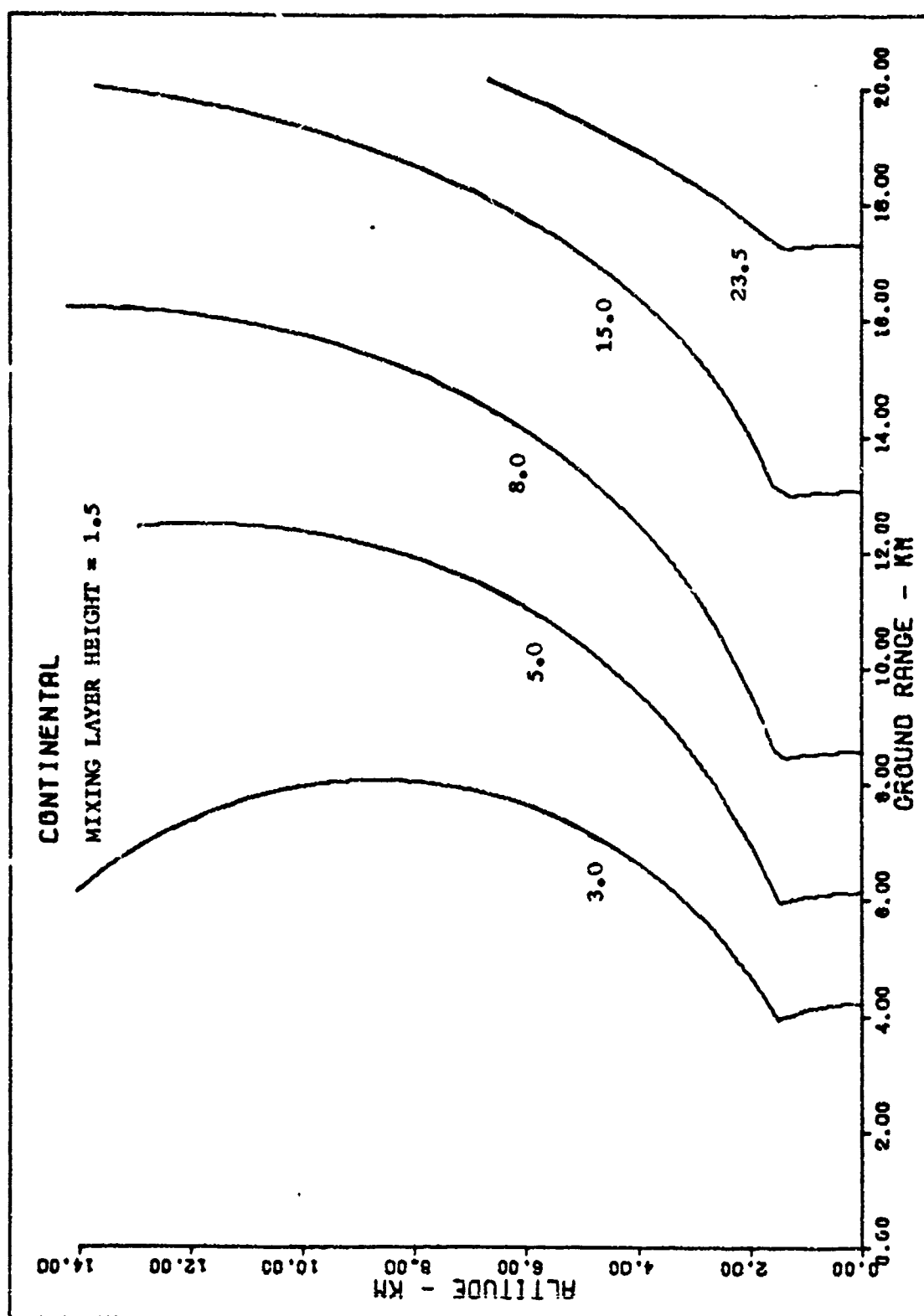
Fig. 24 A Maximum Lock-on Range with Designator and Receiver Collocated for Several Meteorological Ranges - Homogeneous Mixing Layer Model.
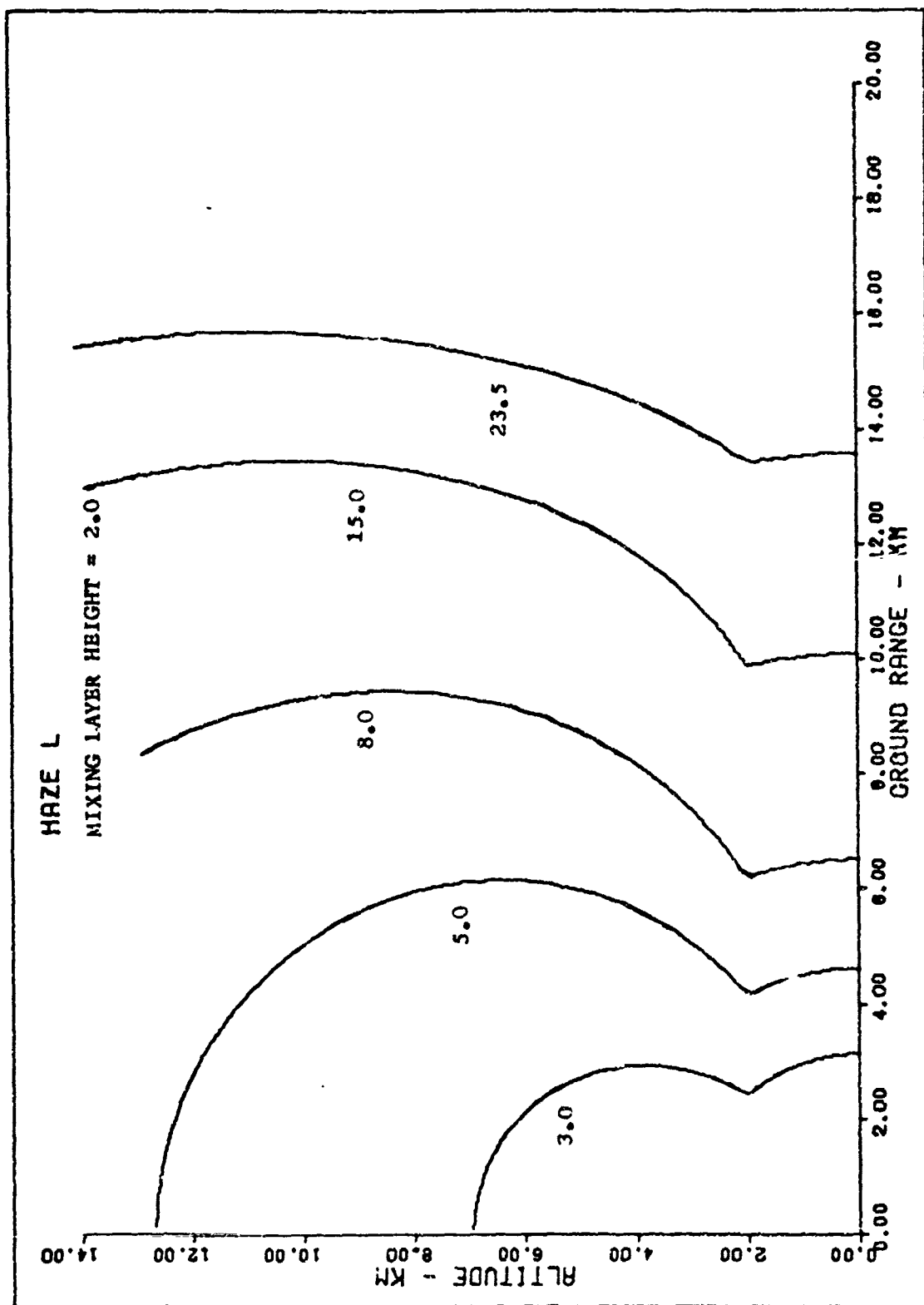
Fig. 24 B Maximum Lock-on Range with Designator and Receiver Collocated for Several Meteorological Ranges — Homogeneous Mixing Layer Model.
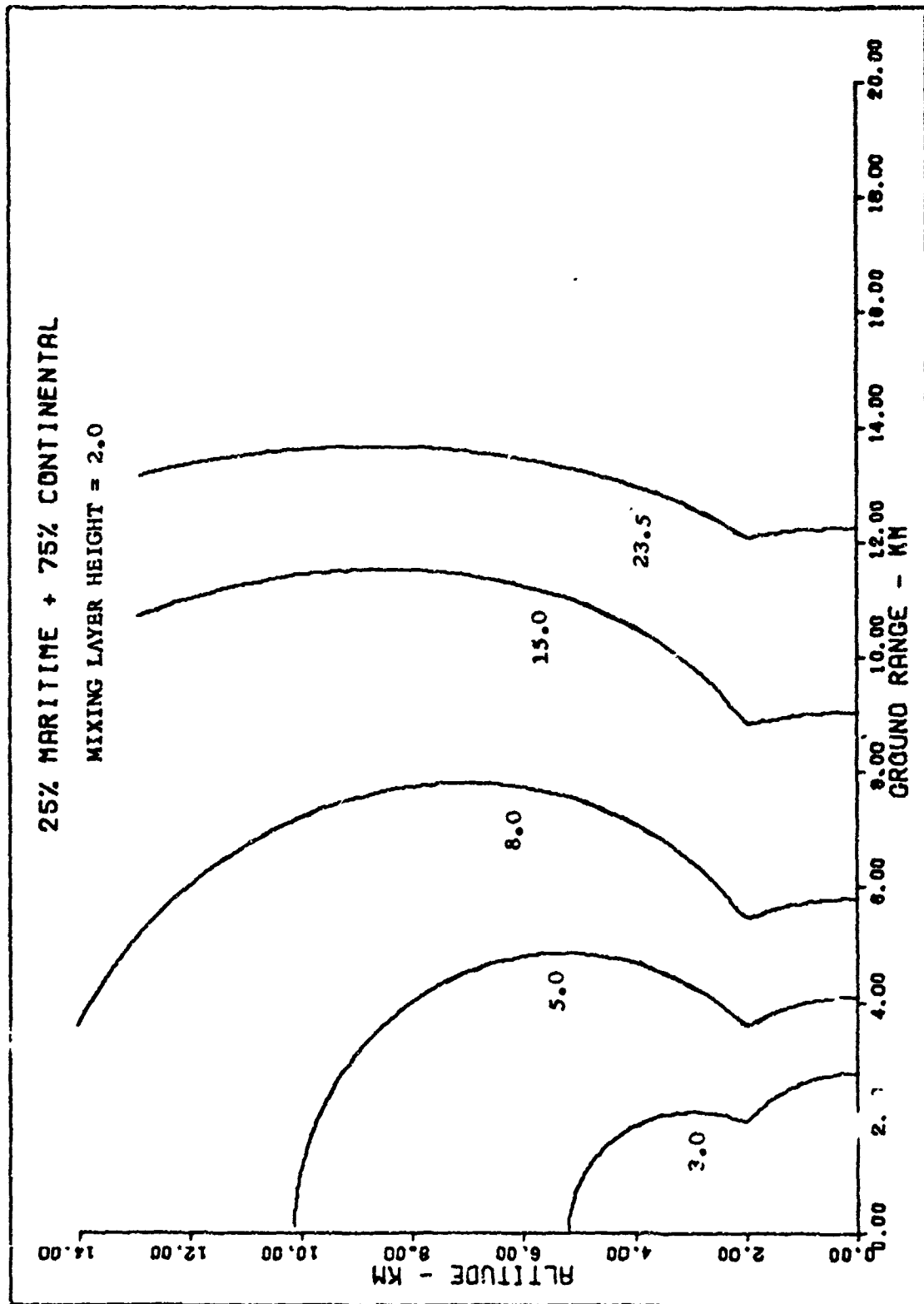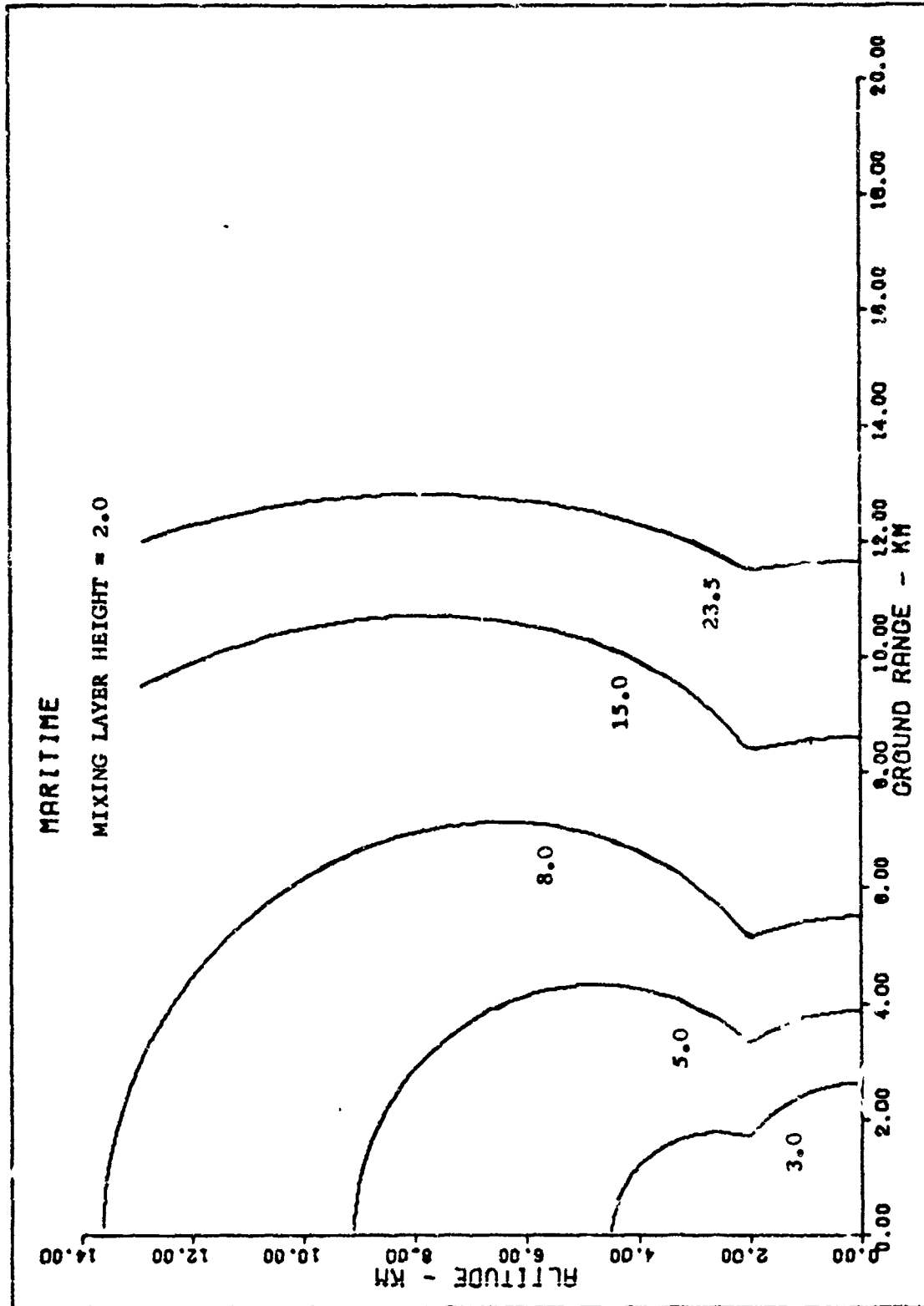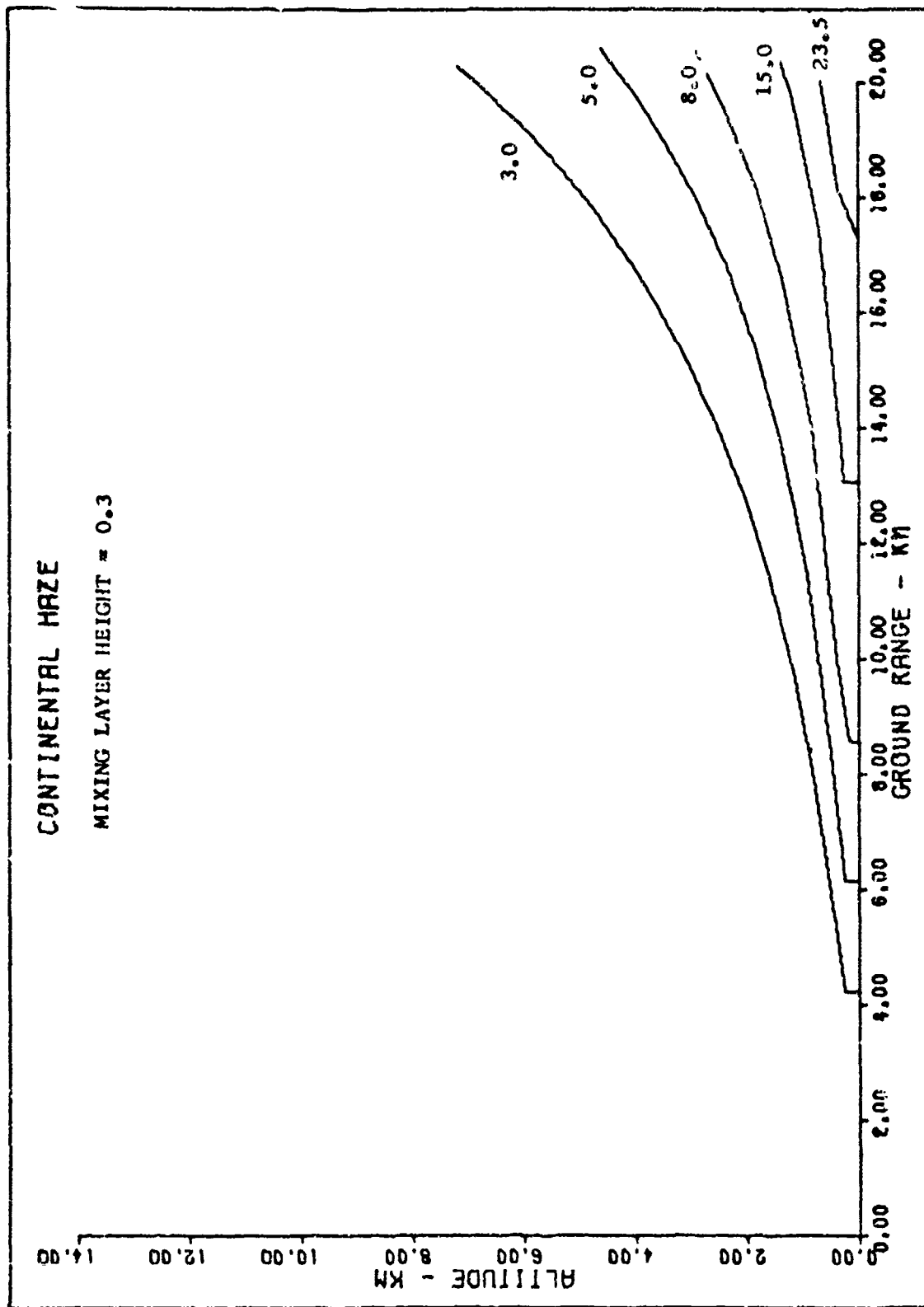
Fig. 24 C Maximum Lock-on Range with Designator and Receiver Collocated for Several Meteorological Ranges - Homogeneous Mixing Layer Model.
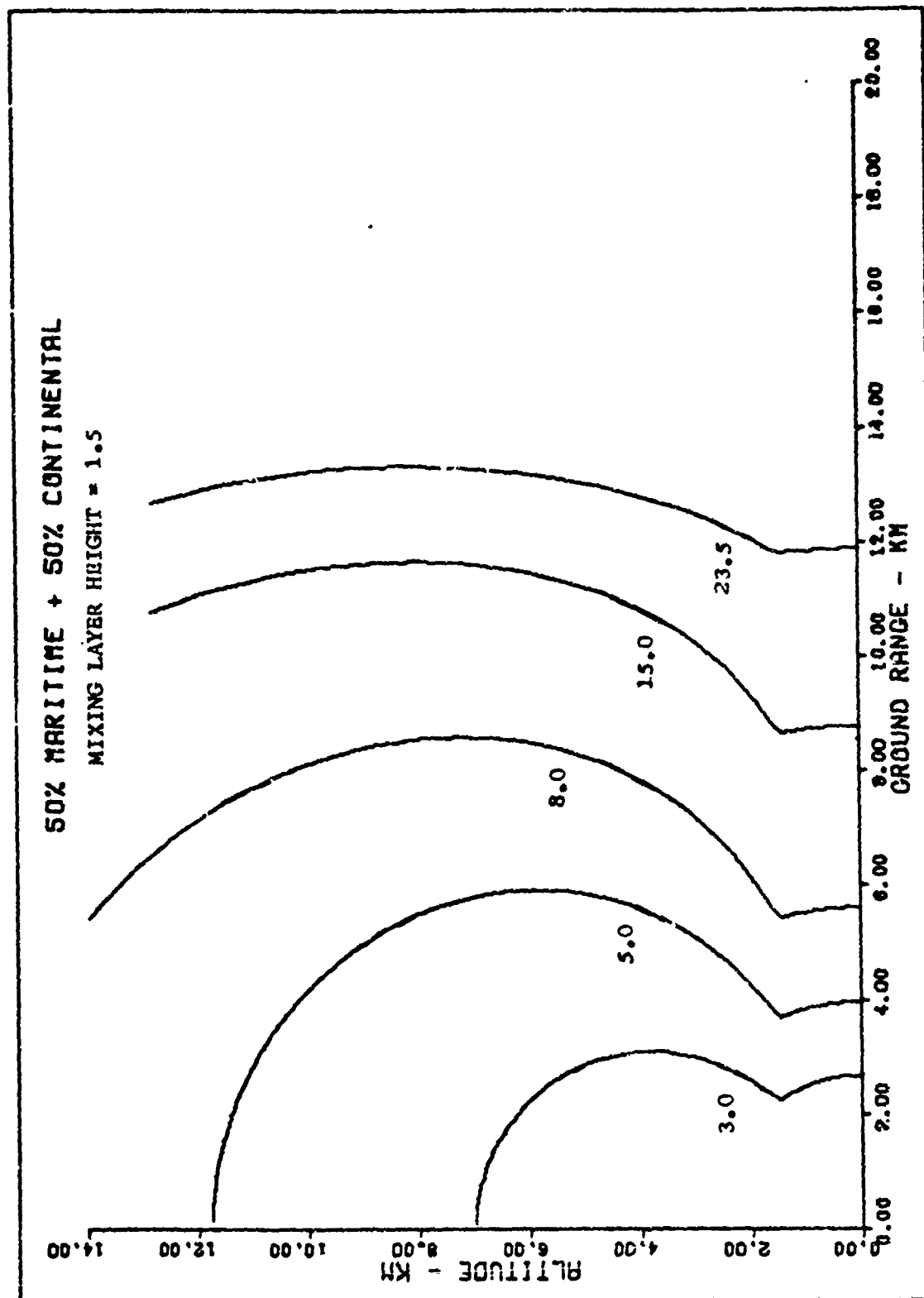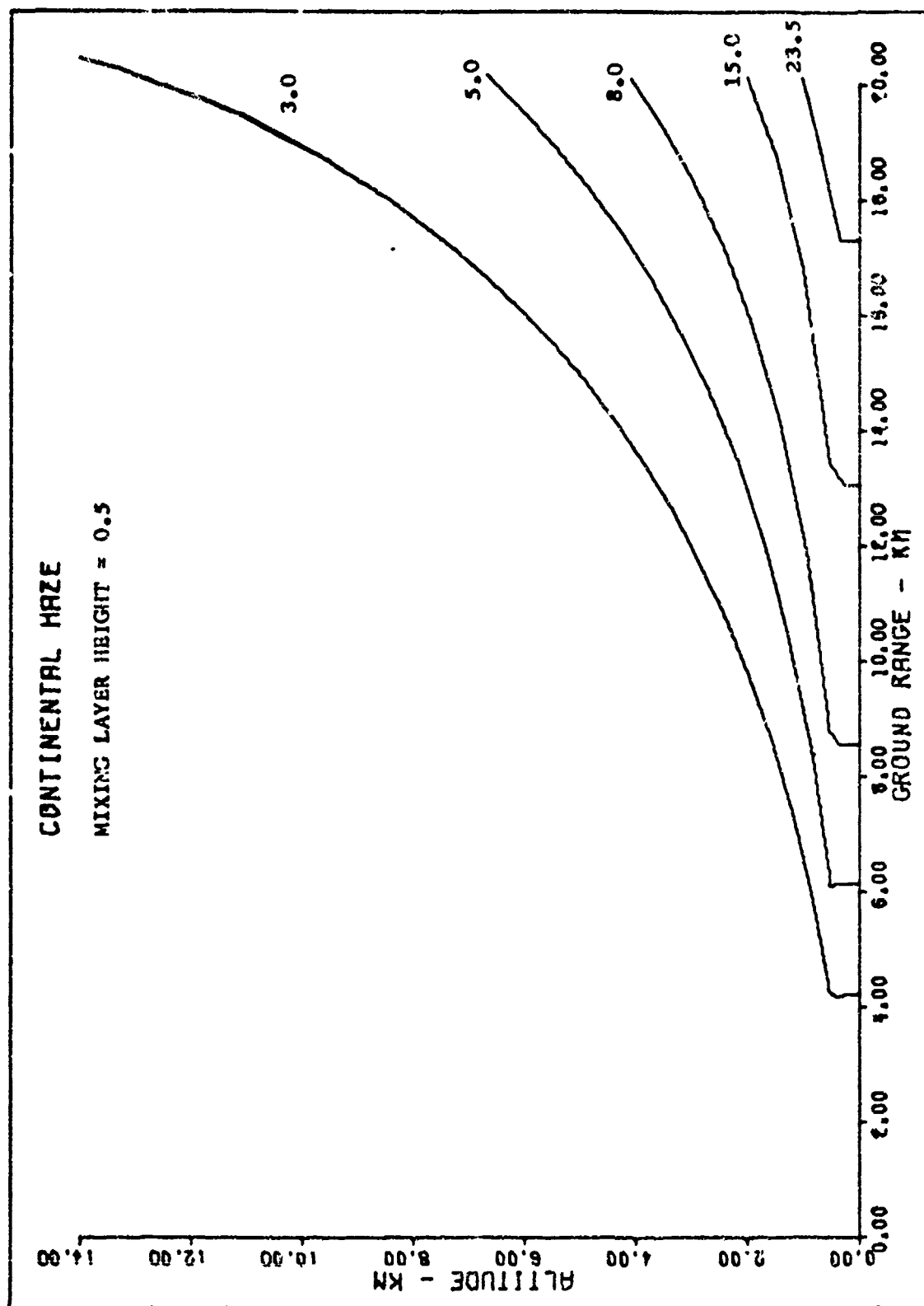
Fig. 24) Maximum Lock-on Range with Designator and Receiver Collocated for
Several Meteorological Ranges - Homogeneous Mixing Layer Model.

Fig. 24 E   Maximum Lock-on Range with Designator and Receiver Collocated for
Several Meteorological Ranges - Homogeneous Mixing Layer Model.
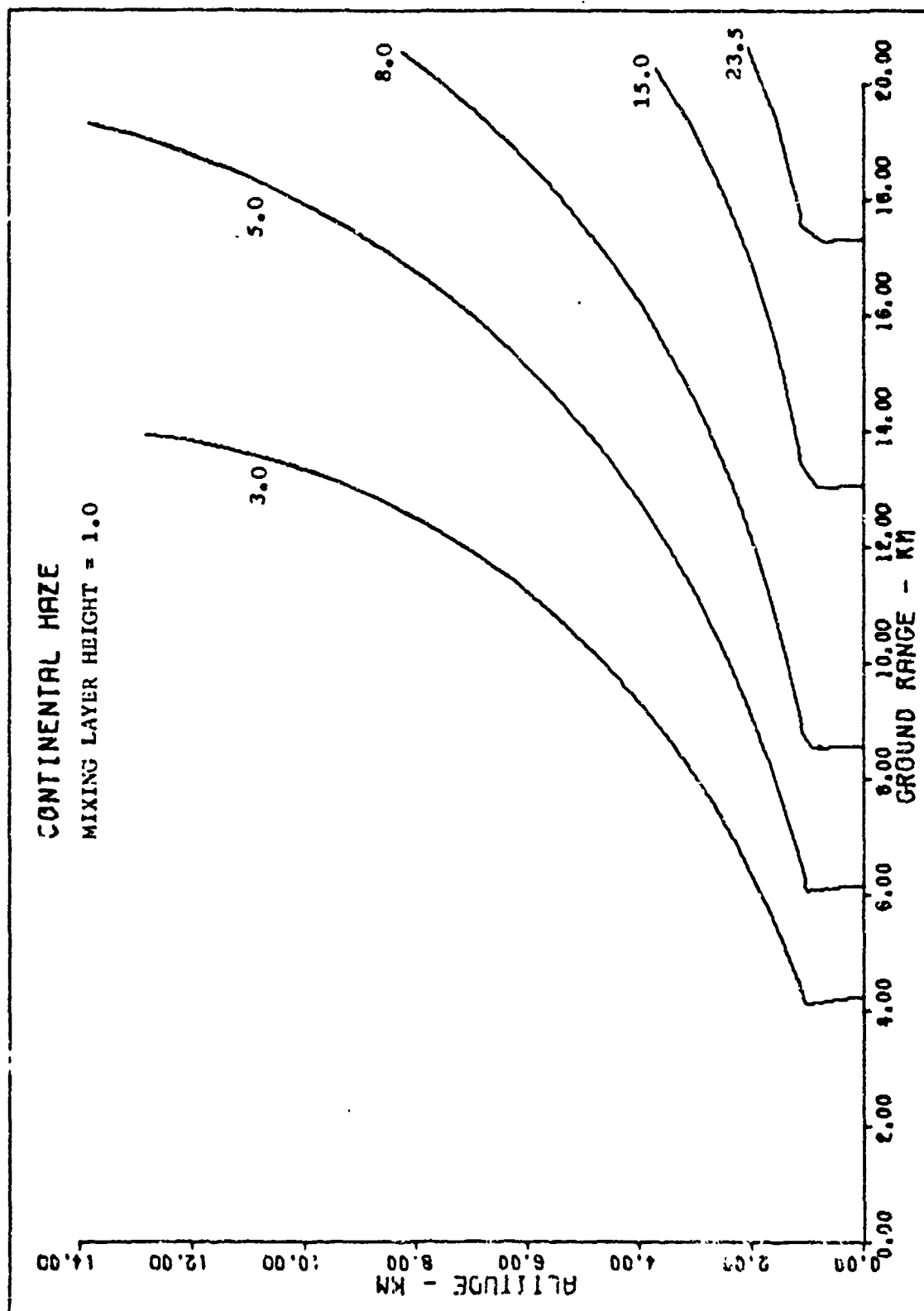
Appendix D

Effects of Mixing Layer Height Variations

Fig. 25 A Maximum Lock-on Range with Designator and Receiver Collocated for Several Meteorological Ranges – Homogeneous Mixing Layer Model.

Fig. 25 B Maximum Lock-on Range with Designator and Receiver Collocated for
Several Meteorological Ranges — Homogeneous Mixing Layer Model.

Fig. 25 C Maximum Lock-on Range with Designator and Receiver Collocated for Several Meteorological Ranges - Homogeneous Mixing Layer Model.
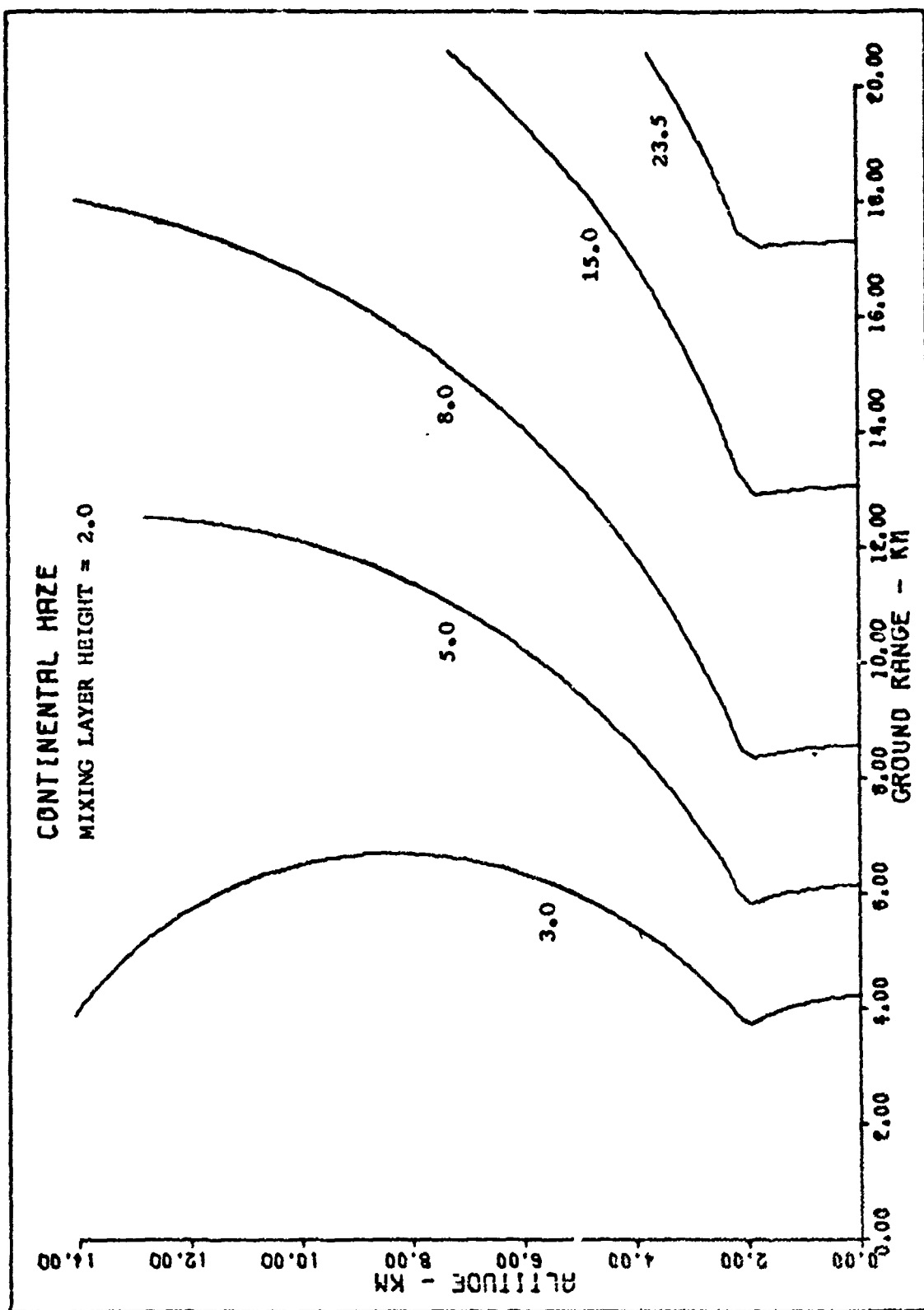
Fig. 25 D Maximum Lock-on Range with Designator and Receiver Collocated for Several Meteorological Ranges - Homogeneous Mixing Layer Model.
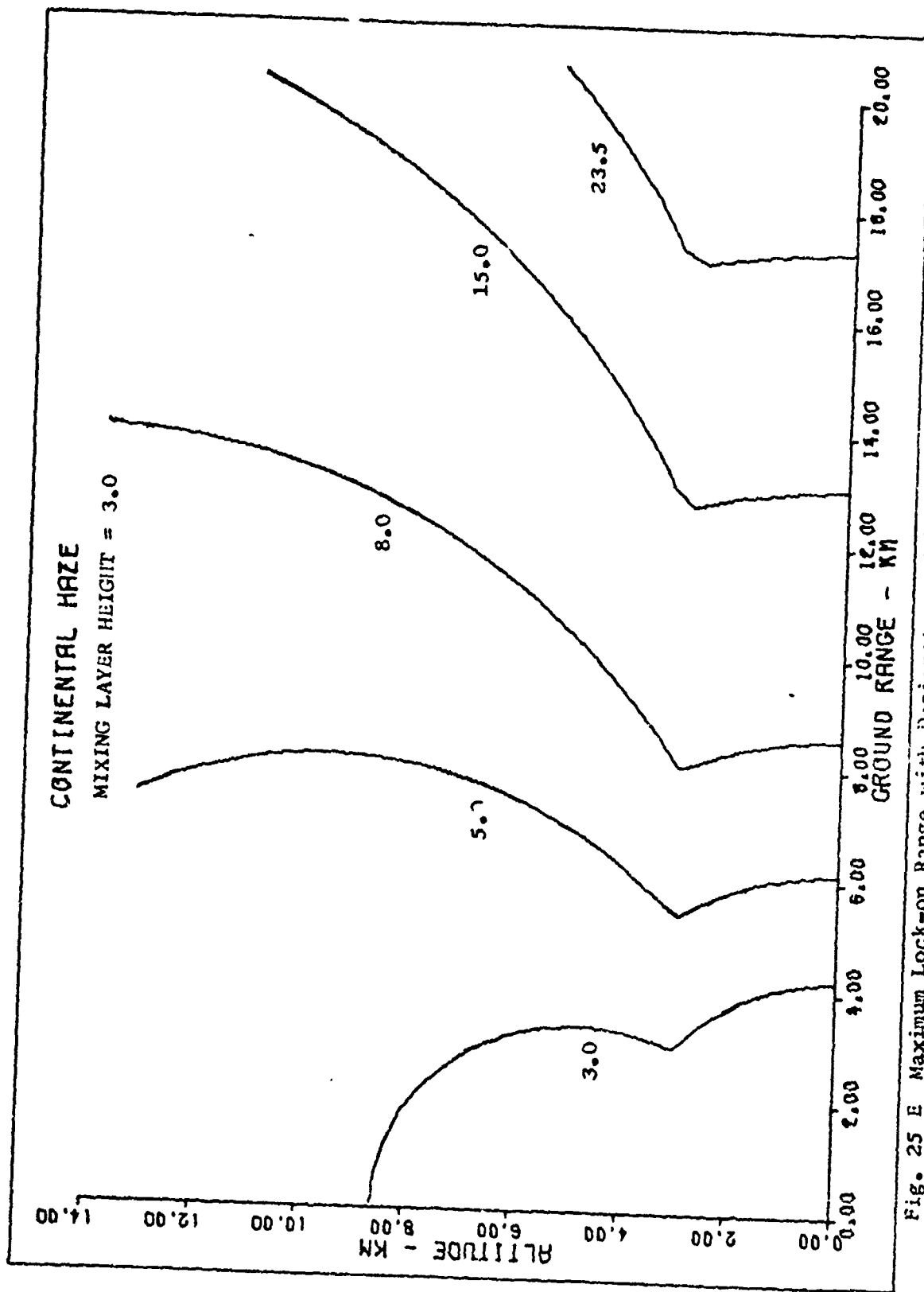
Fig. 25 E Maximum Lock-on Range with Designator and Receiver Collocated for Several Meteorological Ranges - Homogeneous Mixing Layer Model.

Appendix E

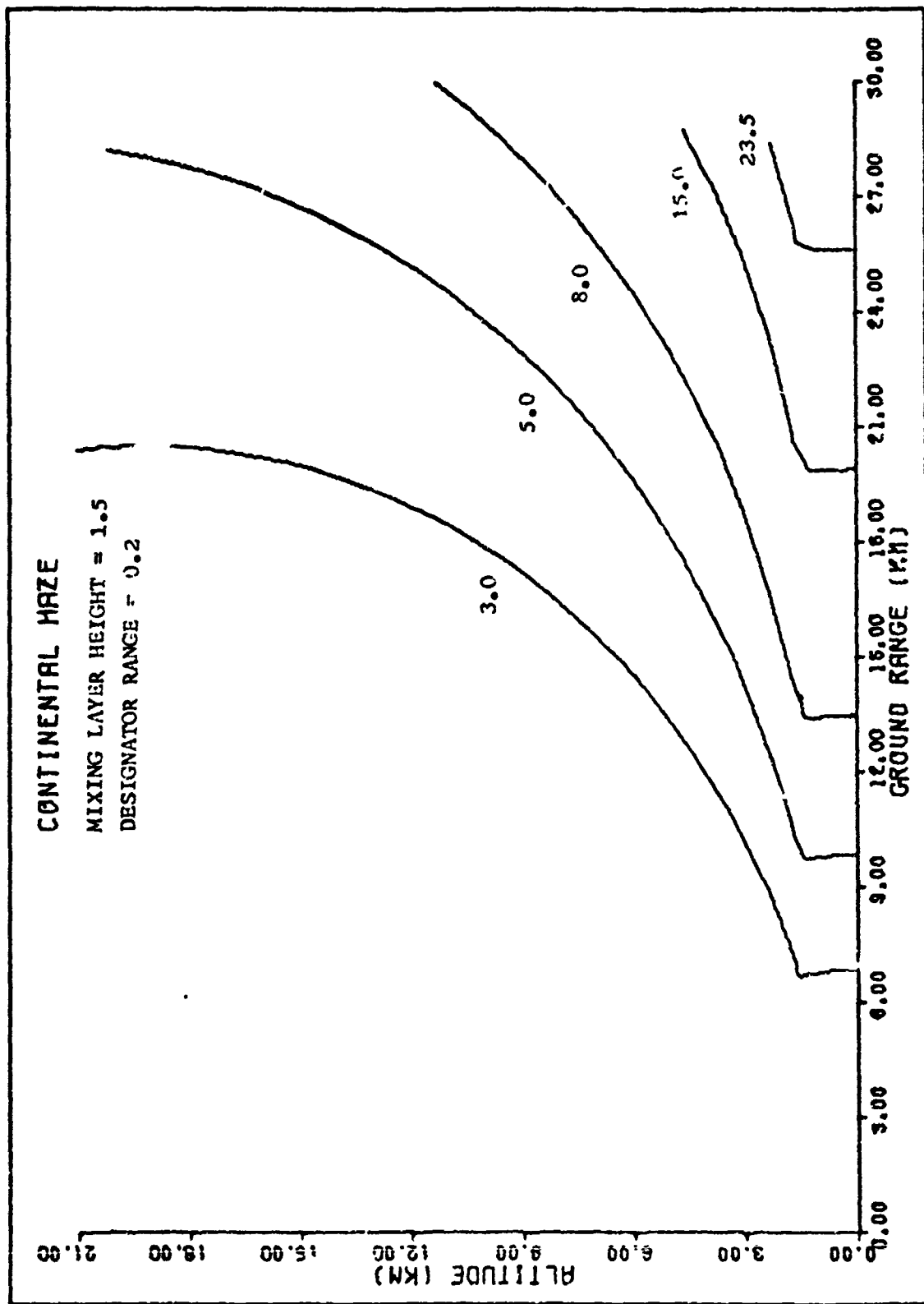## Maximum Lock-on Range Curves - Ground Designator

Fig. 26 A Maximum Lock-on Range with Ground Designator for Several Meteorological Ranges - Homogeneous Mixing Layer Model.
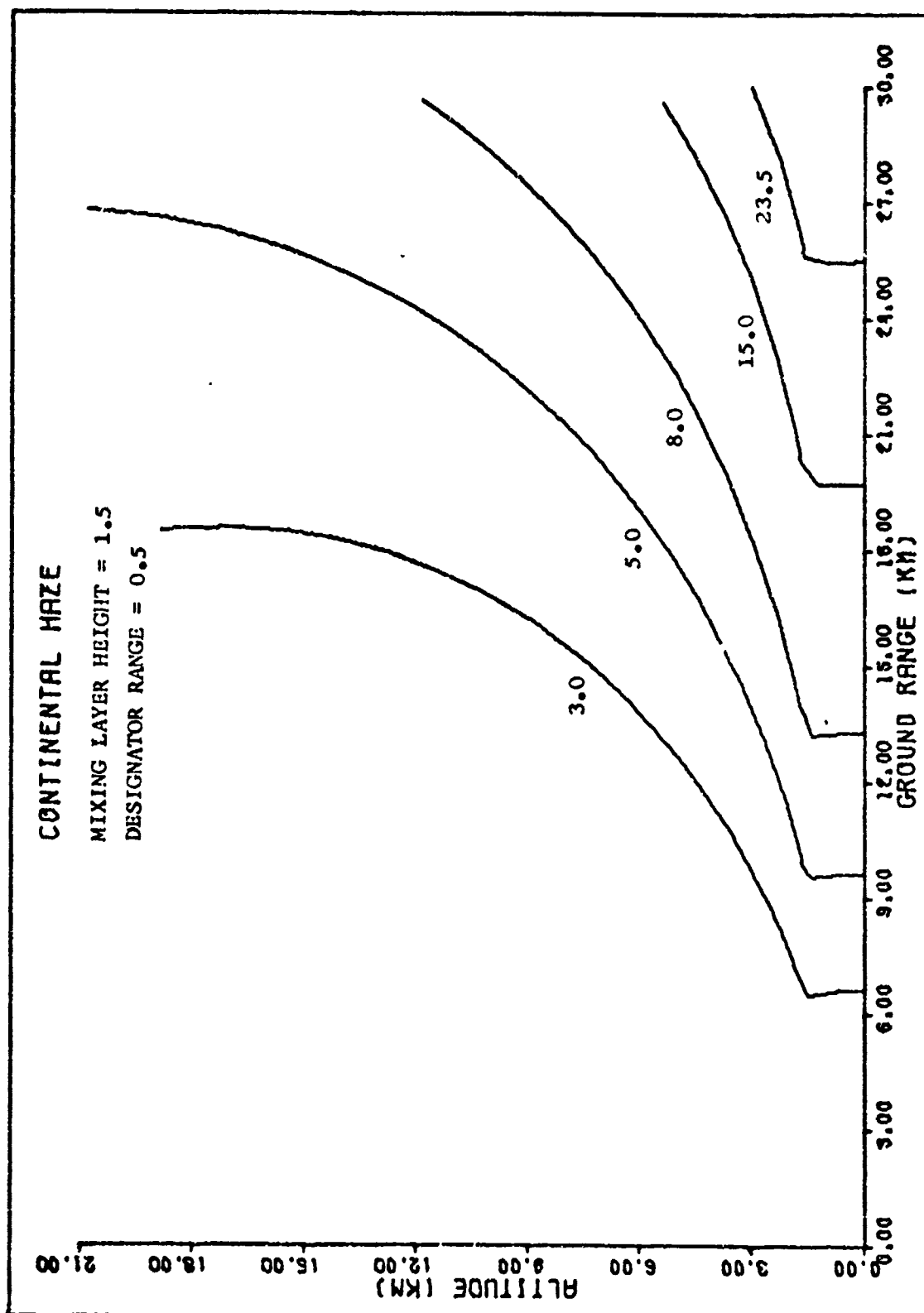
Fig. 26 B Maximum Lock-on Range with Ground Designator for Several
Meteorological Ranges – Homogeneous Mixing Layer Model.

Fig. 26 C Maximum Lock-on Range with Ground Designator for Several
Meteorological Ranges – Homogeneous Mixing Layer Model.

Fig. 26 ○ Maximum Lock-or Range with Ground Designator for Several
Meteorological Ranges - Homogeneous Mixing Layer Model.

Fig. 26 E Maximum Lock-on Range with Ground Designator for Several Meteorological Ranges - Homogeneous Mixing Layer Model.
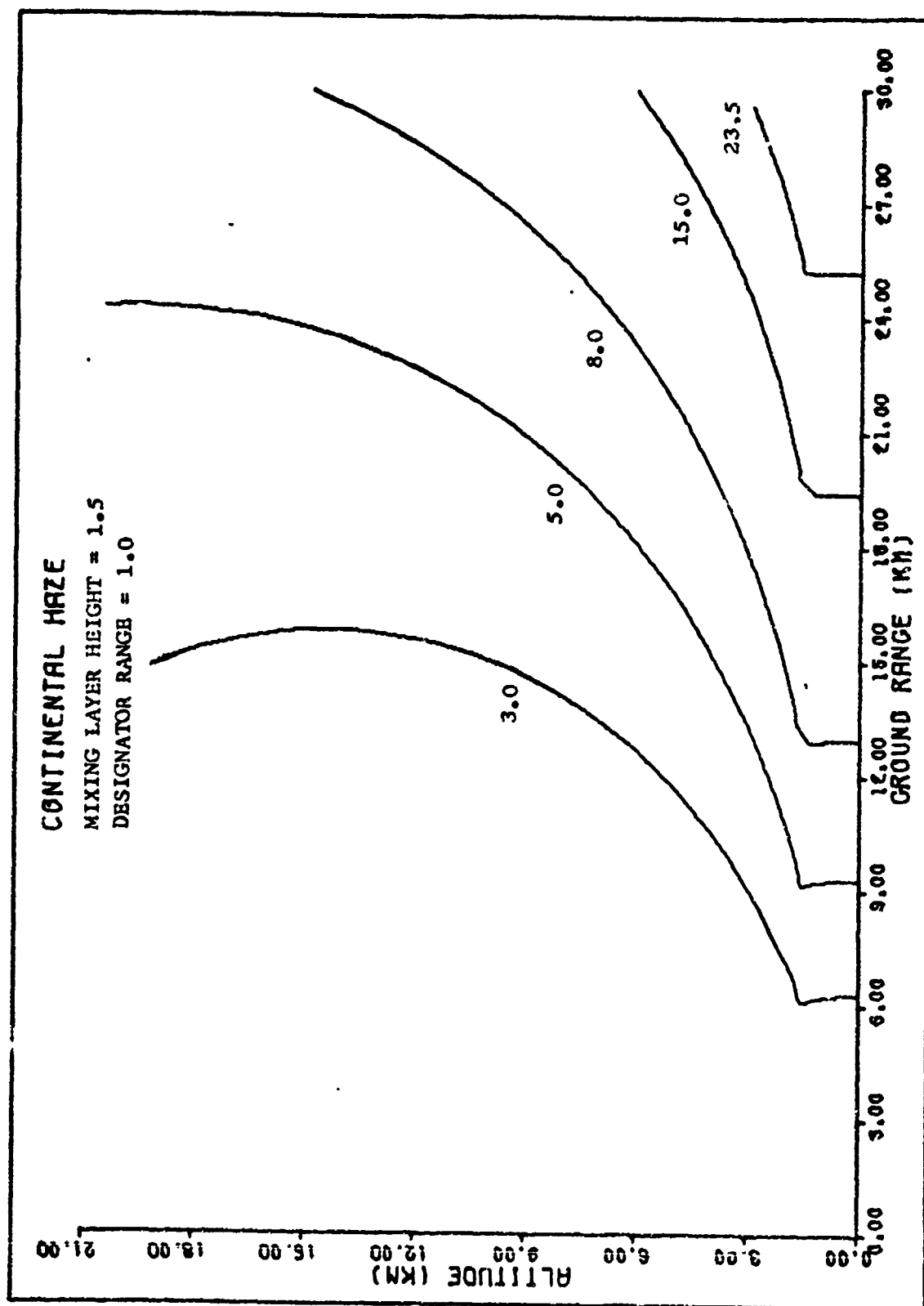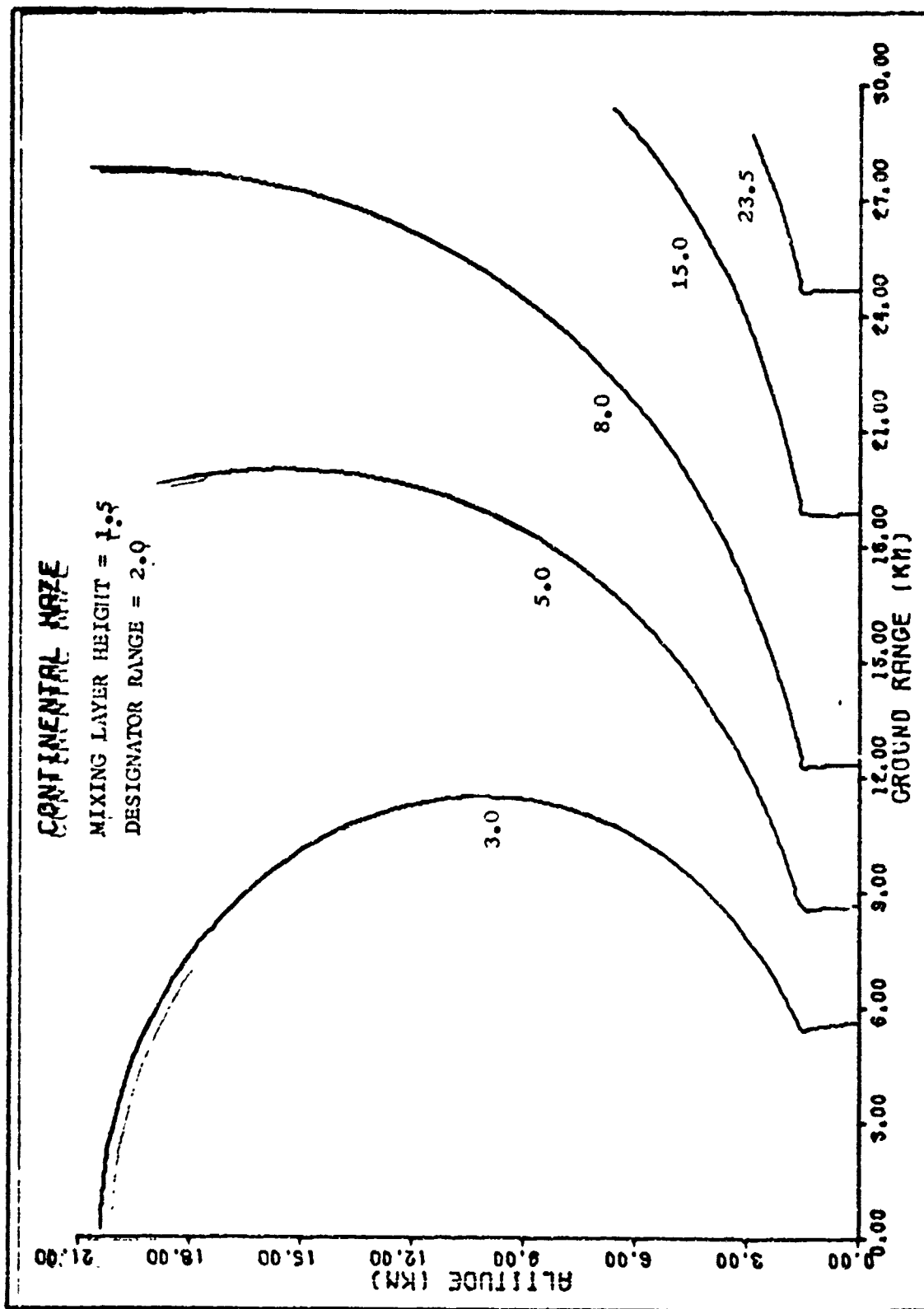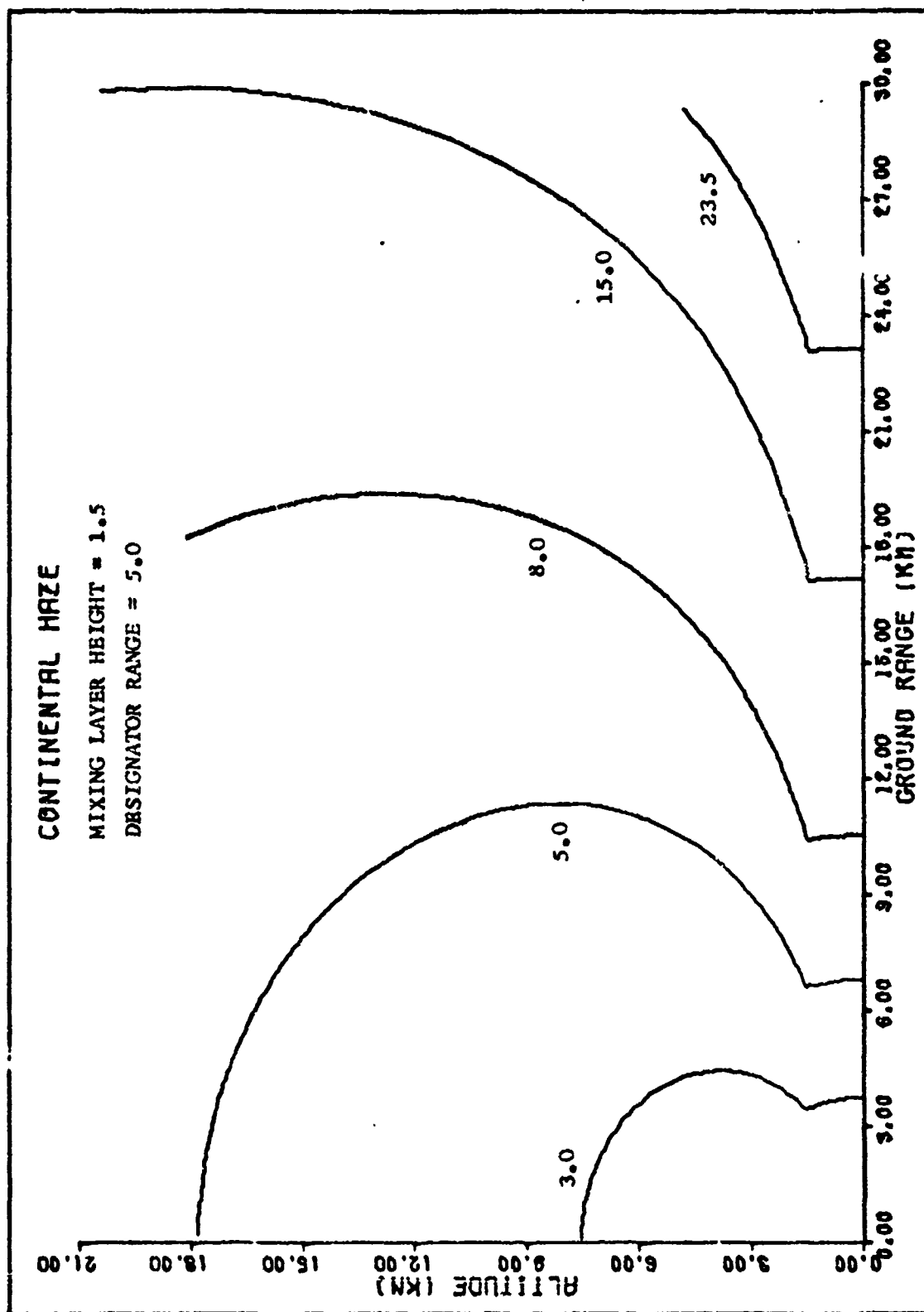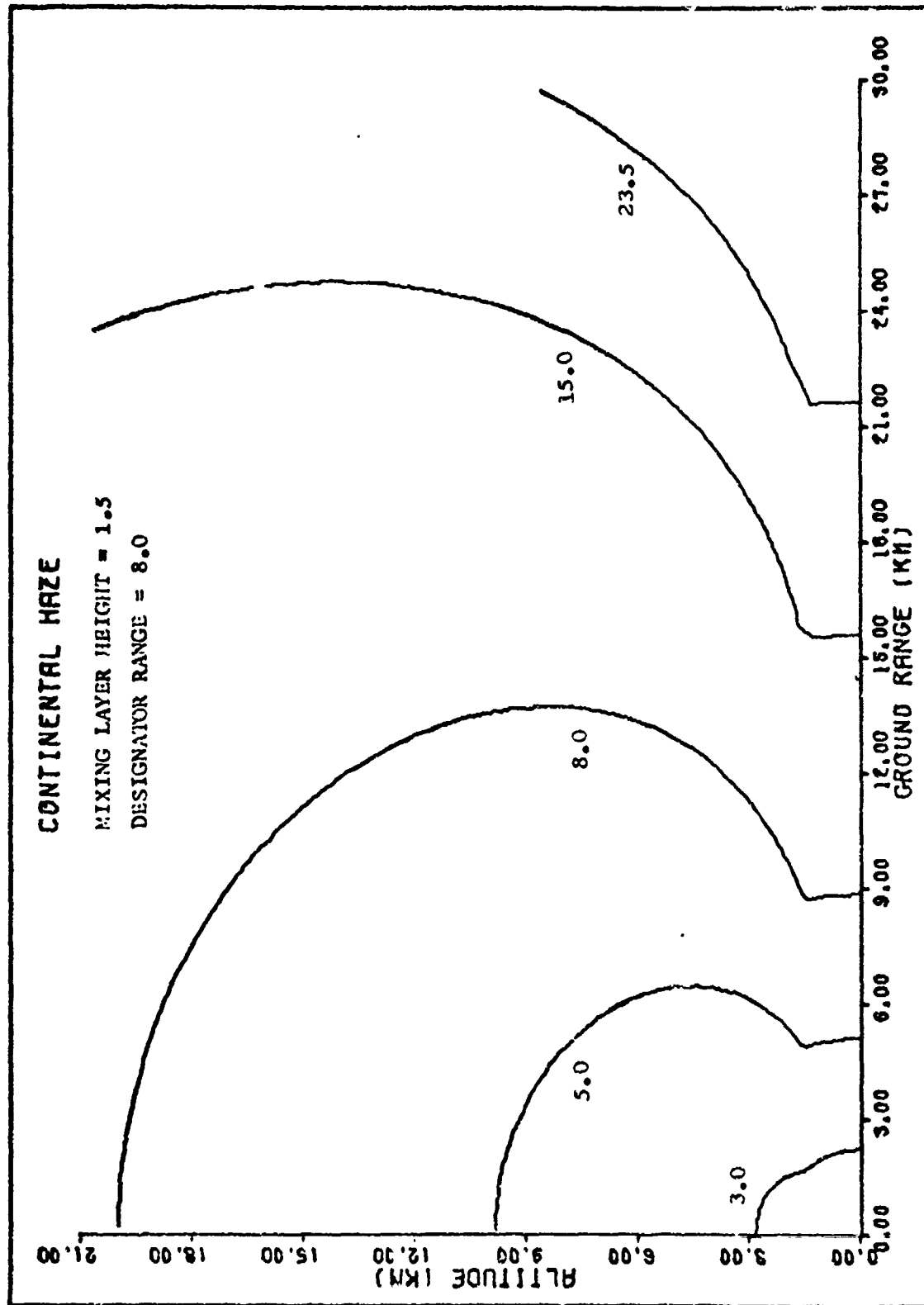
Fig. 26 F Maximum Lock-on Range with Ground Designator for Several Meteorological Ranges — Homogeneous Mixing Layer Model.

Appendix F

Development of the Lock-on Range Equation

The following is a list of symbol definitions used in the development of the lock-on range equation:

A_r - collecting area of receiver optics,

P_d - peak designator power,

P_r - received peak signal power,

P_t - power arriving at target,

R_d - designator range,

R_r - receiver range,

T_d - transmittance of designator optics,

T_r - transmittance of receiver optics,

ρ_t - target reflectance,

σ - atmospheric attenuation coefficient,

θ_r - angle between a normal to receiver surface and the target,

θ_t - angle between a normal to reflecting surface and the receiver,

Ω - solid angle subtended by the receiver.

If atmospheric effects are neglected and it is assumed that all radiated power is intercepted by the target, then

$$P_t = P_d T_d \tag{89}$$

Because the target is a Lambertian reflector, the power intercepted by the receiver can be described as

$$P_r = \frac{P_t \rho_t \cos\theta_t \Omega}{\pi} \tag{90}$$

102

where

$$\Omega = \frac{A_r \cos\theta_r}{R_r^2} \tag{91}$$

If the transmittance of the receiver optics is included Eq (90) can be written as

$$P_r = \frac{P_d T_d \cos\theta_t A_r \cos\theta_r T_r \rho_t}{\pi R_r^2} \tag{92}$$

or

$$R_r^2 = \frac{P_d T_d A_r T_r \cos\theta_t \cos\theta_r \rho_t}{\pi P_r} \tag{93}$$

If the atmospheric effects are included the power reaching the target and receiver can be written as

$$P_t' = P_t \exp\left[-\int_0^{R_d} \sigma(1)d1\right] \tag{94}$$

and

$$P_r' = P_r \exp\left[-\int_0^{R_r} \sigma(1)d1\right] \tag{95}$$

Eq (93) can now be rewritten as

$$R_r^2 = \frac{P_d T_d A_r T_r \cos\theta_t \cos\theta_r \rho_t \exp\left[-\int_0^{R_d} \sigma(1)d1\right]}{\pi P_r \exp\left[-\int_0^{R_r} \sigma(1)d1\right]} \tag{96}$$

or

$$R_r^2 \exp\left[\int_0^{R_r} \sigma(1)d1\right] = K \exp\left[-\int_0^{R_d} \sigma(1)d1\right] \tag{97}$$

where

$$K = \frac{P_d T_d A_r T_r \cos\theta_t \cos\theta_r \rho_t}{\pi P_r} \tag{98}$$

For easy calculations θ_t and θ_r are often assumed to be zero.

Appendix G

<u>Guide</u> <u>to</u> <u>Use</u> <u>of</u> <u>the</u> <u>Model</u> <u>for</u> <u>Lock-on</u> <u>Range</u> <u>Calculations</u>

This appendix describes the equations in the Homogeneous Mixing Layer model which can be used directly for computing lock-on range. With designator and receiver collocated (haze only), Eq (46), page 33, and Eq (49), page 34, can be used. With ground based designator (haze only), Eq (53), page 34, and Eq (54), page 35, can be used. Those to be used with designator and receiver collocated (haze and rain) are Eqs (58) and (60), page 35. The variable, β, in these equations is given by Eq (19), page 28. The ratio, α, for various combinations of continental and maritime hazes is given in Table V, page 23, or Eq (84), page 45. Simple algebraic expressions for lock-on range within the mixing layer are given by Eqs (85) and (88), page 67.

Vita

Vance August Hedin was born 5 October 1939 in Preston, Idaho. He attended Preston High School from which he graduated in 1957. He then attended Utah State University where he majored in Soil Science. He spent two and one half years, beginning in 1961, in Sweden as a missionary for the "Mormon" church. He graduated from Utah State and received a commission in the United States Air Force through ROTC in 1965. After completing Undergraduate Pilot Training at Vance AFB, Oklahoma, he received training in the F-4 and spent 8 months flying with the 389th Tac Ftr Sqd in Southeast Asia. Upon returning in 1968 he was assigned to the Aerospace Defense Command and flew F-106's at Loring AFB, Maine. He was assigned to the Air Force Institute of Technology (AFIT) in June 1972 and received an undergraduate degree in Electrical Engineering (Optics Option) in June 1974. He extended his stay at AFIT for one year and is currently working on a Master of Science degree in Electro-optics.

Permanent address: Route # 3, Preston, Idaho 83263